PERFORMANCE EVALUATION OF NANOFLUID BASED SOLAR THERMAL COLLECTORS

A Thesis submitted in the partial fulfillment of the requirements for the award of the degree of

DOCTOR OF PHILOSOPHY

by

J AMALA RANGA BABU
(ROLL NO: 701412)

DEPARTMENT OF MECHANICAL ENGINEERING

NATIONAL INSTITUTE OF TECHNOLOGY

WARANGAL (T.S) INDIA 506 004

May - 2018

PERFORMANCE EVALUATION OF NANOFLUID BASED SOLAR THERMAL COLLECTORS

A Thesis submitted in the partial fulfillment of the requirements for the award of the degree of

DOCTOR OF PHILOSOPHY

by

J AMALA RANGA BABU
(ROLL NO: 701412)

Under the supervision of
Dr. K. KIRAN KUMAR
&
Prof. S. SRINIVASA RAO

DEPARTMENT OF MECHANICAL ENGINEERING

NATIONAL INSTITUTE OF TECHNOLOGY

WARANGAL (T.S) INDIA 506 004

May 2018

THESIS APPROVAL FOR Ph.D.

This thesis entitled **"Performance Evaluation of Nanofluid based Solar Thermal Collectors"** by **Mr. J Amala Ranga Babu** is approved for the degree of Doctor of Philosophy.

Examiners

_____

_____

_____

Supervisor(s)

Dr. K Kiran Kumar

(Supervisor)

Associate Professor, Mechanical Engineering Department, NIT Warangal

Dr. S Srinivasa Rao

(Co-Supervisor)

Professor, Mechanical Engineering Department, NIT Warangal

Chairman

Prof. P Bangaru Babu

Head, Mechanical Engineering Department, NIT Warangal

Dedicated

to

❖ **My beloved Parents & Family**

❖ **All my Teachers and Professors who taught and encouraged me with**

positive thoughts

NATIONAL INSTITUTE OF TECHNOLOGY
WARANGAL (T.S) INDIA 506 004

DECLARATION

I, hereby declare that the matter embodied in this thesis titled **"Performance evaluation of nanofluid based solar thermal collectors"** is the result of research carried out by me under the supervision of **Dr. K Kiran Kumar** and **Prof. S Srinivasa Rao**, Department of Mechanical Engineering, National Institute of Technology (Deemed University), Warangal, Telangana. This work or any part of this work has not been submitted to any other University or Institute for the award of any other degree or diploma.

Date:
Place: Warangal

(J Amala Ranga Babu)
Research Scholar,
Roll No.701412

NATIONAL INSTITUTE OF TECHNOLOGY
WARANGAL (T.S) INDIA 506 004

CERTIFICATE

This is to certify that the thesis entitled **"Performance evaluation of nanofluid based solar thermal collectors"** submitted by **Mr. J Amala Ranga Babu (Roll No. 701412)** for the award of Doctor of Philosophy in the Department of Mechanical Engineering, National Institute of Technology Warangal, is a bonafide research work carried out by him under our guidance and supervision. The results embodied in this thesis have not been submitted to any other Universities or Institutes for the award of any degree or diploma.

Place: Warangal.

Date:

Dr. K. Kiran Kumar
Associate Professor
Department of Mechanical Engineering
NIT Warangal- India.

Prof. S. Srinivasa Rao
Professor
Department of Mechanical Engineering
NIT Warangal - India.

ACKNOWLEDGEMENTS

NIT Warangal   (**J Amala Ranga Babu**)

December 2017

ABSTRACT

Mankind is living in the arena of evolution of technology in which energy is an integral part. However, this enrichment of science and technology has opened new pathways for energy consumption and generation as well. Raise of population density is another root cause for energy demands. Fossil fuels are depleting at faster rate and leaving carbon footprints on environment. In this scenario, it is inevitable to depends on renewable energy sources which are inexhaustible, eco-friendly and abundantly available in nature. Amid all renewable sources, effective utilization of solar energy is a viable alternative to meet the growing energy demands, particularly for low temperature applications. While consumption of solar energy for various domestic applications is not new, but it is suffering from lower effective energy conversion problem.

Solar collectors are the device that absorbs the incident solar radiation and converts into useful form. Among different types of collectors, solar flat plate collectors (SFPC) are the noteworthy devices to convert the incident radiation into heat energy of working fluid. In view of enhancing the thermal efficiency of collectors, there are two major approaches as either changing the geometry and operating parameters or enhancing the properties of working fluid. Since, various geometrical and operating parameters and modifications are more or less saturated, present work is focused on enhancing the thermophysical and optical properties of working fluid by suspending nanoparticle as an approach for effective conversion of solar radiation into useful heat energy.

Thermophysical properties and their influence on thermal performance of SFPC are estimated using the empirical correlations available in open literature and comparisons are made with the experimental outcomes. It is noticed that a substantial variation exists between the analytical and experimental outcomes. Thus, the influence of each parameter on collector efficiency is critically examined. Both thermal conductivity and viscosity of all working fluids are experimentally measured and compared with the existing correlations. It is noticed that, existing correlations are under-estimating the nanofluid properties, particularly this deviation is considerable for the viscosity of nanofluid. For example, 18.58 % deviation is noticed at 1.0 % particle concentration of CuO/water nanofluid. Therefore, a new correlation is developed for precise calculation of viscosity for both mono and hybrid nanofluid and further analysis is carried out using the developed correlation.

In the current research, thermodynamic analysis is carried out using laws of thermodynamics to evaluate the energy, exergy efficiencies, and to study the various parameters that causes entropy generation. Experimental and analytical approaches are conducted based on mode of fluid circulation i.e. forced circulation and natural circulation as well as on type of incident radiation absorption i.e. direct absorption and indirect absorption.

All the experiments are performed as per ASHRAE standards 93-86 to calculate the instantaneous efficiency of SFPC. Experiments are conducted with different nanofluids like Al_2O_3/water, Cu/water, CuO/water, SiO_2/water and TiO_2/water nanofluids. It is observed that among all nanofluids Cu/water and CuO/water nanofluids exhibits higher thermal performance and lower entropy generation than other working fluids.

Along with the enhanced thermophysical properties, optical properties of Cu/water and CuO/water nanofluids are found to be enhanced. Therefore, by amalgamating Cu with CuO nanoparticles, a new hybrid nanofluid is developed. It is found that Cu-CuO/water hybrid nanofluid exhibits enhanced optical properties than the individual constituents and exhibits higher collector efficiency than its constituents in the direct absorption mode of operation.

It is noticed from the experimental outcomes that, instantaneous efficiency of SFPC is increasing with particle concentration and mass flow rate. In case of forced circulation indirect absorption, SFPC with Cu/water nanofluid is 16.86 % more efficient, while that with Cu-CuO/water and CuO/water are 10.55 % and 9.81 % more efficient for respectively compared to water.

While in case of direct absorption, SFPC with Cu-CuO/water hybrid nanofluid exhibits higher instantaneous efficiency of 18.45 % compared to that of water. While, SFPC with Cu/water and CuO/water nanofluids are exhibiting 13.64 % and 11.34 % enhancement compared to water.

By comparing indirect and direct absorption collectors, direct absorption collector is exhibiting 7.9 % higher instantaneous efficiency with Cu-CuO/water hybrid nanofluid under similar operating conditions.

Similar to forced circulation, in natural circulation also SFPC with Cu/water nanofluid exhibits 11.51% higher instantaneous efficiency. While SFPC with Cu-CuO/water and CuO/water nanofluids exhibits 8.12% and 6.84% more instantaneous efficiency respectively compared to water.

In natural circulation direct absorption, SFPC with Cu-CuO/water nanofluid show 13.25 % higher instantaneous efficiency than water and that is 9.53 % and 8.71 % in case of Cu/water and CuO/water nanofluids

From the above experimental analysis, it is noted that no single working fluid is suitable for all modes of operation.

It is noticed that in case of indirect absorption system thermophysical properties play an important role, while in case direct absorption along with thermal properties, optical properties also have a major contribution to absorb the incident solar radiation. It is also noticed that in case of forced circulation, more amount of incident radiation is collected due to lower heat loss because of reduced temperature difference between absorber plate and bulk working fluid, whereas, in natural circulation mode, higher convection and radiation losses lead to reduce the thermal efficiency of the collector.

CONTENTS

Chapter 3 Nanofluid Preparation and Estimation of Thermophysical Properties

Chapter 4   Performance Evaluation of Forced Circulation Solar Flat Plate Collector

Chapter 5 Performance Evaluation of Natural Circulation Solar Flat Plate Collector

List of Tables

List of Figures

xiii

Nomenclature

Nomenclature

A_c	Area of the collector	m^2
C_o	Speed of light in vacuum	2.9979×10^8 m/ s
C_b	Bonding coefficient	-
C_p	Specific heat	J kg^{-1} K^{-1}
D	Riser diameter	m
$\dot{Ex}$	Exergy flow rate	Js^{-1}
F	Fin efficiency	-
F'	Collector efficiency factor	-
F_R	Heat removal factor	-
f	Darcy friction factor	-
H	Height of the collector	m
h	Planck constant	6.6256×10^{-34} J s
h_l	Total head loss due to friction	m
h_w	Wind Convective heat transfer coefficient	Wm^{-2}K^{-1}
I_t	Solar radiation	W m^{-2}
k	Thermal conductivity	W m^{-1} K^{-1}
K	Radiative coefficients	/m
k_B	Boltzmann constant	1.38×10^{-23} J /K
K_L	Loss coefficient	-
$\dot{m}$	Mass flow rate	kg s^{-1}
$\dot{m}_r$	Mass flow rate in each riser	kg s^{-1}
m	Complex refractory index	
N_g	Number of glass covers	
ΔP	Pressure drop	Nm^{-2}
Q_i	Energy due to incident solar radiation	W
Q_u	Useful energy gain	W
$\dot{S}_{gen}$	Entropy generation rate	W K^{-1}
t	Thickness	m
T	Temperature	K
T_{sun}	Apparent sun temperature	K
U_l	Overall heat loss coefficient	Wm^{-2}K^{-1}
V_w	Wind velocity	ms^{-1}
W	Tube pitch	m
W_{lost}	Work lost	J

Subscripts

a	ambient
avg	average
b	bottom of the collector
bf	base fluid
c	collector
dest	destroyed
e	edge of the collector
f	fluid
fm	mean fluid condition
s	Sun
leak	leakage
max	maximum
min	minimum
nf	nanofluid
np	nanoparticle
p	plate
in	inlet
out	outlet
opt	optimum

Greek symbols

β	Collector tilt angle
ρ	Density, $kg\ m^{-3}$
ϕ	Volume fraction
μ	Viscosity, $N\ S\ m^{-2}$
τ	Transmittivity
α	Absorbivity
η	Efficiency
ε	Emissivity
σ	Stefan Boltzmann constant, $Wm^{-2}K^{-4}$
λ	Wave length, /m

Chapter 1

Introduction

1.1   Background

Energy is becoming the integral part of human life. Escalation of technology and acclivity in population growth rate accelerating the energy demands at an exponential rate. Past few decades are clear evidence of potential growth in various fields like automobile, electronics, power generation, etc., where energy becomes an intrinsic requisite. However, this progress of technology is driving the mankind towards the energy crunch. Thus, energy generation technologies are seeking for an innovative and cutting edge method. The prevalent fossil sources are non-replenish in nature and have finite availability. However, these formal energy sources are reaching to the verge of obliterating out and eventually leaving carbon footprints on environment either directly or indirectly [1]. The dependence on these depleting energy sources and consequent greenhouse gas emissions can be effectively reduced by the use of different renewable energy sources. Therefore, the sustainable development of renewable energy utilization is an effective and unsurpassed approach to meet the future energy needs with minimum environmental vulnerability. In the recent past, the people from different communities like expert researchers and scientific communities to common man and governments are well aware the need of benign renewable energy. Classification of various solar collectors are presented in Fig. 1.1. Amid all renewable energy sources, solar energy is a

widespread and viable alternative with its clean, profuse, inexhaustible and eco-friendly nature.

```
                          ┌──────────────┐
                          │    Solar     │
                          │    Energy    │
                          └──────┬───────┘
                  ┌──────────────┴──────────┐
          ┌───────────────┐         ┌───────────────┐
          │  Electrical   │         │   Thermal     │
          │    Energy     │         │    Energy     │
          └───────────────┘         └───────┬───────┘
                                    ┌────────┴──────┐
                                    │    Solar      │
                                    │  Collectors   │
                                    └───────┬───────┘
        ┌───────────────────┬───────────────┴───────────────────┐
┌───────────────┐   ┌───────────────┐               ┌───────────────┐
│ Concentrated  │   │  Flat Plate   │               │  Evacuated    │
│  Collectors   │   │  Collectors   │               │  Collectors   │
└───────────────┘   └───────┬───────┘               └───────────────┘
              ┌─────────────┴─────────────────┐
      ┌───────────────┐               ┌───────────────┐
      │    Active     │               │   Passive     │
      │  Collectors   │               │  Collectors   │
      └───────┬───────┘               └───────┬───────┘
        ┌─────┴─────┐                   ┌──────┴──────┐
┌──────────┐ ┌──────────┐       ┌──────────┐ ┌──────────┐
│  Direct  │ │ Indirect │       │  Direct  │ │ Indirect │
│Absorption│ │Absorption│       │Absorption│ │Absorption│
└──────────┘ └──────────┘       └──────────┘ └──────────┘
```
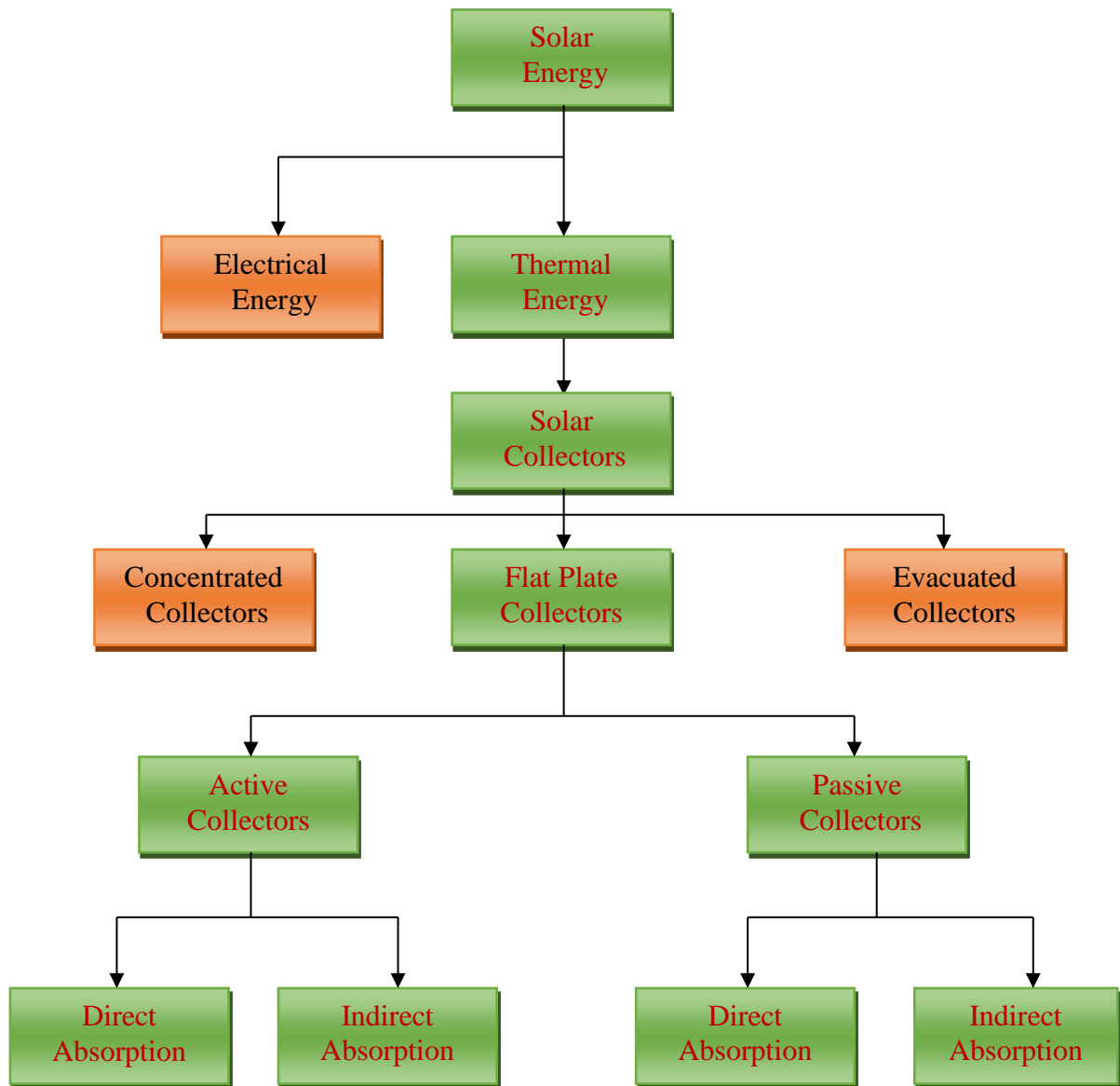
Fig. 1.1 Classification of solar collectors for the current research

The sun will be the fuel of the future, the solar resource is an enormous and it has huge potential. This solar energy can be captured and transformed into useful energy form like heat. The intensity of solar energy will be varies in quantity and quality from place to places and also with time. In recent years, the utilization of solar energy is growing at the faster rate even it is suffering from lower efficacy. Judicious utilization of solar energy is a potential alternative to combat with increasing critical energy needs at ecological balance. Around the world, most of the countries are harvesting solar energy on an unprecedented scale to mitigate the environmental effects. However, while sun rays passing through space, partial amount of solar

energy is attenuated by absorbing and reflecting by both the atmosphere and clouds and reaming is only reaches to the earth's surface [2]. Fig. 1.2 depicts the distribution of solar energy on the earth's surface. The average amount of the solar radiation that penetrates into the atmosphere and reaches the ground is only 51 % of the total incoming solar energy. In the remaining, 30 % is reflected back into space and 19 % is absorbed by the atmosphere and clouds. The total solar energy absorbed by Earth's atmosphere, oceans and land masses is in one hour more than that of the world energy needs in a year.
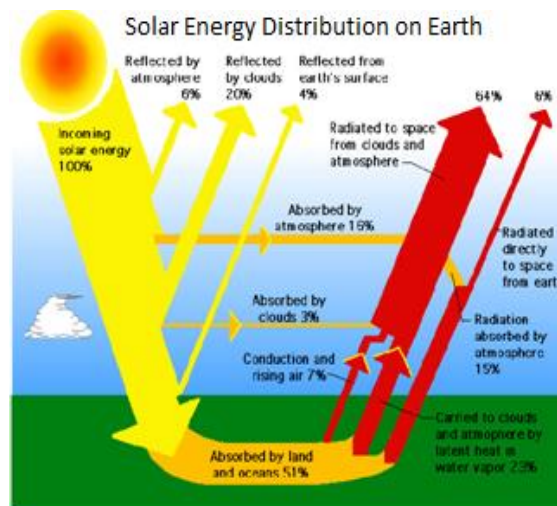
Fig. 1 2 Solar energy distribution on earth

Incident solar radiation is in the form of electromagnetic waves and it is spreads over a wide range of solar spectrum. In precise, the irradiation is in the form of ultraviolet, visible and infrared waves. However, most of the energy inhibited in solar radiation is filtered before it reaches to the earth surface. Fig. 1.3 elucidates the spectral distribution of solar irradiation over a range of wavelengths up to 2400 nm. As depicted in Fig. 1.3, the longer wavelengths (infrared) have less energy than shorter wavelengths (visible or UV). It can also be observed from Fig.1.3 that, most of the energy is inhibited in the UV and visible region only and peak of the spectral irradiance is within the visible region thereby, higher amount of energy of the solar radiation is abides in this region only. Therefore, the substance having good optical properties like higher absorption and extinction coefficients in visible region would absorb more amount of solar energy.

In spite of its low energy intensity and unsteady nature, solar energy has been a prominent substitute to meet the consistently raising energy requirements. The solar energy can be effectively harnessed by using the renowned devices called solar collectors. The solar collector will absorb the solar radiation incident on their surface and converts this incident energy into

useful form. The collectors are categorized based on design, working, operating range etc. However, the basic motto of all the collectors is to harness the available solar energy and transforms into desired form.
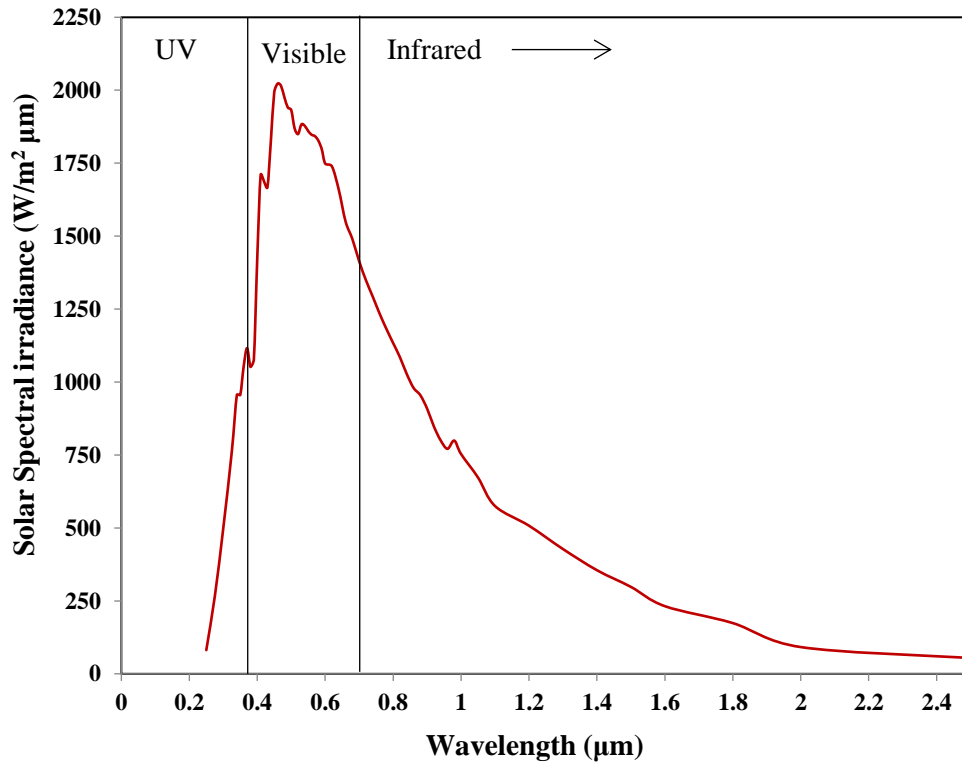
Fig. 1.3 Solar irradiation spectrum over a range of wavelengths

The basic classification of solar collectors based the structure and operating mode is illustrated in Fig. 1.1. Amid all, Solar Flat Plate Collectors (SFPC) are the most conventional and noteworthy device for water and space heating particularly for low temperature domestic applications. Solar radiation incident on collector is absorbed by the absorber plate and convert this radiation into heat, and this heat energy is transforms to the working fluid as useful gain. The schematic views of active and passive solar collectors operated under direct and indirect configurations are presented in Fig 1.4. The detailed explanation on its working is presented in successive chapters at relevant sections. The heat absorbed by the working fluid can be used for many commercial and domestic applications, such as domestic water heating, air conditioning, swimming pool heating for houses, hotels, hospitals etc. [3].
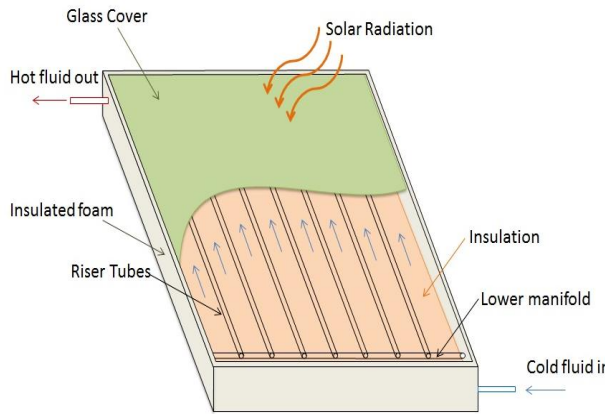
Fig. 1.4 (a) Indirect absorption solar collector
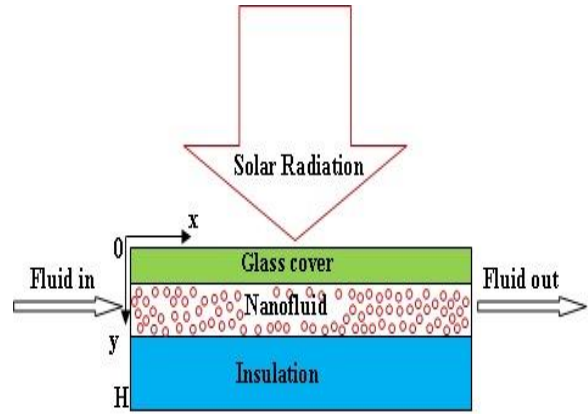
Fig. 1.4 (b) Direct absorption solar collector
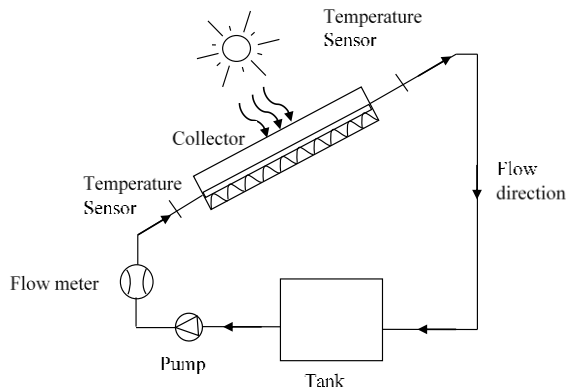
Fig. 1.4 (c) solar collector operating under forced circulation mode
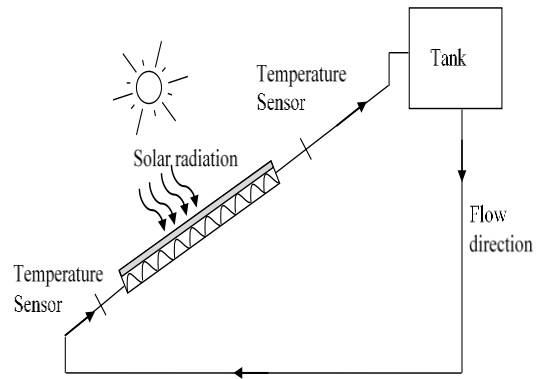
Fig. 1.4 (d) solar collector operating under natural circulation mode

India is a tropical country, it has an immense potential to tap and harness the solar energy round the year. Therefore, by adapting appropriate solar thermal collectors, one can harness the plenty of solar energy available in nature to meet the energy needs which has been reduce the dependence on conventional energy resources and also can maintain environmental sustainability. Even though, the solar collectors are exists from long time, they are suffer from lower thermal efficiency. However, the thermal efficiency of collector depends on geometry, orientation, heat transfer properties of the working fluid and climatological and geographical conditions [4]. Somehow, for a given location the geographical and climatic factors are inconsistent and uncontrollable. On the other hand, various traditional heat transfer enhancement techniques like geometrical and material optimization methods to improve the performance of solar collectors are more or less saturated [5]. Therefore, an alternative approach to increase the collector performance is improving the thermophysical properties and heat transfer characteristics of working fluid. However, the technology of heat transfer to

improve the thermal characteristics of working fluid is standing at the critical juncture and it take paradigm shift with an innovative cutting edge technology called nanotechnology.

1.2 Nanofluids

A novel strategy to improve the thermal properties of working fluid is suspension of high thermal conductive solid particles in inherently poor conductive conventional working fluid. However, suspension of solid particles in base fluid is in not a new idea, it is traced back from the 19th century. Maxwell [6] is the pioneer in the area of dispersing solid particles in a liquid medium to augment the effective thermal conductivity of the working fluid. And also proposed an appropriate theoretical basis, to estimate effective thermal conductivity of particle suspended fluids. In continuation to this, Hamilton-Crosser [7] carried out an outstanding research on particles suspended fluids and modifies the Maxwell correlation [6] to estimate effective thermal conductivity of working fluid more precisely. But both [6], [7] dispersed micro sized solid particles in base fluids, thus their studies are limited by some flaws like the rapid settlement of the solid particles, need of more pumping power, wall erosion and clogging of flow passage in flow field. However, advancement in material technology facilitates to produce nano sized solid particles and give uniqueness to introduce an innovative and novel heat transfer fluid. For the first time, Choi [8] addressed the phenomenon of suspending nano size solid particles in base fluid and this particles suspended fluids are noted as nanofluids. Homogeneous suspension of solid nanoparticles in conventional base fluids will recasts the thermophysical properties of base fluid and promotes the heat transfer rate. This enhanced thermophysical properties of nanofluids provide an influential support to many researchers to employ the nanofluids as a new generation heat transfer fluid in various engineering applications. Therefore, using of these nanofluids as working fluid in solar collector is a novel approach to improve collector performance. Valence electron confinement regime within the nanoparticle defines the thermophysical and optical properties of a nanofluid. Hence, these nanofluids exhibit some superior characteristics such as high specific surface energy, higher thermal conductive capabilities and enhanced photo-thermal properties, which are the favorable characteristics to use nanofluids in SFPCs [9].

In recent years, several researchers analyzed the synthesis, preparation and characterization of various nanofluids for different heat transfer applications [10]–[15]. Many numerical and experimental results are reported on various combinations of nanoparticles and base fluids. Among many kinds of nanoparticles, some commonly used nanoparticles are Al, Ag, Au, Cu,

Fe (metals), Al_2O_3, CuO (metal oxides), SiC, TiC (carbide ceramics), AlN, SiN (nitride ceramics), SiO_2, TiO_2 (semiconductors), carbon in various forms (like nano-diamond, graphite), carbon nanotubes with single wall, double wall and multi walls, fullerene and shell composites. Conventional base fluids are water, polymer solutions, transformer oil, and ethylene glycol.

Many of earlier researchers are reported on the enhancement of thermophysical properties exhibited by the nanofluids. Few notable works on this enhancement of heat transfer characteristics are presented here and detailed information regarding nanofluid characteristics and their usage in solar collectors are discussed in subsequent literature review chapter. Pak and Choi [8] were examined the heat transfer behaviour of water based Al_2O_3 and TiO_2 nanofluids at different Reynolds and Prandtl numbers. They found that convective heat transfer coefficient is linearly increased with particle volume concentration. Sharma et al. [16] attained 23.7 % improvement in heat transfer coefficient at 0.1 vol. % with Al_2O_3/water nanofluid. Sajadi et al. [17] obtained 22 % enhancement in heat transfer coefficient with TiO_2/water nanofluid at 0.25 vol. %. Zhu et al. [18] analytically investigated heat transfer coefficient enhancement with Fe_2O_3/water nanofluid and reported 38 % improvement in heat transfer coefficient at 4 % volume concentration. Lee et al. [19] conducted experimental investigation on SiC/DI water nanofluid and reported 102 % enrichment in heat transfer coefficient at 3 vol. %. Ding et al. [20] analytically examined the heat transfer enhancement with CNT/water nanofluid and reported 350 % enhancement at 0.5 wt. %. The reliable refinement in heat transfer and fluid transport properties, make the nanofluids versatile to use for many engineering applications like heat exchangers [11], [21], car radiator [22], electronic cooling [23] and solar collectors [24]–[26] etc.

In recent past, research on nanofluids utilization for various heat transfer applications is increasing. It has been noticed that most of the studies are focused on synthesis, preparation, characterization, but relatively limited studies are focused on deployment of nanofluids in various domestic, industrial and commercial applications. Fig. 1.5 is evident for the intensive interest among scientific community on nanofluids research. In the year 2016 alone 1259 articles were published on nanofluids whereas 46 articles were published on hybrid nanofluids (papers listed in SCOPUS are only considered). However, it is clear from Fig. 1.5 that comparatively very least amount of research has been carried out on hybrid nanofluids.
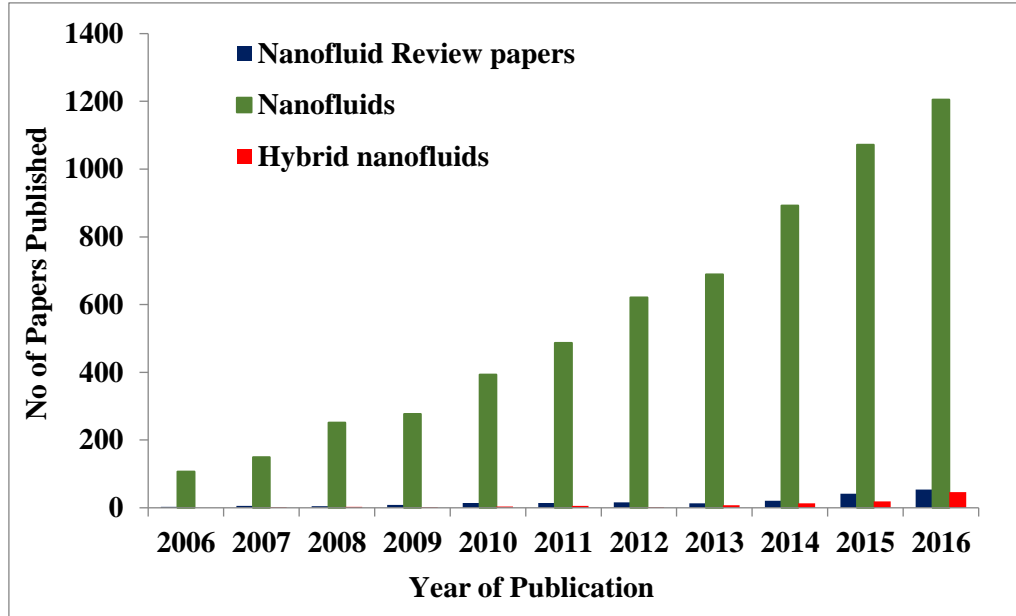
Fig.1.5 Number of articles published reports by Scopus from 2006 to 2016 retrieved by the key word nanofluid and hybrid nanofluid.

1.3   Need of hybrid nanofluids

The fundamental issue with the mono kind nanofluids is either they have a good thermal network or better rheological properties. But, the mono nanofluids solely may not possess all favorable characteristics necessary for a specific application. However, many real time applications demand trade-off among several characteristics/properties of nanofluids. For example, metal oxide nanofluids like Al_2O_3/water exhibits good chemical inertness and stability, but possess lower thermal conductivity while nanofluids prepared from the metallic nanoparticles like Aluminium, Copper, Silver would possess higher thermal conductivities, but, they are chemically reactive and unstable. Therefore, by hybridizing such metallic nanoparticles with ceramic or metal oxides, the resulting hybrid nanofluid may exhibit superior thermo-physical properties and rheological behavior together with the refined heat transfer characteristics.

This opens the new arena of hybrid nanofluid to use them for different heat transfer applications. Hybrid nanofluid is a homogeneous mixture of two or more nanoparticles with new physical and chemical bonds. The primary idea of hybrid nanofluid is to achieve a promising improvement in thermophysical, hydrodynamic and heat transfer properties, compared to mono nanofluids due to the synergistic effect [27]. By hybridizing the appropriate combination of nanoparticles, one can get the desired heat transfer effect even at low particle

concentrations [28]. In the current research, both mono and hybrid nanofluids are used in SFPC, estimated their performance/thermal efficiency analytically and experimentally.

1.4   Organization of the Thesis

The current thesis comprises a total of five chapters inclusive of the present chapter. In which the prominent features of various chapters are enunciated.

Chapter 1 provides a general introduction to the research problem tackled in the present thesis. This chapter also describes the broad organization of the thesis spelling out as to what is expected in each of the chapters.

In chapter 2 contributed to give an exhaustive review on the literature related to the research problem taken up in the present thesis. This is accompanied by the research gaps identified and conclusions drawn from the literature review are furnished. All the major objectives and the scope of the research work are also included in the same chapter.

Chapter 3. The method adapted for nanofluid preparation in the current research is provided. This chapter also scrutinizes the estimation of various thermophysical properties of mono and hybrid nanofluids from the correlations available in open literature. It also compares the experimentally measured properties with the empirical correlations. A considerable deviation is observed between the measured results and the empirical solutions, therefore, a new correlation is developed to estimate the viscosity of nanofluids. Reasons to establish the new correlation is also discussed in that chapter.

Chapter 4 gives the elaborative discussion on thermodynamic analysis (energy and exergy) of SFPC absorbing incident radiation at direct and indirect configurations and operated under forced circulation modes. Experimental studies are carried out with different working fluids such as Al_2O_3/water, Cu/water, CuO/water, TiO_2/water and SiO_2/water as working fluids and comparative studies are presented. It is noticed that, among all the nanofluids, Cu/water and CuO/water nanofluid exhibiting higher thermal efficiency and lower entropy generation. Nevertheless, the Cu/water nanofluid is highly reactive and economically not feasible. Therefore, by combining those two individual nanoparticles, a new hybrid nanofluid called Cu-CuO/water is proposed and studied in the current research. In further analysis, the instantaneous efficiency of nanofluid based SFPC is studied in different configurations under forced circulation is discussed.

Chapter 5 provides a detailed discussion on thermodynamic analysis of SFPC that absorbs the incident solar radiation in both direct and indirect configurations operated under natural circulation mode. Both analytical and experimental studies are carried out using Cu/water, CuO/water and Cu-CuO/water nanofluids and comparative studies are presented.

Chapter 6 provides the conclusion derived from the research work and scope of future work.

1.5   Closure

The present chapter clearly speaks about the background and motivation concerning the research problem taken up for investigation in current thesis. It also documents the various relevant features of all the chapters of the thesis, which provides a clear idea to the reader.

Chapter 2

Literature Review

2.1   Introduction

As spelt out in the earlier chapter, the current thesis will address the interaction of incident solar radiation with the solar collector. By keeping this in mind a comprehensive review of literature concerning to SFPC and its thermal efficiency/performance has been presented. The entire literature is split into ten different phases. The first phase concentrated on the influence of various geometrical and operating parameters on performance of SFPC. While the foregoing sections focuses on synthesis, preparation of nanofluid and their stability. While the fifth section concentrated on preparation of nanofluids and their thermophysical properties whereas consequent section is consolidates the refinement of thermophysical properties of hybrid nanofluids. In seventh section describes the influence of ethylene glycol on solar collector performance. In eighth section, a brief literature is presented on the performance of forced circulation/active solar thermal collectors using different nanofluids. In most of the real time domestic applications, solar collectors are run on natural circulation mode only hence the thermal performance of solar collectors under natural circulation/passive mode is presented in foregoing section. Thermodynamic second law analysis and entropy generation due to heat transfer and flow friction on solar collectors is discussed in tenth section. Comparative studies on solar thermal collectors operated on different absorption configurations and operating modes are presented in the subsequent section. The consequent sections accomplishes the concluding

remarks from the literature review flowed by the gaps identified from literature. Major objectives and scope of the present work is presented as separate section.

2.2 Literature addressing the geometry and operating conditions of SFPC

Though the reasonable amount of work is carried out on geometrical and operating conditions optimization of SFPCs, considerable milestones in this area is presented in the current section. Hottel and Whillier [29] modified the existing SFPC by that time and developed a new model. it is the most commonly used geometry of flat plate collector till the date.

Ackermann et al. [30] investigated the effect of internal fins in SFPC and noticed a marginal improvement in collector performance. A notable thing that they mentioned is, the collector performance can be further improved either by reducing the fin pitch or by using the higher thermal conductive materials for fin material.

Hellstrom et al. [31] examined the influence of geometrical changes of absorber plate on performance of SFPC. They also studied the effect of thermal and optical properties of collector materials on collector performance. They reported that, thermal efficiency of SFPC can be improved by 12.1 % by introducing honeycomb structure on the absorber plate. They also suggested that, the collector efficiency can be further improved by using high thermal conductive material for honeycomb structure and also, using optically polished glass, which would act as transparent to short waves and opaque to long waves. Hence, potent green house effect is created.

Kalogirou [32] carried out a comprehensive study on solar collectors and reported the progress of research on solar thermal collectors. He suggested few passive techniques like changing of geometry of collector, introducing internal inserts, modifying the absorber plate structure to improve the SFPC efficiency. He also consolidated the development of SFPCs in a chronological order.

Chen et al. [33] conducted experiments by introducing porous structure on absorbed plate. They concluded that, the enhanced surface area of absorber plate by porous structure would increase the heat transfer coefficient of working fluid that consequently leads to raise the outlet temperature of working fluid. Siddiqui et al. [34] conducted an extensive study on various approaches proposed by the researchers and suggested that, creating turbulence in flowing fluid by introducing different elements is an effective approach to enhance the collector efficiency

than the passive heat transfer enhancement techniques like changing the surface geometry of the absorber plate.

Abdin et al. [1] discussed different modern solar energy collection technologies, and they suggested some efficiency improving techniques such as dimple structure on absorber plate, introducing twisted inserts and using of nanofluids as working fluids. Francia et al. [35] also reported the reduction in heat loss with the insertion of honeycomb structure between absorber plate and glass.

Selmi et al. [36] examined the radiation absorption capabilities of collector with single and multiple glazing structures. They reported that, multiple glazing structure will absorbs more incident radiation by effective green house effect but, the total radiation incident on the top of the collector may not be able to reach the absorber plate due to its lower wavelength, whereas, the single glazing structure will allow more incident radiation on the absorber plate. Tian et al. [37] addressed the influence of collector material properties on collector performance. They suggested, low iron glass for glazing material, which have high transmittivity and hence, allow more incident radiation on to the absorber plate. They also suggested, black painting on absorber plate to improves the absorptivity and reduce the emissivity of plate, that causes to enhance the absorption rate of incident radiation and consequently improves the collector performance.

In recent years, Saedodin et al. [38] experimental studies are conducted by deploying porous metal foam on the absorber plate and reported that the maximum thermal efficiency of SFPC is increased by 18.5% compared to non foamed absorber plate. Nima et al. [39] also studied the effect of metal foam on collector performance, but they placed copper metal foam in the riser tube and noticed that, metal foam riser is more effective to absorb the incident radiation. They reported that, the convective heat transfer coefficient is almost double with 8.2 ℃ reduction in plate temperature.

Raimonda Soloha et al. [40] conducted a case study on Latvia city (European country) at large scale with 20,000 inhabitants living area. They reported approximately 30 to 78 % of heat load required for the residential applications can be collected from the solar radiation, particularly for space heating and water heating requisites.

2.3 Literature addressing nanoparticle synthesis

2.3.1 Synthesis of mono nanoparticles

Thermophysical properties of a nanofluid are strongly influenced by the successful synthesis and stable suspension of nanoparticles in base fluids. Top-down (break down) approach and bottom-up (build up) approaches are the most familiar methods of nanoparticle synthesis [41]. In the top-down approach, external forces are applied on bulk materials to break down into fine particles, whereas, in bottom-up approach, atomic transformation or molecular condensation techniques are used. Detailed classification of various methods to synthesis the mono nanoparticle is given in Fig. 2.1.
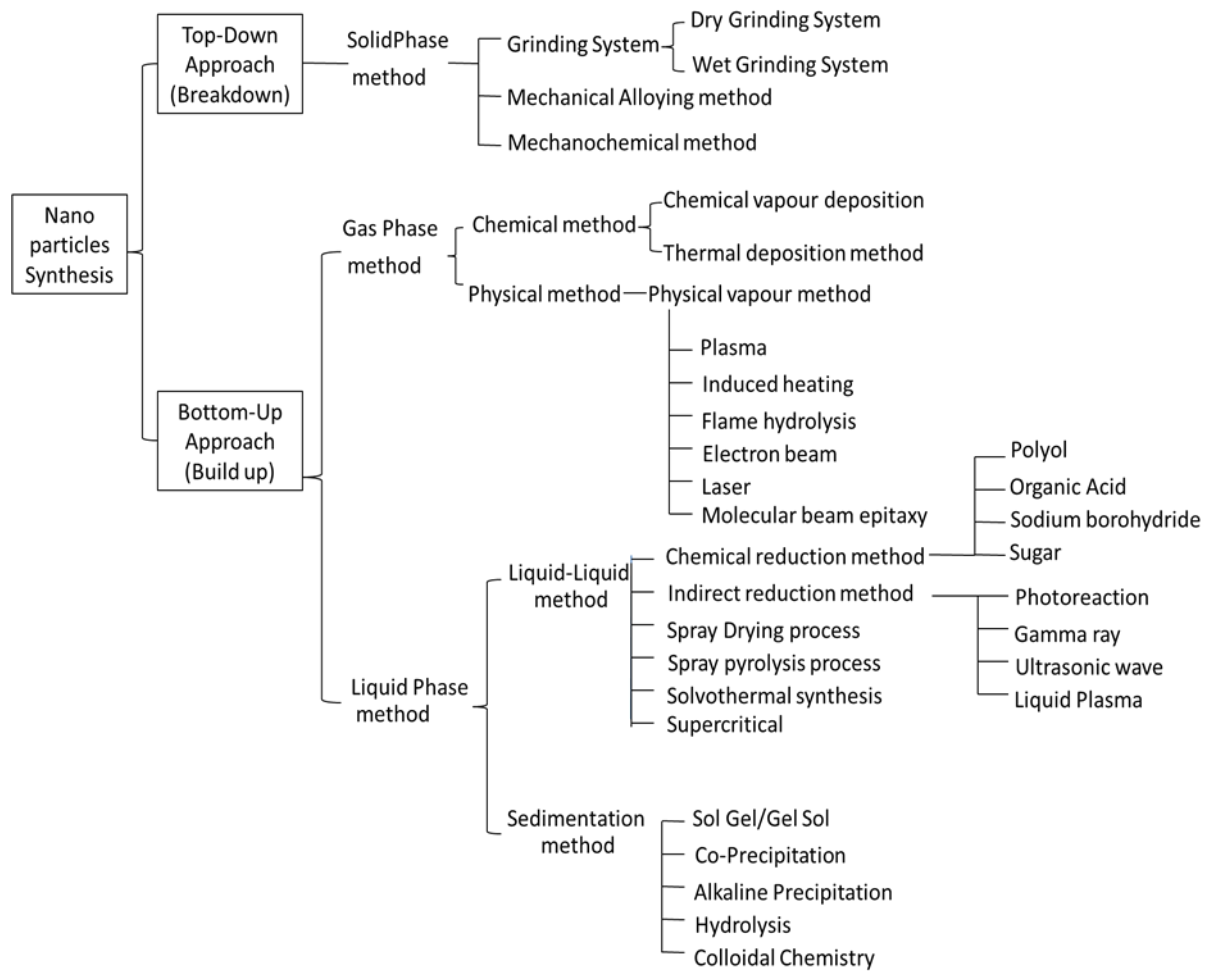
Fig. 2.1 An assortment of mono nanoparticle synthesis methods at a glance [42]

Mono nanoparticles are widely synthesized by either of the approaches mentioned in the earlier section. The top-down approach can be sub-divided into dry grinding [43] and wet grinding [44]. In any grinding process, solid substance breaks into nanoparticles by the applying

mechanical energy in terms of shock, compression or friction. In dry grinding, the process is carried out in the presence of air or gas, whereas, in wet grinding, the process is carried out in the liquid environment. Some of the common dry grinding methods are jet milling [45], hammer milling, shearing milling, roller milling, shock shear milling, ball milling and tumbling milling. Common wet grinding methods are tumbling ball milling, vibratory ball milling [46], planetary ball milling [47], centrifugal fluid milling [48], agitating bead milling, flow conduit bead milling, annular gap bead milling and wet jet milling. It is worth noting that agglomeration of nanoparticles is relatively more with the dry grinding methods as compared to wet grinding methods [49]–[51].

The bottom-up approach is broadly divided into gaseous phase methods and liquid phase methods. Chemical vapour deposition (CVD) [52], [53], Physical vapour deposition (PVD) [53], [54] and thermal decomposition methods [55] fall under gaseous phase methods. CVD and PVD methods can produce nanoparticles ranging from 10 nm to 100 nm, whereas thermal decomposition method can produce 4-18 nm sized nanoparticles. Thermal decomposition method is widely for producing metal oxide particles on a commercial scale. Liquid phase methods are further classified into liquid-liquid method and sedimentation methods. Chemical reduction [56]–[58] of metal ions is an exemplary liquid-liquid method. The principle advantage of this method is that, the particles can be produced in different shapes and sizes by using appropriate reducing agent. Along with these methods, solvo-thermal synthesis [59], spray pyrolysis [60], spray drying are some other typical liquid-liquid methods. While, the sol-gel process is an extensively used sedimentation method, which is used to produce polymer nanoparticles and metal oxide nanoparticles [42]. Detailed classification of mono nanoparticle synthesis methods is given in Fig. 3.1.

2.3.2 Synthesis of hybrid nanoparticles

This section describes the distinct synthesis methods adopted by various researchers to fabricate the hybrid nanoparticles.

2.3.1 Synthesis of Al_2O_3-Cu nanocomposite

Suresh et al. [61] prepared nano crystalline Al_2O_3-Cu hybrid nanocomposite by thermochemical method. In this method, a solution is prepared by mixing copper nitrate $Cu(NO_3)_2.3H_2O$ and aluminum nitrate $Al(NO_3)_3.9H_2O$ with water. The proportions of these precursor salts are chosen based on the proportions of alumina and copper mixture in the nanocomposite. The prepared solution is spray dried at 180 °C to get the Al_2O_3-Cu composite powder. This powder

is heated at 900 °C in the still air for 1 hour to form stable alumina and copper oxide mixture. Then this mixture is heated for 1 hour in a hydrogen atmosphere at 400 °C inside a tubular furnace to reduce CuO to Cu however, the structure of the alumina is remains unchanged during this reducing process. Then this Al_2O_3-Cu nanocomposite is ball milled at 400 rpm to obtain homogeneous Al_2O_3-Cu nanocomposite powder for experimentation.

2.3.2 Synthesis of MWCNT-Fe₃O₄ nanocomposite

Sunder et al. [62] prepared the MWCNT-Fe_3O_4 nanocomposite by in-situ method. In this technique, initially the MWCNTs are carboxylated by dispersing the MWCNTs in mixture of strong hydrochloric and nitric acids (1:3 polar ratios). Then the MWCNTs are washed with acetone followed by distilled water. The compound is then dried at 80 °C over a period of 24 hrs. The carboxylated-MWCNT is dispersed in distilled water and then the blend is mixed with ferric chloride ($Fecl^{3+}$) and ferrous chloride ($Fecl^{2+}$) slats. For uniform dispersion of the iron chlorides, an aqueous sodium hydroxide solution is gradually added until the reaction completed, which is indicated by colour change. Throughout this process, the solution is continuously stirred and the pH value is maintained about 12. Then, the produced MWCNT-Fe_3O_4 nanocomposite is washed with acetone and distilled water thereafter dried for 24 hrs at 80 °C.

2.3.3 Synthesis of Cu-TiO₂ nanocomposite

Madhesh et al. [63] synthesized Cu-TiO_2 hybrid nanocomposite by mechanical milling method. The titania nanoparticles are uniformly dispersed in aqueous solution by ultra-sonication and then copper acetate is added to the mixture. Ascorbic acid and sodium borohydrides are used as reducing agents and continued the sonication for 2 hrs at 45 °C temperature and ambient pressure to produce hybrid nanocomposite. The produced nanocomposite particles are washed with distilled water, followed by vacuum drying.

2.3.4 Synthesis of MWNT-GO nanocomposite

Baby et al. [52] synthesized the MWNT-GO nanocomposite. MWNTs (Multi Walled Nano Tubes) are functionally treated by catalytic chemical vapour deposition (CCVD) technique using hydride catalyst. Graphite Oxide (GO) is prepared by Hummers method. It is a specific method to treat graphene nanoparticles, in which, graphite is treated with H_2SO_4 in an ice bath. Sodium nitrate and $KMnO_4$ are supplemented to this solution at 1:6 ratio to accelerate the reaction, on completion of reaction, the suspension is treated with H_2O_2. Further, the solution is washed with (De Ionized) DI water, followed by oven drying at 40 °C for 8 hrs.

2.3.5 Synthesis of GNP-Ag nanocomposite

Yarmand et al. [64] synthesized GNP-Ag nanoparticles by following the same procedure followed by Sunder et al. [62]. Inherently the Graphene nano platelets (GNP) are hydrophobic in nature, so, they do not dissolve in polar solvents like water. Therefore, these GNPs are treated with a mixture of strong nitric acid and sulphuric acid under bath sonication to transform them into hydrophilic carboxyl functional group platelets. Then, the GNPs are washed with distilled water and oven dried for more than 24 hrs at $70^{o}C$. Separately, the solution of Ag $(NH_3)_2OH$ is prepared by compounding the ammonia at 1 wt.% to 0.01 L of silver nitrate solution and this prepared Ag $(NH_3)_2OH$ solution is blended with pre functionalized GNP in 1:6 molar ratio to get the hybrid nanocomposite. The nanocomposite is collected from the solution by centrifugal action. The obtained nanocomposite is washed with distilled water and oven dried for 4 hrs at $60^{o}C$.

2.3.6 Synthesis of TiO_2-CNT nanocomposite

Megetif et al. [65] produced TiO_2-CNT hybrid nanoparticles by functionally treating CNT's with strong HNO_3-H_2SO_4 at 1:3 v/v for 3 hrs at $70^{o}C$ to transform the CNTs from hydrophobic to hydrophilic. The functionalized CNTs are dispersed in water by sonication. Subsequently 1.5 mL of ethylene glycol and 20 mL of 2-propanol are added to aqua CNTs solution under N_2 atmosphere. 1mL of $Ti(OBu)_4$ is also added to this suspension by drop wise and continued sonication. The resultant precipitate is vacuum filtered and washed with 2-propanol and dried in air at $60^{0}C$ for 12 hrs to obtain CNT-TiO_2 hybrid nanocomposite.

2.3.7 Synthesis of Ag-TiO_2 nanocomposite

Batmunkh et al. [66] prepared Ag-TiO_2 hybrid nanocomposite by mechanical stirring method. Initially TiO_2 nanoparticles suspended in water by ultra-sonication and silver particles are synthesized by Pulse Wire Evaporation method, Ag nanoparticles are grounded using planetary ball mill and then TiO_2 particles are mixed with Ag particles to attain the Ag-TiO_2 nanocomposite.

2.3.8 Synthesis of ϒ-Al_2O_3-MWCNTs

Abbasi et al. [59] made a successive attempt to prepare hybrid ϒ-Al_2O_3-MWCNT nanocomposite by solvo-thermal process. Initially MWCNTs are functionalized by acid treatment[62]. Aluminium acetate powder is dispersed in pure ethanol. The functionalized MWCNTs are suspended in that solution and continued sonication until no visible black agglomerates are noticed. Ammonia solution is added to the mixture to maintain pH above 9 and to obtain a more stable suspension. This solution is kept in vacuum chamber (50 cm Hg)

for 24 hrs. Later, the compound is transferred to teflon lined stainless steel auto clave chamber which is maintained at 200℃ and 16 bar pressure and kept inside for 24 hrs wherein nanocomposite precipitates at the bottom. The precipitate is cooled to room temperature and washed with absolute ethanol till the nanocomposite attains neutral pH. Thereafter, the resultant nanocomposite is vacuum dried at 60℃ for 6 hrs.

2.3.9 Synthesis of Cu/Cu₂O nanocomposite

Nine et al. [47] produced Cu/Cu_2O nanocomposite by wet ball mill method. To make Cu_2O nanoparticles, 99 % pure copper nanoparticles of 200nm size are ball milled under wet condition. Planetary ball mill is used to grind nanocomposite to desired shape and size. 0.5 g Cu particles with 20 ml of DI water are fed to ball mill and it is run for 90 min at 500 rpm by maintaining the temperature below 50 ℃. The synthesized sample is oven dried at 60 ℃.

2.3.10 Synthesis of Ag-MWNT nanocomposite

Chen et al. [67] synthesized Ag-MWNT nanocomposite by ball milling. To functionalize the MWNTs 0.5 g of MWNT and 3.2 g of ammonium bicarbonate are rolled in ball mill for 5 h at 25 rpm. To produce the nanocomposite, 0.2 g of functionalized MWNTs are added with silver nitrate under mild stirring, 0.5 g formaldehyde is used as reducing agent and stirring is continued for 30min at 60℃. the resultant nanocomposite is collected by centrifugation and then washed with pure water and ethanol.

Summary of various synthesis methods adapted by previous researchers is presented in table 2.1.

Table 2.1 Summary of various synthesis methods of hybrid nanoparticles

Reference	Hybrid nanoparticle	Base fluid	Synthesis method
Madhesh et al. [63]	$Cu-TiO_2$	DI Water	Mechanical milling
Sundar et al. [62]	$MWCNT-Fe_3O_4$	Distilled Water	In-Situ and Chemical co-precipitation
Baby et al. [52]	MWNT-GO	DI Water	Catalytic Chemical Vapour Deposition
Yarmand et al. [64]	GNP-Ag	Water	Chemical Vapour Deposition
Batmunkh et al. [66]	$Ag-TiO_2$	Water	Mechanical Stirring
Abbasi et al. [59]	$\Upsilon-Al_2O_3-MWCNT$	Water	Solvo-thermal

Nine et al. [47]	Cu-Cu$_2$O	Water	Wet ball milling
Chen et al. [67]	Ag-MWCNT	Water	Ball milling
Suresh et al. [68], [69]	Al$_2$O$_3$-Cu	Water	Thermo chemical
Li et al. [70]	CNT-SiO$_2$& CNT-SiO$_2$-Ag	Water	Plasma Treatment
Chen et al. [71]	MWCNT-Fe$_3$O$_4$	Water	Ball milling

2.4. Literature addressing the nanofluid preparation

Nanofluid preparation is the pivotal stage that decides the stability and thermophysical properties of a nanofluid. Nanofluid is not a simple binary mixture of liquid-solid. The prepared fluid must possess some essential requirements including durability, being chemically inert, and stable with minimal agglomeration for considerable duration are essential to use nanofluid for real time applications. Two wide spread approaches for the preparation of nanofluids are: one step method and two step methods.

2.4.1 One Step Method

In one-step method, nanoparticle generation and dispersion in base fluid are one ago [18], [72]. This is the most suitable method for high thermal conductive metals to avoid oxidation. High stability and uniform dispersions are the principle advantages of this method. Even rate of agglomeration is relatively much low, producing the high concentration nanofluid at predefined concentration is difficult by this method. In addition, tedious sequence of steps like drying, storing, dispersing of the nanoparticles can be avoided. The major drawback of this method is, nanofluids cannot be produced at commercial scale and also it is not a cost effective approach for the production of nanofluids at large scale.

2.4.2 Two Step Method

In the two-step method, nanoparticles are separately synthesized and suspended in base fluid independently, with assistance of mechanical aids at desired concentration [8], [73]. The primary advantage of this method is that the thermophysical properties can be controlled comparatively in a better way than single step method. The notable interest with this method is the nanoparticles can be produced economically on a large scale. However, the prime intricacy is the unavoidable agglomeration by virtue of cohesive and Vander Waal forces among the

nanoparticles. This agglomeration can be fairly controlled by employing appropriate surfactant or dispersant at critical micelle concentration. The agglomeration can also be minimized by using appropriate mechanical dispersing devices like ultrasonic bath, magnetic stirrer, high-pressure homogenizer and ultrasonic disrupter.

Both, mono and hybrid nanofluids can be prepared by the two step method. The typical approach to prepare hybrid nanofluid is, either by simultaneously dispersing the individual constituents of nanoparticles or by dispersing the synthesized nanocomposite in a base fluid at a predefined proportion. To attain the homogeneous and stable dispersion sonication can be adapted. By blending an appropriate surfactant in the base fluid agglomeration can be further suppressed.

2.5 Literature addressing stability of nanofluids

Stability of nanofluid is a key parameter for the consistent functioning of a thermal system at designed capacity. Therefore, preparation of stable nanofluid for a considerable duration is a technical difficulty to the researchers. The possible reason for agglomeration of nanofluids is, strong Vander Waal forces and cohesive forces among the nanoparticles. These forces may be the root cause for agglomeration. The agglomerated nanofluid loses its potential to transfer heat by diminishing the Brownian motion of particles. It also deteriorates the flow behaviour by amplifying frictional resistance and consequently increases the pressure drop. Therefore, stable suspension of the nanoparticles is essential to get desired properties.

Underlying principles for the stable suspension of nanoparticles are (1) Diffusion Principle: nanoparticles are scattered by fluid medium and hence dispersed into it by electric double layer repulsion. (2) Zeta Potential Principle: the absolute zeta potential value of the nanofluid must be more to the extent possible. As the zeta potential diverges from the iso-electric point, strong repulsive forces will develops among particles and reduces the agglomeration. Teng et al. [74] observed Al_2O_3/water nanofluid is stable and gave good thermal conductivity by maintaining the pH value 8. Suresh et al. [69] produced stable Al_2O_3-Cu/ water hybrid nanofluid by maintaining the pH value 6.

Typical instruments that are used to check the relative stability are sedimentation photographs, zeta potential test, centrifugation, UV-Vis spectrophotometer, SEM (Scanning Electron Microscope), light scattering, and TEM (Transmission Electron Microscope).

From the literature, it is found that, a number of effective strategies were developed to minimize the agglomeration. The most common methods are (i) adding surfactant (ii) electrostatic stabilization by controlling the pH value and (iii) ultrasonic vibration. However, the method of adding a suitable surfactant is widely employed by the researchers in the preparation of a stable nanofluid.

2.5.1   Surfactant addition

Surfactant is a surface-active agent, which creates electrostatic repulsion among the nanoparticles in the base fluid to compensate Vander Wall attractions [75]. It enriches the affinity between the nanoparticles and base fluid. These surfactants are the complex chemical compounds, which lower interfacial tension between base fluid and suspended nanoparticles. In addition, they help to stabilize the suspension by increasing the electric double layer repulsion between nanoparticles (one layer is formed on the surface of particles by the corresponding ions within the crystal lattice and second diffusion layer is formed on the base fluid. When these double-layered particles come closer repulsive forces develop and thereby diminish the agglomeration). Surfactants chemically convert nanoparticles from hydrophobic to hydrophilic and vice versa, based on the type of host fluid and nanocomposite/nanoparticle. On the other hand, surfactant can also increase the zeta potential of nanofluid, which magnifies the surface charge of dispersed nanoparticles in the host fluid [76], [77]. The conventionally used surfactants are Sodium Dodecyl Benzene Sulfonate (SDBS) [78], [79], Sodium Dodecyl Sulphate (SDS) [76], [80], [81], Cetyl Trimethyl Ammonium Bromide (CTAB) [82], Dodecyle Trimethyl Ammonium Bromide (DTAB) [83], Hexa decetyl trimethyl ammonium bromide (HCTAB), Salt and OlicAcid [84], [85] Sodium Octonate (SOCT) [83], Poly Vinyl Pyrolidone (PVP) [86], [87], Gum Arabic [88] and Octylsilane [89]. To obtain favorable results, selection of appropriate surfactant should be made in conjunction with the combination of nanoparticles and base fluid.

2.5.2   Electrostatic stabilization

The stability of nanofluid is directly related to the electro kinetic properties of nanoparticles. An electric charge exists in the atoms in the outer most orbital. This charge is the root cause of kinetic behaviour of nanoparticles in base fluids. In Electrostatic stabilization, stable suspension can be attained by forming an electric static double layer by the ions of particles and host fluid. The diffusion layer is initiated at the iso-electric point at which zeta potential is zero. As the pH

values of solution move away from this iso-electric point, these repulsive force increases and hence stability of nanofluid improves. This electrostatic stabilization method is pH sensitive [61].

2.5.3 Ultrasonic Vibration

It is a typical nanofluid stabilization inducing method. It is an effective method for homogeneous dispersion of nanoparticles and breaking the agglomeration. Many researchers are use this technique, because of its simple and easiness. The key principle of this technique is the nanoparticles are continuously subjected to high frequency vibrations and particles are uniformly dispersed in the base fluid. It is to be noted that the surface properties of suspended nanoparticles are not changed like in other methods. The optimized duration of sonication depends on the size, type and concentration of nanoparticles. Ultrasonic bath, ultrasonic vibrator and homogenizers are the most common devices to impart ultrasonic vibrations.

The stability of the nanofluid can be measured by the sedimentation rate in terms of particle velocity in host fluid. According to Stoke's law [90] speed of nano particle sedimentation can be decreased by decreasing the nanoparticle size (R), increasing host fluid viscosity (μ), and decreasing the density gradient between the nanoparticle and host fluid $\left(\rho_{np} - \rho_{bf}\right)$. Among all the parameters, the most significant parameter is R. From the theory of colloid chemistry, the sedimentation is zero due to Brownian motion of nanoparticle, if the particle size reaches the critical size (R_c) [91]. One can estimate the critical size of nanoparticle/nanocomposite using the equation (1).

$$V = \frac{2R^2}{9\mu}\left(\rho_{np} - \rho_{bf}\right) \tag{3.1}$$

From the equation of sedimentation velocity, stability of nanofluid can increase by reducing the size of nanoparticle, reducing the density difference between nanoparticle and base fluid and increasing the viscosity of base fluid.

2.6 Literature addressing nanofluids - Heat Transfer

Nanofluids are relatively new class of heat transfer fluids spread over all fields of technology and engineering due to their prevalent properties. Higher thermal conductivity of nanofluids attracts and encourages the researchers to use them in many technological applications. The other pivotal thermophysical property is viscosity which defines the hydrodynamic behaviour

of a fluid. Both thermal conductivity and viscosity are increasing with the particle concentration. Along with particle concentration other considerable parameters influences the thermophysical properties of nanofluid are such as temperature, size of particle, properties of base fluid etc. Suspension of solid particles in fluids to promote their thermal properties is not a new idea. Maxwell et al. [6] dispersed solid particles in liquid medium to enhance the thermal conductivity of the working fluid and developed a correlation to estimate the thermal conductivity of particle suspended fluid. Hamilton Crosser et al. [7] extended the Maxwell research and modified the Maxwell thermal conductivity correlation for more precise prediction. But both [6], [7] in their research they suspended micro-size particles in flowing fluids.

Capability to produce nano sized solid particle with the advanced material technology create a new platform for the new class and innovative heat transfer fluids. First time Choi et al. [92] addressed the phenomenon of suspending nano sized solid particles in base fluid to augment its thermal and flow properties and entitled those fluid as nanofluid.

Wen and Ding [93] conducted experiments with Al_2O_3/water nanofluid in a test tube and reported 47 % augment in heat transfer coefficient with at 1.6 vol. %. In their extended work Ding et al. [20] used CNT/water nanofluid as working fluid in horizontal tube and reported 350 % enhancement in heat transfer coefficient at Reynolds number of 800 with 0.5 wt.%.

Philip et al. [94] reviewed and summarized the research progress on nanofluids preparation, stability, thermal and rheological characteristics of alumina (Al_2O_3) nanofluids. While Fotukian et al. [95] reported 25 % heat transfer enhancement at 0.24 vol. % of CuO/water nanofluid with 20 % penalty of pressure drop.

Ahammed et al. [96] experimentally examined the viscosity and surface tension of graphene-water nanofluid at different concentrations and temperatures. They reported that viscosity of nanofluid following the incremental trend with the particle concentration and following inverse trend with the temperature, while surface tension is decreasing with both particle concentration and temperature as well. At 1.5 % particle concentration and 50 ^{o}C viscosity of nanofluid augmented by 47.12 % while surface tension is reduced by 18.7% for same concentration and temperature.

Ramanujam et al. [97] conducted experiments to study the influence of base fluid properties on enhancement of thermal conductivity of nanofluid. For their study, they considered toluene,

xylene, mesitylene, and kerosene as base fluids and magnetic nanoparticle coated with oleic acid as suspended particles. They observed that, the base fluid having lower thermal conductivity will exhibits the maximum thermal conductivity enhancement. They also noticed that, below certain limit of particle concentration, there is no considerable improvement in thermal properties and that concentration is termed as critical concentration. The critical concentration is different for different base fluids and among all the considered working fluids kerosene exhibits the lower critical concentration and higher thermal conductivity enhancement than other working fluids. They mentioned that, the base fluid and nanoparticle interactions at the interface is a critical parameter which will directly influences the stability and thermophysical properties of a nanofluid. If the particle concentration is above the critical concentration, nano clusters may form due to Van der Waals interactions and contributed for the enhancement of thermal conductivity.

Ghasemi et al. [98] experimentally evaluated the performance of circular heat sink with Al_2O_3/water nanofluid at different flow rates and particle concentrations. They reported that, Nusselt number and consequent heat transfer coefficients are also increasing volume flow rate the heat sink, but the pumping power also proportionally increasing with flow rate whereas the friction factor is decreasing with the flow rate.

Ilyas et al. [99] experimentally investigated the stability and thermophysical properties of MWCNT/thermal-oil nanofluid up to 1.0 % concentration. To conduct the experiments, the MWCNTS are neither functionally treated nor surfactant is used to prepare the stable nanofluid. At 1.0 % particle concentration, viscosity and thermal conductivities are augmented by 76 % and 33.6 % respectively than that of thermal oil. Since, there is a considerable variation between the empirical and experimental results they proposed new correlations for both thermal conductivity and viscosity of nanofluids.

Ueki et al. [100] experimentally studied the thermal conductivity and specific heat of water based nanofluids. They conducted experiments on two water based nanofluids, which are prepared from soot Carbon Black (CB) and Carbon Nano Powder (CNP). In their work, CB particles are synthesized by the combustion process, while CNP are purchased from vendor. It is clear from their experimental results that, the nanoparticle shape and nanofluid temperatures had more influence on enhancement of thermal conductivity. The effective thermal conductivity of CB and CNP are augmented by 7 % and 19 % at the particle concentration of 1.5 %. They mentioned that, the fine soot CB particles can be produced either by thermal

decomposition or by incomplete combustion of hydrocarbons at commercial scale relatively at low cost, which is the prime motto of their experimental work.

2.7   Literature addressing hybrid nanofluids - Heat Transfer

As mentioned earlier, all favourable characteristics for a specific application may not possible with the dispersion of single type of nanoparticle (mono nanofluids). The mono nanofluid may possess either good thermal network or better rheological properties. It opens a new arena for hybrid nanofluids. In the recent past, hybrid nanofluids are becoming the cutting edge heat transfer fluids for diversified and conceivable technical applications. The desired and expected characteristics can be obtained only with appropriate combination of individual constituents. The synergistic effect of individual constituent particles of hybrid nanofluid may possess higher thermal and hydrodynamic properties than the nanofluid prepared from the individual constituent nanoparticles.

Suresh et al. [61] conducted experiments with Al_2O_3-Cu/DI water hybrid nanofluid and reported Nusselt number is increased by 13.56 % at 1730 Reynolds number, but the friction factor is increased by 16.97 % when compared to water. Baby et al. [101] synthesized Ag-HEG nanocomposite and tested with water as base fluid. They reported 25 % enhancement in thermal conductivity of hybrid nanofluid compared to water. In their extended work, they conducted experiments with MWNT-HEG/water hybrid nanofluid at the particle concentrations of 0.005 % and 0.05 % and reported that, thermal conductivity of hybrid nanofluid is enhanced by 9 % and 20 % respectively [52]. In the another work, Baby et al. [52] conducted experiments with MWNT-HEG/EG and they reported that thermal conductivity and heat transfer coefficients are enhanced by 20 % and 294 % respectively compared to base fluid at the volume concentration of 0.01 %.

Munkhbayar et al. [102] examined the thermal conductivity of Ag-MWCNT/water hybrid nanofluid and obtained 14.5 % enhancement compared to base fluid. Chen et al. [103] reported 28 % enhancement in thermal conductivity with MWCNT-Fe_2O_3/water hybrid nanofluid. Syam et al. [62] conducted experiments with MWCNT-Fe_3O_4/water hybrid nanofluids and reported that Nusselt number is enhanced by 31.10 % with the penalty of 1.86 % pumping power.

Abbasi et al. [59] examined the TCE of Υ-Al_2O_3-MWCNT/water hybrid nanofluid at the particle concentration of 0.1 % and reported 20.68 % enhancement compared to water.

Madhesh et al. [63] investigated the convective heat transfer coefficient, overall heat transfer coefficient and Nusselt number enhancements with Cu-TiO$_2$/water nanofluid are reported as 52 %, 68 % and 49 % respectively at the concentration of 1.0 % but at the cost of 1.7 % friction factor and 14.9 % pressure drop. Megetif et al. [65] estimated the convective heat transfer coefficient of CNT-TiO$_2$/water hybrid nanofluid at 0.2 wt % concentration and reported 38 % increment compared to base fluid. Yarmand et al. [64] conducted experiments on Graphene-Ag/water hybrid nanofluid to evaluate the heat transfer coefficient enhancement. From their outcomes, 32.7% increment in Nusselt number with the penalty of increment in the friction factor by 1.08 times.

Motahari et al. [104] experimentally estimated the dynamic viscosity of MWCNT-SiO$_2$/Engine Oil hybrid nanofluid as function of particle concentration and temperature. They reported that at 4 % particle concentration hybrid nanofluid exhibits 171 % enhancement in viscosity. They stated that, the available empirical models are not able to precisely predict the dynamic viscosity of hybrid nanofluid. Therefore, they proposed a new correlation to estimate dynamic viscosity of hybrid nanofluid at closer approximation.

2.8   Literature addressing solar collectors with ethylene glycol based nanofluids

In recent days, researchers are investigating the influence of ethylene glycol and its mixture with water as base fluids to prepare the nanofluids. Influence of nanoparticle suspensions in such base fluids are discussed in this section.

Li et al. [105] experimentally examined thermophysical properties of ethylene glycol based ZnO nanofluid. They reported that thermal conductivity of nanofluid is increasing with particle concentration and mass fraction and viscosity of nanofluid is increasing with particle concentration and diminishing with temperature.

Soltani et al. [106] conducted experimental studies on viscosity of MgO-MWCNT/Ethylene glycol nanofluid and reported that the viscosity of hybrid nanofluid is increased by 168 % at 1 % particle concentration.

Delfani et al. [107] carried out experimental studies on direct absorption solar collector using MWCNT with water ethylene glycol mixture at 70 % , 30 % and reported that direct absorption collector with nanofluid exhibits 10-29 % higher collector efficiency compared to based fluid

Karami et al. [108] studied the influence of CuO/water+EG in direct absorption solar collector. They reported that thermal conductivity of nanofluid is increased by 13.7 % and suspension of nanoparticle improves the energy absorbed fraction by 4 times than that of base fluid.

Zamzamian et al. [109] investigated the performance of solar flat plate collector using Cu/EG nanofluid and they reported that collector efficiency is increased up to 81 % at 0.3 wt. % nanoparticle suspensions.

Meibodi et al. [110] conducted experimental studies on SiO_2/EG nanofluid at different particle concentrations and mass flow rates. They reported that collector efficiency is increasing with particle concentration and mass flow rate as well. They noticed that collector efficiency is maximum enhanced by 4 % compared to base fluid at 1 % particle concentration.

Karami et al. [111] investigated the performance of direct absorption collectors with the suspension of CuO nanoparticles in ethylene glycol and water mixture at 70 % and 30 %. They reported that by using nanofluid, collector efficiency is improved by 9 – 17 %.

Kaya et al. [112] experimentally investigated the influence of ZnO nanoparticle suspensions in EG and water (50% - 50%) in evaluated U- tube solar collectors at different particle concentrations. They reported that collector efficiency is raised up to 62.87 % with the nanofluid, which is 26.42 % higher than that of base fluid.

2.9   Literature addressing forced circulation solar thermal collectors

Many researchers were investigated, the influence of nanoparticle suspensions in working fluid of solar collector to enhance its thermal efficiency. Few notable works are presented in this section.

Yousefi et al. [24] experimentally investigated the effect Al_2O_3/water nanofluid on the efficiency of SFPC and reported that instantaneous efficiency is improved by 28.3 % compared water. They mentioned that, while estimating instantaneous efficiency, heat removal factor for both nanofluid and water are closer to each other, but the absorbed energy parameter for the nanofluid is 28.3 % more than water at 0.2 wt % particle concentration that leads to enhance the thermal efficiency of the collector. In their extended work, Yousefi et al. [113] conducted experiments with MWCNT/water nanofluid at different concentrations, and reported that thermal efficiency of SFPC increases with the particle concentration. They also determined the optimum pH value of MWCNT/water nanofluid for maximising the efficiency of SFPCs. The

results reveal that, as pH value of nanofluid diverges positively or negatively from the iso-electric point, the charge of particles increases thus reduces agglomeration and consequently improve the performance.

Chaji et al. [114] run the experiments on SFPC with TiO_2/water nanofluid as working fluid and obtain 7 % enhancement in its performance compared to water. Tiwari et al. [115] estimated the efficiency of with Al_2O_3/water nanofluid based SFPC operating at different mass flow rates and volume fractions. They reported that, with the use of nanofluid collector efficiency was enhanced by 31.64 % at 2 LPM and 1.5 % volume fraction.

Abad et al. [116] investigated the performance of Cu/water nanofluid based SFPC at different volume fractions of 0.05 % to 0.1 % and reported that the instantaneous efficiency of SFPC was enhanced by 24 % compared to water. Kabeel et al. [117] estimated the thermal efficiency of SFPC operating Cu/water nanofluid and reported 17.5 % improvement at 5 % particle concentration.

Ali et al. [26] examined the performance of SFPC with CuO/water nanofluid as working fluid and attained 16.7 % improvement in thermal efficiency at 0.4 % volume fraction.

Vincely et al. [118] conducted experiments on Graphene Oxide/water nanofluid based SFPC at different particle concentrations of 0.5 %, 1 % and 2 % and experiments are conducted in laminar regime. They reported that, higher convective heat transfer coefficient and collector efficiencies of 11.5 % and 7.3 % respectively are obtained at 2 % concentration and 1 LPM flow rate. Meibodi et al. [119] experimentally examined the performance of SFPC with SiO_2-EG/water nanofluid at different volume fractions. The efficiency of SFPC is increasing with particle concentration and attained maximum enhancement of 8 % at 1 vol. % of nanoparticle concentration compared to water. Therefore, it is recommended to use lower concentration to attain more stable nanofluid and to minimize the operating cost.

Sint et al. [120] examined instantaneous efficiency of SFPC with CuO/water nanofluid up to 2 % particle concentration. They reported that, the collector performance was improved by 5 % compared to water at higher particle concentration. Jouybari et al. [38] experimentally observed the performance of metallic porous foam filled on the absorber plate of SFPC and SiO_2/water nanofluid was used as working fluid at the particle concentrations of 0.2 %, 0.4 %, and 0.6 % and they reported 8.1 % enhancement in SFPC performance. It is observed from their experimental results that, collector instantaneous efficiency is increasing with mass flow rate

and heat loss parameters are linearly decreasing. They also noticed that, by increasing the particle concentration collector instantaneous efficiency heat losses are also increased.

In case of direct absorption solar collectors, fluid medium will directly absorb the incident solar radiation and possess promising enhancement in collector efficiency than surface collectors. This is due to the reduced temperature difference between absorber plate and bulk fluid by the direct contact of working fluid, which subsequently causes to reduce the convective and radiative losses as well. Suspension of nanoparticles in base fluid will augment the optical and radiative properties along with the thermophysical properties of working fluid that enhance the absorption capability of working fluid for a wide range of wavelengths. The considerable refinement in base fluid properties encourages the researchers to use them for cultivating the solar energy. It is noticed from the experimental outcomes that the suspension of nanoparticles increasing the range of band width of solar spectrum. Particularly, metallic nanoparticles have superior solar radiation absorption due to Plasmon resonance effect in the visible and near IR region of solar spectrum.

Auffan et al. [121] carried out a brief study on nanoparticle suspension for solar thermal applications and he noticed few points. Such as, the properties of material at nano scale are different from the bulk materials, at the nano scale its surface to volume ratio is abnormally increased and hence more atoms are available at the surface of material which results for high specific surface energy and the particles becomes thermodynamically unstable and become a good carrier of energy which leads to absorb more incident solar radiation.

Tyagi et al. [122] investigated the performance of Al_2O_3/water based Direct Absorption Collector (DAC) at different particle concentrations and flow rates. They reported that, at lower concentrations collector efficiency is gradually increasing with particle concentration and it is maximum improved by 9 % at particle concentration of 2 %, if the concentration is beyond 2 % performance is nearly constant. They also stated that the collector instantaneous efficiency is gradually enhanced by reducing the particle size.

Saidur et al. [123] studied the effect of Al_2O_3 nanoparticles suspension in water for direct solar absorption system. Pure water is transparent at visible wave length and has higher solar radiation absorption ability at longer wave lengths of above 2000 nm however, by suspending the Al_2O_3 nanoparticles, the nanofluid exhibits stronger extinction coefficient at shorter wavelengths of 300 nm and enhances absorption capability at visible wavelengths as well. They

reported that the nanoparticle size has nominal impact on extinction coefficient while the particle concentration plays intuitively a vital role to enhance the absorption capabilities of nanofluid and this improvement is promising within 1% particle concentration. Luca et al. [124] investigated the scattering and absorption properties of nanofluids in aqueous and glycol suspensions. They observed that, the influence of scattering is negligible at lower concentration and as the particle concentration increases radiative losses from the collector could be declined and causes for more solar radiation absorption.

Ladjevardi et al. [125] experimentally examined the solar radiation absorption with silver nanoparticles and reported 22 % improvement in incident radiation absorption with Ag/water nanofluid. In contemporary, He et al. [126] analytically estimated the optical properties of Cu/water nanofluid and compared with the experimental measurements. They reported that transmittance of working fluid is reduced with the increasing particle size and particle concentration while the optical absorption is increased with the particle concentration. The enhanced absorption capabilities of nanofluid causes for higher outlet temperatures of working fluid, which is the primary objective of solar water heater.

Gorji et al. [127] examined the stability and radiative properties of CNT/water nanofluid for direct absorption. They reported that, the functionally treated CNTs are able to surmount their inherent hydrophobic nature and stable for longer periods. Suspension of CNTs in base fluids will exceptionally ameliorate its thermophysical and optical properties. They reported that, the prepared nanofluid is stable for more than 90 days and exhibits stable radiative properties under direct radiation.

Karami et al. [107] experimentally investigated the performance of DAC with CuO nanoparticle suspensions in water-EG at 70:30 proportions. Experiments are conducted with and without black coating on absorber plate at different mass flow rates. They reported that the collector exhibits higher thermal efficiency at higher mass flow rates and also mentioned that black coated collector with particle suspensions give 11.4 % higher thermal efficiency than non coated collector operated with base fluid.

Gupta et al. [128] conducted experiments on DAC with $Al_2O_3–H_2O$ nanofluid at 0.005 % particle concentration and 1.5 LPM, 2 LPM, 2.5 LPM mass flow rates. They observed that, the instantaneous efficiency of collector is augmented with the nanofluid, at all flow rates when

compared to base fluid and this enhancement is relatively more at the higher mass flow rates. They reported 8.1 % improvement in collector efficiency 2.5 LPM.

Khosrojerdi et al. [129] conducted experiments with GO/Water nanofluid in DAC and reported that, with the refined thermo-physical and optical properties of nanofluid leads to absorb more incident solar radiation and causes to obtain higher instantaneous efficiency . Ramsatish et al. [130] analytically estimated the thermal and optical properties and corresponding efficiency of DAC with gray and non gray fluids (graphite and copper sulphate suspensions in respectively) and compared the analytical solutions with the experimental results. They reported that the improved absorption characteristics and reduced heat loss of gray fluid improves the collector efficiency up to 28 % compared to water.

Chen et al. [131] investigated the thermo-physical and optical properties of SiC/ionic nanofluid for DASC and reported 5.2 % improvement in instantaneous efficiency at 0.03 wt.% compared to water.

Water, Ethylene glycol are the common SFPC working fluids for various engineering applications. The lower thermal conductivity of working fluid causes for lower heat transfer rate in many thermal applications. Therefore, by adapting high thermal conductive working fluids in solar collectors, that will enhance the performance and miniaturise the collector dimensions as well. By suspending the high thermal conductive ultrafine solid particles in the collector fluid will promotes the heat transfer properties and consequent thermal efficiency of the solar collector. In recent years, many researchers choosing nanofluid is as a unanimous option to improve the performance of SFPC. Many investigations are carried out on thermophysical properties of nanofluid and their influence on collector performance both analytically and experimentally. Nanofluids exhibit higher convective heat transfer coefficients than the base fluid due to reduced heat capacities and enhanced conduction currents. For the desired exit temperatures, effective utilisation of these favourable thermophysical properties is essential.

From the aforementioned open literature, it can be observed that a significant amount of research is being carried out on the usage of mono nanofluids in SFPC to improve its performance. Particularly, the metallic nanofluids have high potential to absorb more solar radiation. The credible reason for this enrichment may be, for the high conductive metals like Cu, Ag, Au the frequency of free electron vibrations at the outer most orbital is closer to the

frequency of visible light wavelength. When such metals are subjected to solar radiation, free electrons in the surface atoms are excited and resonance is created at the interface and this resonance is termed as localised surface plasmonic resonance. This optical phenomenon results, a strong enhancement in both absorbing and scattering properties of nanofluid. This creates a new platform for generating hybrid nanofluids particularly for solar thermal applications. Therefore, by hybridising the metallic nanoparticles with ceramic or metal oxide nanoparticles, the resulting hybrid nanofluids may exhibit the superior thermophysical properties and refined rheological behaviour by accompanied with the ameliorated absorbing characteristics

Xuan et al. [132] studied the effect of plasmon effect on TiO2-Ag/water nanofluid in direct absorption solar collector and identified that TiO2-Ag plasmonic nanoparticle exhibits a strong light absorption due to plasmonic effect. They reported that the temperature rise by the hybrid nanofluid is higher than that of TiO_2 nanofluid for the same intensity of solar radiation.

2.10 Literature addressing natural circulation/passive solar thermal collectors

In natural circulation mode, working fluid will circulates in the collector due to buoyancy. When the collector exposed to incident solar radiation, the radiation fall on the collector is converted into heat and this heat is transformed to the working fluid. By absorbing the heat from the absorber plate, temperature of the working fluid gets raised and that causes to reduce the density of the working fluid. This reduced density gradients creates buoyancy in working fluid and leads to circulation in collector.

Shitzer el al. [133] conducted analytical and experimental studies on SFPC under natural circulation mode with water as working fluid. They reported that analytical approach is approximately 18 % over estimate the experimental outcomes. Zerrouki et al. [134] conducted analytical and experimental evaluation of collector performance and outlet temperatures with parallel tube design. They reported that, most of the experimental and predicted results should have satisfactory qualitative and quantitative agreement, but it is inconsistent with natural circulation/thermosyphon solar collector. In their extended work, Zerrouki et al. [135] experimentally evaluate the thermal performance of a solar water heater with multiple risers, run the experiments under thermosyphon-flow and compared the results with analytical calculations. They observed that higher outlet temperatures are obtained about 1 PM. They also

pose the similar comment, that in natural circulation water heating, analytical approach is overestimating the collector efficiency.

In the recent years, Jung et al. [136] conducted experiments on SFPC in thermosyphon mode and obtained 56.43 % instantaneous efficiency with water. They reported that average tapping water temperature across the day is 55.92 ^{o}C. Koca et al. [137] considered Ag/water nanofluid as working fluid to run the experiments. They experimentally measure the thermophysical properties and performance of SFPC under natural circulation/passive operating mode. They measure thermal conductivity and viscosity at different concentrations of 0.25 % to 1.0 % and over a temperature range of 20 to 50 ^{o}C. They reported that the existing correlations to estimate the viscosity and thermal conductivity of existing correlation in open literature are underestimating at all volume fractions and temperatures. The same nanofluid is used to estimate the performance of SFPC and they reported that the performance is improved by 11 % compared to water.

Saravanan et al. [138] investigated solar water heater performance under thermosyphon mode with twisted tape inserts at different twist ratios. They also conducted experiments with V-trough and plain flat plate collectors and compared the performance. They reported that V-trough collector gives 13.64 % higher thermal performance than that of flat plate collectors due to added solar intensity with trough. The performance is further improved by 19.01% at twist ratio of 3 due potent swirling action in flow field and increased hydraulic flow length.

Ghaderian et al. [139] evaluated the performance of CuO/water nanofluid based solar collector with internal coil operated under natural circulation mode. The analysis carried out with different volume concentrations and flow rates. They reported that, collector gave the maximum enhancement of 14 % in collector efficiency at 0.03% particle concentration compared to water.

Sundar et al. [140] conducted experimental studies on Al_2O_3/water nanofluid based solar collector operated under thermosyphon/passive mode. Twisted tapes are instead in riser tubes to enhance the heat transfer rate. They reported that, by introducing the twisted tapes, the heat transfer coefficient is enhanced by 21 % with plain riser and that of 49.75 % with twisted tape risers compared to water. The enhanced heat transfer coefficient leads to increase the collector efficiency to 58 % and 76 % without and with twisted tapes compared to water.

2.11 Literature addressing exergy analysis of solar thermal collectors

Mahian et al. [141] conducted experimental study on SFPC using Al_2O_3/Water nanofluid as working fluid and evaluated the entropy generation at different volume fractions and particles sizes. They noticed, outlet temperature is increased with the particle concentration while the entropy generation is reduced by increasing the volume fraction and reducing the particle size. They also reported that tube roughness also play role in entropy generation.

Parvin et al. [142] investigate the heat transfer performance and entropy generation using CuO/Water nanofluid and they reported that Nusselt number and entropy generation increases with volume fraction.

Shojaeizadeh et al. [143] investigated the exergy efficiency of SFPC with Al_2O_3/Water with different flow rates and concentrations. They noticed that inlet and ambient conditions are also effect the collector exergy efficiency along with its flow rate and concentration.

Said et al. [144] conducted experiments on SFPC with Al_2O_3/water nanofluid with different particle diameters. They reported that lower size particles will exhibits better thermodynamic behaviour and enhances both energy and exergy efficiencies.

Alim et al. [145] theoretically analyzes heat transfer rate and entropy generation with water based Al_2O_3, CuO, SiO_2, TiO_2 nanofluids in SFPC. They reported that among all the nanofluids, CuO/water nanofluid exhibits higher heat transfer rate while the entropy generation is reduced by 4.34 % compared to water at the cost of 1.58 % pumping power.

2.12 Literature addressing comparison of absorption types (Direct & Indirect) and operating modes (Active & Passive)

Tyagi et al. [122] experimentally examined and compared the performance of direct absorption collectors with SFPC under active mode of operation using Al_2O_3/Water nanofluid. They reported that the instantaneous efficiency of direct absorption collector using nanofluid is improved up to 10 % more than that of SFPC.

Otanicar et al. [146] constructed a nanofluid-based micro solar thermal-collector using Al_2O_3/Water as working fluid. From their experiments they observed that instantaneous efficiency of collector is considerably increasing with increasing of particle volume fraction. However, when the volume fraction increased above certain level (2 %) the efficiency is slightly

decreased. They reported that, the instantaneous efficiency of solar collectors are improved compared to particle-free fluids, and also reported that instantaneous efficiency of direct absorption system is approximately 9 % more than indirect absorption SFPC.

Siddiqui et al. [147] experimentally investigated the performance of SFPC with CuO/water nanofluid in both natural and forced circulation modes and reported that under similar operating conditions and at the same particle concentration forced circulation/active mode gave 6.3 % higher thermal efficiency than natural circulation/passive mode.

Michael et al. [148] experimentally studied the CuO/water based SFPC with Sodium dodecyl benzene sulfonate (SDBS) surfactant and obtained 6.3 % enhancement in thermal efficiency. The instantaneous efficiency of the collector is tested over a day with water and CuO/water nanofluid as working fluids. They experiments are conducted in both natural and forced circulation modes, and observed that, the instantaneous efficiency in natural circulation mode is approximately 8.1 % lower than that of forces circulation mode. In forced circulation mode, higher instantaneous efficiency of 57.98 % is noticed at 0.1% particle concentration that is 52.33% for the water based SFPC under similar operating conditions.

2.13 Conclusions from Literature Review

A thorough review of literature is conducted on various parameters influencing the energy and exergy performance of nanofluid based solar thermal collectors. The total literature is presented in seven segments and each segment is focused on a particular area of research. The review started with the active and passive heat transfer enhancement techniques for geometrical and operating conditions. Then the survey is extended on enhancing the heat transfer properties of working fluid by suspending the nanoparticles (both mono and hybrid) in conventional base fluids. Further it is extended on type absorption system (direct or in-direct) and mode of operation (active or passive). It is noticed that very few studies are available in open literature on the comparison of the performance of SFPCs based on absorption configuration and operating modes.

2.14 Research gap observed from the literature

- Though numerical studies on nanofluid based solar flat plate collectors have been carried out by some researchers in the recent past, experimental studies are relatively scarce.

- Based on thermo-physical and optical properties of nanofluids, choice of nanofluid for different solar collectors is different.

- Few researchers analysed the mono-nanofluids, but analysis of hybrid nanofluids are relatively less.

- Very few studies are made on comparison of absorption modes and operating modes.

2.15 Objectives and scope of the present work

The preceding sections provided an exhaustive summary of the literature pertaining to the problem considered in the current thesis work. The above exercise made it quite clear that a number of avenues are still open in the studies pertaining to nanofluid based solar thermal collectors, in particular use of hybrid nanofluids in solar collectors. It is quite obvious that any solar thermal collector working under real time environment, it is mandatory to consider the type of absorption and mode of operation to calculate convection and radiation losses while conducting energy and exergy studies. There seem to be very few works that comprehensively address all the aspects of absorption and operating modes on thermal efficiency of solar collectors. Not many studies were tried to evolve the use of hybrid nanofluids to improve the absorption spectrum of incident radiation of solar thermal collector and its performance. In view of the above, the present research work has been taken up to make comprehensive analytical and experimental studies on hybrid nanofluids based SFPC's and comparison of results with individual constituents and water, in different absorption types (direct and In-direct) and operating modes (active and passive). The prominent objectives of the work thus taken up include:

- To select appropriate nanofluid to improve the efficiency of solar flat plate collector

- To estimate the influence of thermophysical properties of nanofluids on solar thermal collector performance.

- To accomplish thermodynamic analysis (Energy and Exergy) on different collectors such as flat plate collector and direct absorption collectors.

- To carry out analytical and experimental studies in order to compare the performance of solar flat plate collector using different nanofluids (mono-nanofluid and hybrid nanofluid) and at different operating modes.

2.16 Research approach

In the current research, analytical and experimental investigations are carried out to evaluate the thermal efficiency of SFPC operated at different absorption (in-direct and direct) modes and operating modes (forced and natural convection). Comparative study is conducted among different modes with different working fluids.

1. Selection and preparation of different nanofluids. The nanoparticles and base fluids for the preliminary studies are chosen from the open literature.

2. Thermodynamic analysis is conducted on different working fluids and identified the preliminary nanoparticles.

3. Developed two experimental test rig that is capable for conducting the experiments for all modes of operations with minor peripheral changes and attachments. The test setups are capable to produce the repeatable and reliable results.

4. To choose the appropriate nanoparticle, pilot experimental trails are and conducted with different working fluids and considerable deviation is noticed between analytical and experimental results.

5. Critically analyse the reasons for the deviation, and presumed that fluid transport and thermal transport properties are considerable parameters for this deviation. Thus, viscosity and thermal conductivity of nanofluids are experimentally measured and compared with the analytical solutions. It is noticed that thermal conductivity of nanofluids has relatively less deviation from the experimental out comes whereas, a substantial deviation is noticed in dynamic viscosity and hence, a new correlation is proposed and all other calculations are conducted with the developed correlation.

6. Experiments are conducted in two absorbing configuration of indirect and direct absorption and operating modes of forced and natural circulation.

7. Analysed the effect of nanoparticles on the thermal efficiency of solar collector and noticed considerable enhancement in collector efficiency. Comparative studies are conducted by considering the all possible errors while conducting experiments.

2.17 Closure

A comprehensive review of literature concerning the synthesis and thermophysical properties of mono nanofluids, and hybrid nanofluids are provided. With the exhaustive exploration of literature, various parameters those control the thermal efficiency of SFPCs' are

(i) geometrical & operating conditions (ii) properties of working fluid (iii) type of absorption of incident radiation (indirect or direct) (iv) and mode of operation (active or passive) has been documented in the present chapter. In conclusion to the literature review, the factors that are useful and provide the appropriate information of consideration to the present research problem are provided. The different principal objectives of current research work are provided, which will provides a bird's-eye view on the current thesis. The ensuing chapter is devoted to the present extensive details on estimation of necessary thermophysical properties, using the empirical correlations available in open literature. Thermal conductivity and viscosity of the considered nanofluids are experimental estimated and compared with the empirical correlations. A new viscosity model is developed to precisely estimate the dynamic viscosity of all nanofluids.

Chapter 3

Nanofluid Preparation and Estimation of Thermophysical Properties

3.1   Introduction

Nanoparticle production, homogeneous suspension and producing stable nanofluids are the key issues with the particle suspended fluids. The method of nanoparticle synthesis and its dispersion depends on the type of bulk material and its properties. With updated technology, various synthesis methods are available to produce the nanoparticles at commercial scale. Few of the synthesis methods to produce mono and hybrid nanoparticles are discussed in the chapter 2 literature addressing the synthesis and stability of nanofluids section.

3.2   Nanofluid preparation for the current work:

For the current research, all the nanoparticles (Al_2O_3, Cu, CuO, SiO_2, and TiO_2) of sizes 30-50 nm are purchased from SISCO Research Laboratory Pvt. Ltd India. The size of particles is assumed to be same as quoted by the supplier. Distilled water is taken as the base fluid for nanofluid preparation as well as for conducting experiments for comparison of collector performance. Both mono and hybrid nanofluids are prepared by two step method. Nanoparticles are dispersed in the base fluid using ultra-sonicator (supplied by Electrostatic Industries, India) to brake the agglomerated particles and to obtain stable and homogeneous suspension. Fluid is

subjected to continuous sonication for 2 hrs and the sonicator produced the ultrasonic waves at 180 W. CTAB is used as a surfactant to increase the dispersion stability of nanoparticles in base fluid. Both sonication and surfactant are used to control the agglomeration while preparing stable nanofluid.

Fig 3.1. Preparation of nanofluids by ultrasonic sonicator (i) Al$_2$O$_3$/water nanofluids

(ii) CuO/water (iii) Cu/water

All the nanofluids are prepared at 0.125 % 0.25 %, 0.5 %, 0.75 % and 1 % particle concentrations, which are the suitable particle concentration for solar applications. It is noticed that, all the nanofluids are stable for 36 h at least without any visual settlement. Hybrid nanofluid is prepared at 50%: 50% (Cu-CuO) to conduct experiments.

3.3   Estimation of thermophysical properties of mono nanofluids and hybrid Nanofluid

To precisely measure the performance of a nanofluid based thermal system, accurate information about thermophysical properties of the working fluid is necessary. To evaluate the thermophysical properties of nanofluid analytically the particles are assumed to be uniformly dispersed in host fluid. These properties strongly depend on the quantity of nanoparticles added to base fluid. The weight of the nanoparticles required to prepare the nanofluid for a particular volume fraction can be estimated by using Eq (3.1) [1]

$$\emptyset = \frac{\frac{W_{np}}{\rho_{np}}}{\frac{W_{np}}{\rho_{np}} + \frac{W_{bf}}{\rho_{bf}}} \qquad (3.1)$$

Several researchers from the past decades proposed many correlations to precisely evaluate the effective thermophysical properties of mono nanofluids by considering different constraints such as particle size, base fluid properties, operating temperature so on and these correlations

are well acceptable with the experimental results. Most of the existing correlations for mono nanofluid possess good agreement with the experimental outcomes. However, empirical correlations to estimate the thermophysical properties of hybrid nanofluids are not reported much in open literature so far. A significant amount of experimental work needs to be carried out to develop new correlations to appropriately estimate the thermophysical properties and consequent heat transfer characteristics and flow behaviour of a hybrid nanofluid. It is observed that the classical models used for estimating the properties of mono nanofluid are extended for hybrid nanofluids and these modified correlations are presented in the foregoing sections. Some of the thermophysical properties like density, dynamic viscosity, specific heat, thermal expansion coefficient and thermal conductivity of typical mono nanofluids and hybrid nanofluids are estimated using analytical correlations which are having closer approximations with the experimental results.

In the current research all the nanoparticles of sizes 30-50 nm. Cu, CuO, Al_2O_3, TiO_2 and SiO_2 are initially considered for the analysis to choose suitable nanoparticle for solar thermal applications. The particle concentration for this analysis is 0.125 %, 0.25 %, 0.5 %, 0.75 %, and 1.0 % are chosen based on independent scattering phenomenon to precisely predicts the thermophysical properties and subsequent influence on solar collectors. The properties of nanoparticles are presented in table. 3.1

Table 3.1 Thermophysical properties of various nanoparticles considered for the current research.

Property / Material	Thermal conductivity (W/m K)	Density (kg/m^3)	Specific heat (J/kg K)
Copper (Cu)	400	8900	385
Aluminium Oxide (Al_2O_3)	37	3970	765
Copper Oxide (CuO)	69	6300	551
Titanium Oxide (TiO_2)	8.9	4250	686
Silicon dioxide (SiO_2)	1.4	2220	745

3.3.1 Selection of nanoparticle concentration:

The principle benefit of particle suspensions in base fluid is, to have better control over the properties of nanofluid by particle concentration. Little changes of particle concentration will have greater influence on resultant properties including thermophysical and optical properties. In particular, to refine scattering and extinction coefficients are ameliorated by the suspension of solid particles at nano size. By suspending the nanoparticles in base fluid, a tiny layer formed on nanoparticle and it is participated in absorption of solar radiation [151]. At the higher concentrations, these layers are closer to each other, which results higher convective and radiative losses. In contrary, at the lower concentrations, the fluid layer around the nanoparticles may not absorb incident radiation. Therefore, to absorb maximum possible radiation with minimum losses, precise selection of particle concentration is a key parameter for solar thermal applications. It is noteworthy that, the extinction coefficient of nanofluid is a decisive parameter that defines the absorption capability of solar radiation. To restrict the independent scattering, the particle concentration is limited to less than 1.0 %. Independent scattering is nothing but the scattering of neighbouring particles will not infer with each other [152]. Fig. 3.2 shows the scatter separating regime and particle concentration. The scatter separation line can be estimated by:

$$\frac{c}{\lambda} = \frac{\alpha}{\pi}\left[\frac{0.905}{\phi^{0.333}} - 1\right] > 0.5 \tag{3.2}$$

where, 'c' is the particle spacing, and 'λ' incident light wavelength, and 'α' a non-dimensional particle size parameter that correlates the diameter of nanoparticle and incident light wavelength.
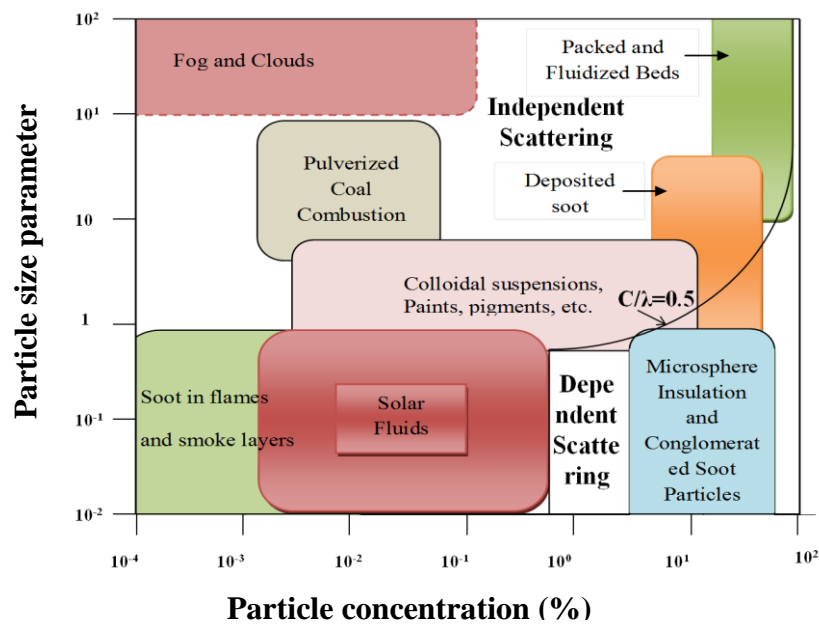
Fig. 3.2 Particle concentration based on the scattering regime

Based on the independent scattering principle, the particle concentration is limited to 1 % in current work. However, which does not mean that scattering is not exist, but the scattering of neighbouring particles does not infer with each other. In view of the fact, that the contribution of scattering coefficient is much low in extinction coefficient due to lower particle concentration, and hence it can be neglected. The details about the estimation and affect of extinction coefficient on the performance of solar collectors are discussed in the thermodynamic analysis of direct absorption collector in the subsequent chapter.

3.4 Estimate the thermophysical Properties of nanofluids - Empirical relations

3.4.1 Density: Density of mono nanofluid is estimated based on the principle of the mixture rule and can be calculated by using Eq (3.4) [149].

$$\rho_{nf} = \left(\frac{m}{V}\right)_{nf} = \frac{m_{bf} + m_{np}}{V_{bf} + V_{np}} = \frac{\rho_{bf} V_{bf} + \rho_{np} V_{np}}{V_{bf} + V_{np}} \tag{3.3}$$

$$\rho_{nf} = \emptyset \rho_{np} + (1 - \emptyset)\rho_{bf} \tag{3.4}$$

By extending the mixture principle, the density of hybrid nanofluid can be estimated by Eq (3.6) and the experimental results of Takabi et al. [153] has good agreement with this correlation

$$\rho_{hnf} = \emptyset_{np1}\rho_{np1} + \emptyset_{np2}\rho_{np2} + (1 - \emptyset_h)\rho_{bf} \tag{3.5}$$

where $\emptyset_h$ is the overall volume fraction of individual nanoparticles suspended in a hybrid nanofluid and it is given by: $\emptyset_h = \emptyset_{np1} + \emptyset_{np2}$

Sundar et al. [62], [154] investigated the density of MWCNT- Fe_3O_4/water and nano-diamond-Fe_3O_4/ water hybrid nanofluids using mixture rule equation (3.5) and achieved good agreement with their experimental results.

3.4.2 Heat Capacity: Heat capacity is a quantitative measure of heat transfer in a SFPC, which governs the amount of heat gain by the SFPC. Specific heat of nanofluid is commensurately decreasing with increment of particle concentration. This reduction in heat capacity leads to increase the outlet temperature of working fluid. The heat capacity of mono nanofluid and hybrid nanofluids can be estimated from the principle of mixture rule by using equations (3.6) and (3.7) respectively [149], [153].

$$C_{p,nf} = (\emptyset \rho_{np} C_{p,np} + (1 - \emptyset)\rho_{bf} C_{p,bf})/\rho_{nf} \tag{3.6}$$

$$C_{p,hnf} = (\emptyset_{np1}\rho_{np1} C_{p,np1} + \emptyset_{np2}\rho_{np2} C_{p,np2} + (1 - \emptyset_h)\rho_{bf} C_{p,bf})/\rho_{hnf} \tag{3.7}$$

The theoretical predictions based on mixture theory for the density and heat capacity of hybrid nanofluid at different volume fractions show good agreement with the experimental outcomes of Ho et al. [155].

The influence of particle concentration on the density and specific heat of various nanofluids at different volume fractions are analytically estimated using Eq 3.4 and Eq 3.6 and described in Fig. 3.3 and Fig. 3.4. It is clear from Fig. 3.3 that the density of all nanofluids is linearly increasing with particle concentration. From Eq (3.2) the properties of nanoparticle material directly influence the density of nanofluid. It can be observed from table 3.1, that the copper material has the higher density, which consequently causes for higher density of Cu/water nanofluid than other nanofluids. Fig. 3.4 elucidates the specific heat of nanofluid as a function of particle concentration. It can be observed from Fig 3.4 that is inversely varying with the particle concentration and it is true for all considered nanofluids. The nanofluid has the lower specific heat, needless quantity of energy to raise unit temperature. The similar results can observe for density as well as the specific heat from many studies [64], [155].
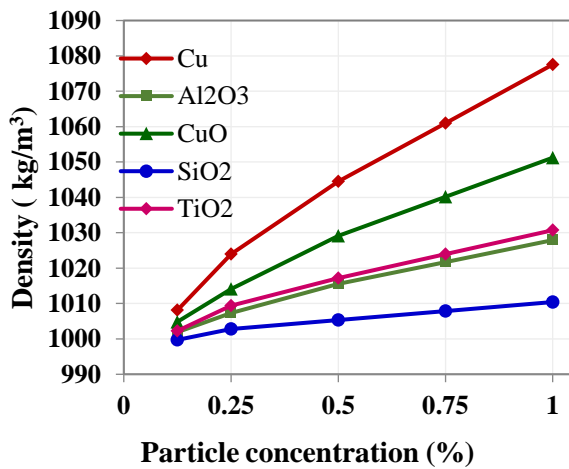
Fig. 3.3 Density variation of different nanofluids at different particle concentration.
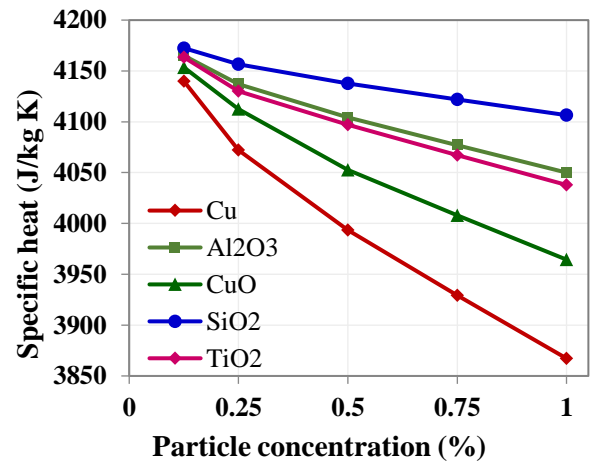
Fig. 3.4 Specific heat variation of different nanofluids at different particle concentration.

The effect of particle concentration on the density and specific heats of hybrid nanofluids at different volume fractions are analytically estimated using Eq 3.5 and Eq 3.7. One can be observed from Fig 3.5 and Fig 3.6 that the hybrid nanofluids are also following the similar trend as mono nanofluids.
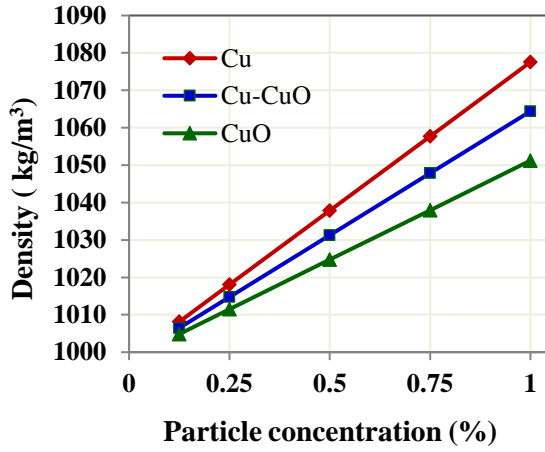
Fig. 3.5 Density variation of mono and hybrid nanofluids at different particle concentration.
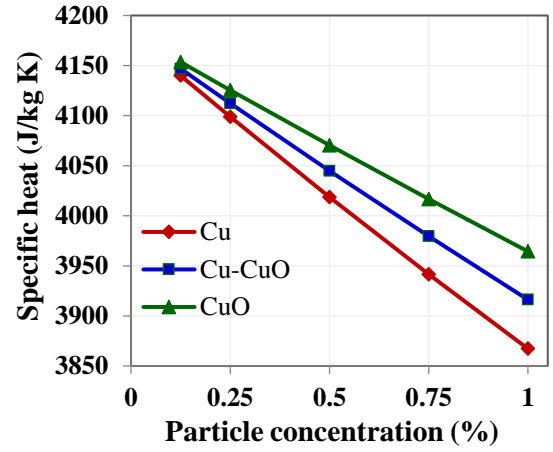
Fig. 3.6 Specific heat variation of mono and hybrid nanofluids at different particle concentration.

3.4.3   Viscosity: In many heat transfer applications, fluid flow properties also play a crucial role in effective thermal management. In a SFPC also, the flow behaviour of a nanofluid is influenced by the dynamic viscosity of the working fluid. Thus, viscosity of nanofluids attains identical priority as thermal conductivity. Plenty of correlations are available in open literature to estimate the dynamic viscosity of nanofluid. Some of the favourable correlations, which will closely predict the dynamic viscosity of nanofluids to the experimental outcomes, are presented in this section. Batchelor, (1977) proposed a correlation to estimate the dynamic viscosity of the nanofluid by considering the Brownian motion as given below:

$$\mu_{nf} = (1 + 2.5\emptyset + 6.2\emptyset^2)\mu_{bf} \tag{3.8}$$

In case of hybrid nanofluids, $\emptyset$ is replaced with $\emptyset_h$.

Nguyen et al. [157] briefly describes the impact of particles size and temperature on the viscosity of a nanofluid. The viscosity of a nanofluid is proportionally increases with size of nanoparticle and reduces with the increase of temperature. The viscosity of nanofluid at different particle sizes can be estimated by:

$$\mu_{nf} = (1.475 - 0.319\emptyset + 0.0512\emptyset^2 + 0.009\emptyset^3)\mu_{bf} \qquad for \ d_p = 29nm \tag{3.9}$$

$$\mu_{nf} = (1 + 0.025\emptyset + 0.015\emptyset^2)\mu_{bf} \qquad for \ d_p = 36nm \tag{3.10}$$

$$\mu_{nf} = (0.904\exp(0.1483\emptyset)\mu_{bf} \qquad for \ d_p = 47nm \tag{3.11}$$

Eq 3.12 gives the influence of temperature on the viscosity of nanofluid, while the Eq 3.13 considers the particle concentration along with the temperature of working fluid [158].

$$\mu_{nf} = (2.1275 - 0.01275T + 0.00027T^2)\mu_{bf} \tag{3.12}$$

$$\mu_{nf} = 4.682 \left(\frac{T_\alpha}{T_{nf}}\right)^{0.00049} \emptyset^{0.1794} \mu_{bf} \tag{3.13}$$

The correlations used to estimate the dynamic viscosity of mono nanofluid can also be employed for hybrid nanofluid by replacing $\emptyset$ with $\emptyset_h$. Hooman et al. [64] estimated the viscosity of GNP-Ag/water hybrid nanofluid with Nguyen et al. [157] correlation and reported close agreement with experimental results.

3.4.4 Thermal conductivity: It is the one of the notable thermophysical property, which governs the heat transfer characteristics of a nanofluid. By suspending the high thermal conductive solid particles in base fluid, net thermal conductivity of the nanofluid enhances due to convection currents between base fluid and solid particles. Many researchers proposed numerous correlations to predict and explain the peculiar enhancement of thermal conductivity by considering various parameters. Maxwell [6] is the pioneer in this area, he proposed a theoretical model to determine the effective thermal conductivity of solid particle suspensions in liquids, which is the base correlation to determine the thermal conductivity of nanofluids till date. This model is effective for homogeneously dispersed the low concentration nanofluids. It is drawing great theoretical and practical attention of many researchers.

$$k_{nf} = k_{bf} \left\{ \frac{[k_{np} + 2k_{bf} - 2\emptyset(k_{bf} - k_{np})]}{[k_{np} + 2k_{bf} + \emptyset(k_{bf} - k_{np})]} \right\} \tag{3.14}$$

Thermal conductivity of hybrid nanofluid can be estimated by modifying the Maxwell model [6]. By extending the principle of mixture rule and is given by

$$k_{hnf} = k_{bf} \left\{ \frac{\left[\frac{k_{np1}\emptyset_{np1} + k_{np2}\emptyset_{np2}}{\emptyset_h} + 2k_{bf} + 2(k_{np1}\emptyset_{np1} + k_{np2}\emptyset_{np2}) - 2\emptyset_h k_{bf}\right]}{\left[\frac{k_{np1}\emptyset_{np1} + k_{np2}\emptyset_{np2}}{\emptyset_h} + 2k_{bf} - (k_{np1}\emptyset_{np1} + k_{np2}\emptyset_{np2}) + \emptyset_h k_{bf}\right]} \right\} \tag{3.15}$$

Bruggemen (1935) proposed a correlation for spherical nanoparticles by considering the influence of nano clusters on the thermal conductivity of nanofluid, and it is given by

$$k_{nf} = \frac{1}{4}(3\emptyset - 1)k_{np} + [(2 - 3\emptyset)k_{bf}] + \frac{k_{bf}}{4}\sqrt{\Delta} \tag{3.16}$$

where, $\Delta = \left[(3\emptyset - 1)^2 \left(\frac{k_{np}}{k_{bf}}\right)^2 + [(2 - 3\emptyset)^2 + 2(2 + 9\emptyset - 9\emptyset^2)]\left(\frac{k_{np}}{k_{bf}}\right)\right]$

For the hybrid nanofluids thermal conductivity can be estimated by extending the Bruggeman (1935) model with the principle of mixture rule as given below

$$k_{hnf} = \frac{1}{4}(3\emptyset_h - 1)\frac{k_{np1}\emptyset_{np1}+k_{np2}\emptyset_{np2}}{\emptyset_h} + \left[(2 - 3\emptyset_h)k_{bf}\right] + \frac{k_{bf}}{4}\sqrt{\Delta} \tag{3.17}$$

$$\text{where, } \Delta = \begin{bmatrix} (3\emptyset_h - 1)^2 \left(\frac{k_{np1}\emptyset_{np1}+k_{np2}\emptyset_{np2}}{\emptyset_h}\right)^2 \left(\frac{1}{k_{bf}}\right)^2 + \\ \begin{bmatrix} (2 - 3\emptyset_h)^2 + \\ 2(2 + 9\emptyset_h - 9\emptyset_h{}^2) \end{bmatrix} \left(\frac{k_{np1}\emptyset_{np1}+k_{np2}\emptyset_{np2}}{\emptyset_h}\right)\left(\frac{1}{k_{bf}}\right) \end{bmatrix}$$

Experimental results of Madesh et al. [63] had good agreement with Eq (3.17).

Koo and Kleinstreuer [160] introduced a new correlation to precisely predict the thermal conductivity of nanofluid by considering both the effects of static and dynamic motion of nanoparticles. In their analysis, Maxwell [6] model is considered as static part where dynamic motion of nanoparticles is ignored, therefore, a Brownian motion term is introduced to account the dynamic motion nanoparticles in base fluid. Maxwell [6] model is considered as static part, while in dynamic part is accountable for the Brownian motion of nanoparticles in the surrounded base fluid.

$$k_{nf} = k_{static} + k_{Brownian} \tag{3.18}$$

$$k_{static} = k_{bf} \left\{ \frac{k_{np}+2k_{bf}+2\emptyset(k_{np}-k_{bf})}{k_{np}+2k_{bf}-\emptyset(k_{np}-k_{bf})} \right\} \tag{3.19}$$

$$k_{Brownian} = 5X10^4 \beta\emptyset\rho_{bf}C_{p,bf}\sqrt{\frac{k_BT}{\rho_{np}d_{np}}}f \tag{3.20}$$

$$k_{nf} = k_{bf} \left\{ \frac{k_{np}+2k_{bf}+2\emptyset(k_{np}-k_{bf})}{k_{np}+2k_{bf}-\emptyset(k_{np}-k_{bf})} \right\} + 5X10^4 \beta\emptyset\rho_{bf}C_{p,bf}\sqrt{\frac{k_BT}{\rho_{np}d_{np}}}f \tag{3.21}$$

where β was introduced for consider the interaction between bulk fluid and nanoparticle, f considered the temperature dependency on thermal conductivity.

$$\beta = 0.0137(100\emptyset)^{-0.8229} \quad \emptyset < 1\% \tag{3.22}$$

$$\beta = 0.0017(100\emptyset)^{-0.0841} \quad \emptyset > 1\% \tag{3.23}$$

$$f = (-134.63 + 1722.3\emptyset) + (0.4075 - 6.04\emptyset)T \tag{3.24}$$

Vast literature is available on the influence of various parameters on thermal conductivity. Summary is given below.

(i) Particle volume fraction: It follows a linear relationship with thermal conductivity [161]

(ii) Particle material: By suspending the nanoparticles in base fluid nanoclusters are formed around the nanoparticle and those causes for the enhancement of thermal conductivity. The size of nanoclusters depends on the type of particle material. The nanoparticles which are capable to form the larger nanoclusters should possess higher thermal conductivity. [155]. Suresh et al.

[118] observed that hybridizing the high conductive nanoparticles with chemically inert particles promotes the effective thermal conductivity of hybrid nanofluid. The enhanced thermal conductivity of hybrid nanofluid may be the driving parameter for improving the heat transfer rate and attain the interest of researchers to use them for many thermal applications [28], [156].

(iii) Base fluid: By suspending the nanoparticles in base fluid, an electronic double layer develops around the nanoparticle and the thickness of the double layer depends on the type of base fluid and suspended particles [162]. The key parameters that affect the thermal conductivity of nanofluid are dynamic viscosity and thermal conductivity of based fluid. Relatively less thermal conductive base fluid will exhibits high thermal conductivity ratio [163]. Whereas, high viscous fluids possess stable nanofluid, but it obstructs the Brownian motion of the nanoparticles as a result, reduces the thermal conductivity of a nanofluid. Still, it needs a systematic experimental work, to establish the impact of base fluid, on thermal conductivity of a nanofluid.

(iv) Particle size: Brownian motion of the nanoparticle is one of the root-cause for the enhanced thermal conductivity of nanofluid. As particle size reduces they moves at a faster rate and hence colloidal motion increases, and improves the energy transport within the liquid medium [164].

(v) Particle shape: Most of the nanoparticles are produced either in spherical or in cylindrical shape. Cylindrical shape particles would exhibits more thermal conductivity than spherical particles. The credible reason maybe, more length of orders of cylindrical particles may enables to promote more heat transfer rate [165].

(vi) Temperature: It will dramatically influence the thermal conductivity of the nanofluid. As the temperature increases the Brownian motion of nanoparticle also increase, and thus, the thermal conductivity of a nanofluid also increases [166]. However, raise in temperature may also affect the size of nanoclusters and electric double layer thickness. Therefore, thermal conductivity of nanofluid follows the decreasing trend at the elevated temperatures [167].

(vii) Acidity of nanofluid: The electrostatic repulsive forces of nanoparticles depend on the pH value of nanofluid. As the pH value of nanofluid moving away from the iso-electric static point, the repulsive forces between the nanoparticles and base fluid is also increases, hence the stability as well as thermal conductivity of a nanofluid increases [61], [168].
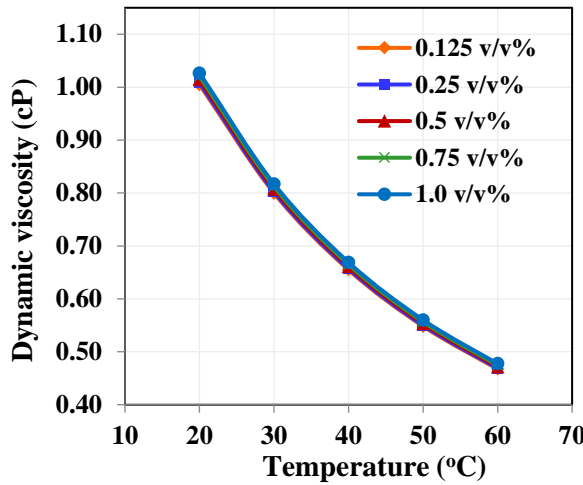
Fig 3.7 Viscosity of nanofluid as a function of particle concentration and temperature
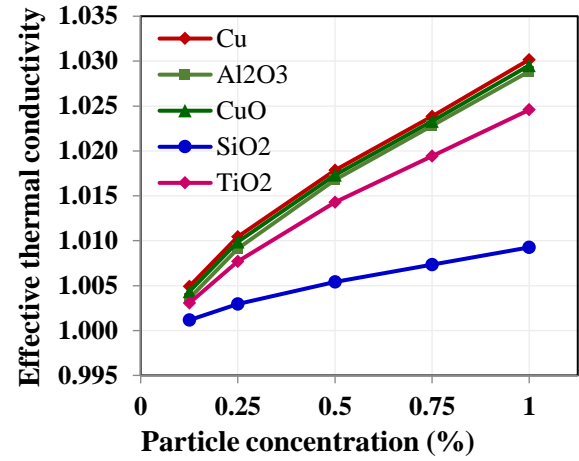
Fig 3.8 Effective thermal conductivities of different nanofluids at different particle concentrations

Viscosity of a nanofluid is gradually decreasing with temperature raise and it is estimated using Eq 3.12. Fig. 3.7 shows the influence of temperature and particle concentration on viscosity of nanofluid. From the most of correlations available in open literature, viscosity is the sole function of particle concentration. Therefore, all the nanofluids exhibit the quantitatively equal variation of viscosity with respect to particle concentration. However, the primary intension of nanofluids development is to use them over a wide range of temperature applications. It is clear from Fig. 3.5 that the viscosity of nanofluid is progressively increasing with particle concentration and declining with the temperature raise and it is true for all nanofluids. Fig. 3.8 shows the enhancement of effective thermal conductivity of nanofluids as a function of particle concentration and it is increasing with the particle concentration. The effective thermal conductivity is nothing but the ratio of thermal conductivity of nanofluid to that of thermal conductivity of base fluid. Thermal conductivity of all considered mono nanofluids are estimated using Eq 3.16. The thermal conductivity of a nanofluid is depends on the properties of the particle material. It can be observed from table 3.1 that the bulk materials of copper and copper oxide have higher thermal conductivity. Therefore, the maximum enhancement of effective thermal conductivity is obtained for Cu/water nanofluid, which is 6.57 % and that of CuO/water nanofluid is 6.43 % compared to water. Similar kind trend in effective thermal conductivity can be observed for hybrid nanofluids as well as shown in Fig. 3.9. Thermal conductivity of the hybrid nanofluid are estimated using Eq 3.17. The most prominent reasons for this improvement are (i) Brownian motion: it is nothing but random

moment of nanoparticles in base fluid. It has been found that the Brownian motion of nanoparticles at molecular and nano scale level is a key mechanism to govern the thermal behaviour of particle suspended fluids. This random motion promotes the collisions between the particles will endorse the micro mixing and localized convection between the particles and base fluid [169], [170]. (ii) Larger specific surface area of particles: the increased specific surface area promotes the more convection currents between nanoparticle and base fluid [73]. (iii) Another possible reason for the amelioration of thermal conductivity is liquid layering: at the liquid/particle interface, a tiny liquid layer is formed around the nanoparticle, which re-orders the ions at the interface and improves local heat transfer rate and thermal conductivity of a nanofluid [171].
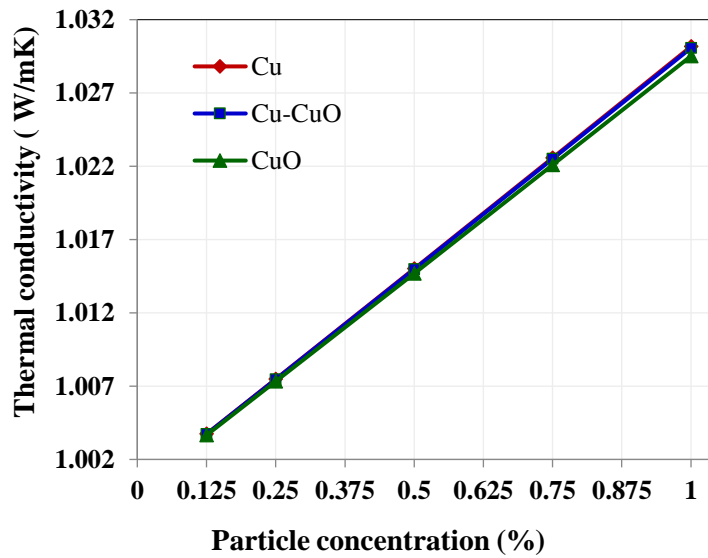
Fig 3.9 Effective thermal conductivities of different nanofluids
at different particle concentrations

3.5   Experimental investigation of thermophysical properties of nanofluids

Among all the thermophysical properties, thermal conductivity and viscosity are two key properties, which govern the heat transfer and flow behaviour of a nanofluid. Many engineering applications demand the trade-off between dynamic viscosity and thermal conductivity of a nanofluid. Enhanced thermal transport properties along with minimal augment of viscosity are the favorable properties for better thermal performance of a SFPC. Both viscosity and thermal conductivity of water and all nanofluids are experimentally measured. Experiments are conducted at different particle concentrations from 0.125% to 1.0% over 20 ºC to 70 ºC temperature range.

3.5.1 Viscosity Measurement:

Dynamic viscosity of water, mono nanofluid and hybrid nanofluids at different particle concentrations and temperatures are measured using Rheolab QC rotational rheometer (Anton Paar supplier, India) as shown in Fig. 3.10. The apparatus is equipped with a peltier temperature controlled thermostatic bath with computer interface to control and measure the rheological behaviour of nanofluid at different temperatures. The apparatus can measure the viscosity over a range of 1 to 10^9 mPa.S and over a temperature range of -20 ^{o}C to 180 ^{o}C. The computer interface facilitates to record the measured data and to vary the temperature of working fluid. For the reliability of measurements, viscosity of distilled water is experimentally measured and compared with the standard data taken from REFPROP tables [172]. The experimental readings have close approximations with standard data with less than 2 % deviation, over the considered range of temperatures. The nanofluid is placed between the concentric cylinders of rheometer. The outer cylinder is rotated by external means, while the inner cylinder remains stationary. When the outer cylinder rotates, the torque is transmitted to inner stationary member through a thin liquid film of nanofluid formed between the cylinders. Based on the speed of rotation, and thickness of fluid film (gap between cylinders), one can measure the viscosity of fluid from its Newtonian behaviour [173].
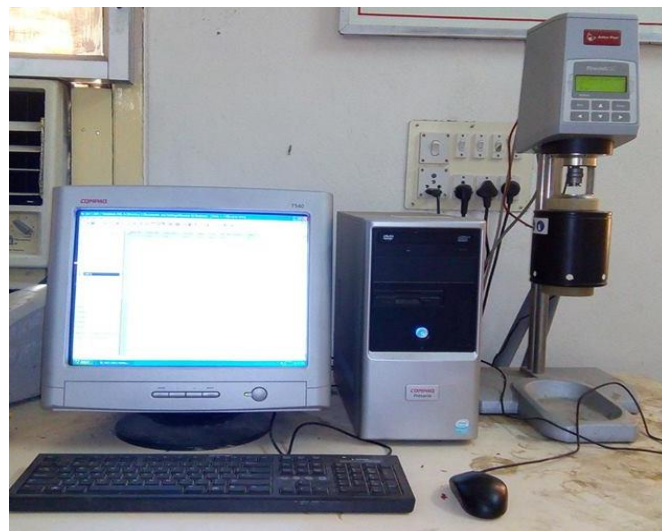
Fig. 3.10 Photographic view of Rheometer with computer interface

Fig. 3.12 shows the variation of empirically estimated and experimentally measured viscosity of a nanofluid as a function of particle concentration. Viscosity of a nanofluid at different particle concentrations is measured and compared with several existing empirical correlations. It can be observed from the experimental results that viscosity of a nanofluid

increases with the particle concentration and this increment is relatively more at the higher concentrations. The increasing particle concentration amplifies the entanglement and resistance between adjacent layers and leads to increase the viscosity of a nanofluid. Many other factors related to intermolecular interactions at the microscopic level also play a concealed role in the enhancement of dynamic viscosity of a nanofluid. The probable reason for the augment of nanofluid viscosity is that the nanoparticles are loaded into base fluid, larger interfacial/contact area of nanoparticles with base fluids promoting shear rates and consequently responsible for higher viscosity [151]. And another possible reason may be the inter-particle forces among the particles causes for higher shear rates and subsequently responsible for the increase of viscosity. It can be observed from Fig. 3.12 that there is a notable deviation between measured and analytical results. For instance, CuO/water nanofluid is considered for the analysis, for CuO/water nanofluid at 20 °C the deviation between empirical and experimental readings are 7.67 % at 0.125 % particle concentration and it is 18.58 % at 1.0 % particle concentration. At the temperature of 20 °C, dynamic viscosity of CuO/water nanofluid is increased from 1.002 mPa (for distilled water) to 1.082 mPa, 1.102 mPa, 1.143 mPa, 1.184 mPa and, 1.218 mPa for the particle volume concentration of 0.125%, 0.25 %, 0.5 %, 0.75 %, and 1.0 % respectively.
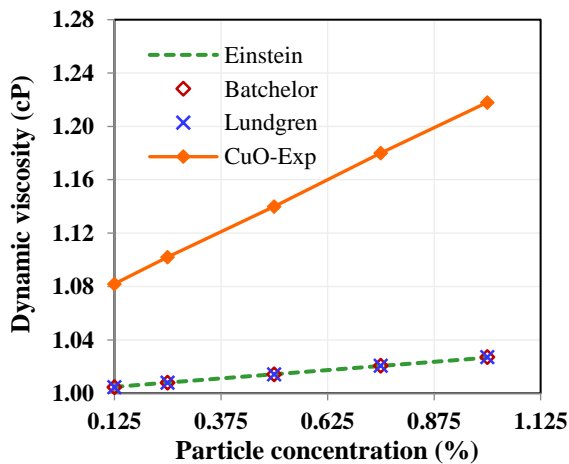
Fig. 3.11 Comparison of empirical and experimentally measured viscosity of CuO/water nanofluid
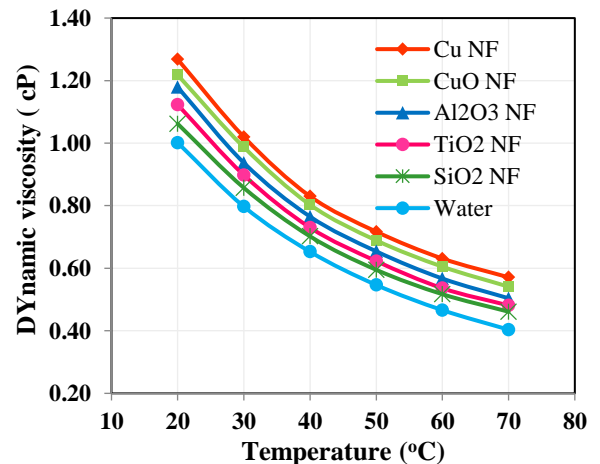
Fig. 3.12 Experimentally measured viscosity of water and different nanofluids as a function of temperatures

The dynamic viscosity of distilled water and different water based nanofluids such as Cu/water, CuO/water, Al$_2$O$_3$/water, TiO$_2$/water and SiO$_2$/water are experimentally measured. The dynamic viscosity of different nanofluids at 1 % particle concentration is measured and presented in the Fig. 3.12. In view of the fact that the solar collector has to operate over a range of temperatures, dynamic viscosity of nanofluids is measured at different temperatures.

52

Unambiguously, viscosity of all nanofluids is declining with increase in temperature and this decrement is relatively more at high temperatures. As the temperature of nanofluid increases, the Van Der Waals forces of attractions are gradually ceased and lead to reduce the viscosity of a nanofluid [169].
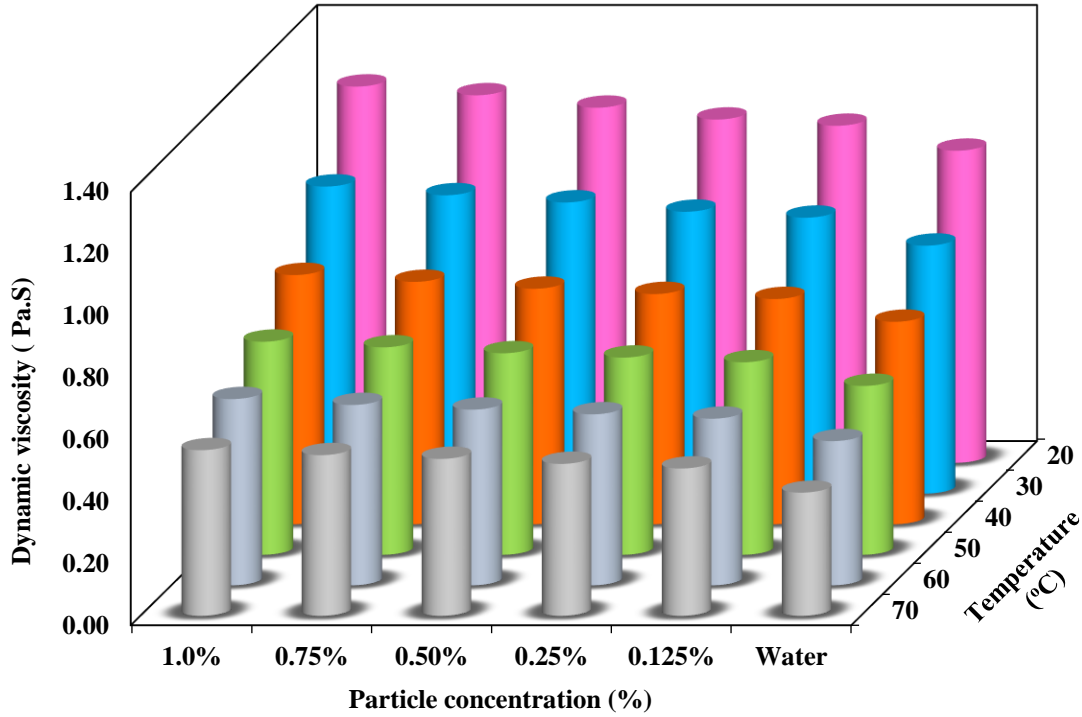
Fig. 3.13 experimentally measured viscosity of water and CuO/water nanofluids as a function of particle concentration and temperatures

Fig. 3.13 elucidates the change of dynamic viscosity of CuO/water nanofluid with respect to particle loading and temperature. It is exculpated from the measured readings that the viscosity of nanofluid is gradually increasing with the concentration and decreasing with the temperature raise [106]. This is due to the fact that, the increment of particle concentration causes to develop strong cohesive forces among the particles and these forces are responsible for the augment of viscosity of a nanofluid. And also, by increasing the particle loading in base fluid, more shear rate is produced between the particles and the base fluid, which is liable for higher viscosities at higher particles concentrations. But, these cohesive forces and share rates are ceases with the temperature rise and leads to curtail the viscosity of a nanofluid [157].

3.5.1.1 Correlation Proposed to estimate the viscosity of nanofluids:

Experimental investigations are necessitates for validating the various empirical correlations used to estimate the viscosity of a nanofluid. Though, plenty of correlations are available in open literature, most of the correlations are not able to precisely predict the viscosity of nanofluid with close approximation to measured values. Because, the correlations available in literature, considers the particle concentration as a sole parameter that influence the nanofluid viscosity [156], [174], [175], but the properties of nanoparticle material are not taken into account. However, few correlations considered the temperature as an influencing parameter [157], [158]. It is clear from Fig. 3.11 that the empirical correlations are under estimating the viscosity of nanofluid. Therefore, to precisely predict the viscosity of nanofluid a new correlation has been developed by considering the all possible influencing parameters. In the developed correlation particle concentration, temperature and density of the nanoparticle are also taken into account and the developed correlation is:

$$\frac{\mu_{nf}}{\mu_{bf}} = 1 + a\phi^b \left(\frac{T_{nf}}{T_0}\right)^c \left(\frac{\rho_{nf}}{\rho_{bf}}\right)^d \tag{3.25}$$

Constants of the developed correlation for different nanofluids of viscosity are presented in table 3.2.

Table 3.2 Correlation constants for different nanofluids

Nanofluid/ correlation constant	a	b	c	d
Cu/water	0.1411	0.0497	1.4751	10.6481
CuO/water	0.1844	0.0856	1.6271	10.2430
Cu-CuO/water	0.1695	0.0384	1.4145	10.8146

It is clear from the constants of correlations that the density of nanoparticle has significant influence on viscosity of nanofluid.

For the proposed correlation, from the curve fit, regression coefficient is 0.9404. It can be observed that the data would correlated with 96% of the data is with the curve fit range. Therefore, it is note to worthy that, the proposed correlation is capable to precisely estimate the viscosity of water based mono nanofluids as well as hybrid nanofluids with a single equation.
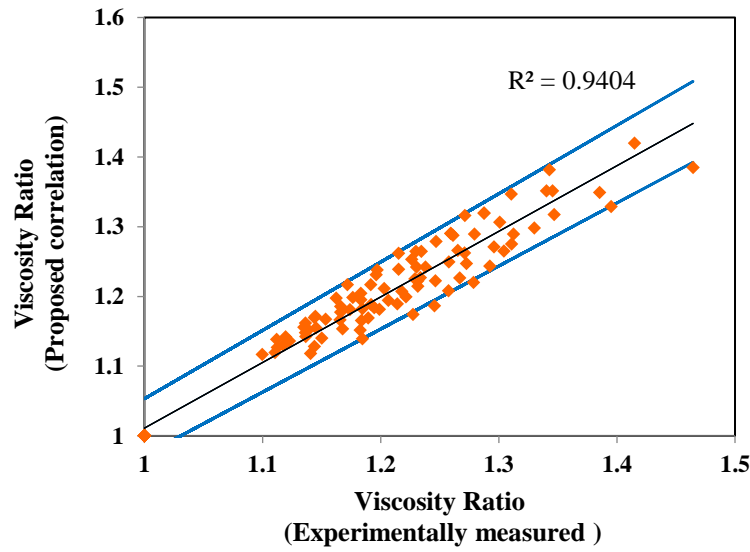
Fig. 3.14 Viscosity ratio for experimental measurements Vs proposed correlation

Fig. 3.15 illustrates the viscosity of both mono and hybrid nanofluids as function of temperature. It can be observed hybrid nanofluids are also following the similar trend of mono nanofluids. Dynamic viscosity of hybrid nanofluid lies between the viscosities of its individual constituents. By suspending the nanoparticles in the base fluid, nanoclusters are formed around the particle and the size of nanoclusters formed is material dependent. By increasing the temperature of working fluid the thickness of these nanoclusters and cohesive forces among the particle are ceased and lead to reduce the viscosity of both mono and hybrid nanofluids.
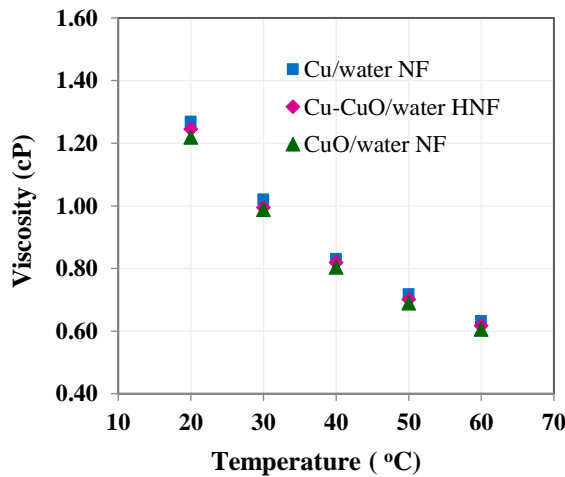
Fig. 3.15 Viscosity of mono and hybrid nanofluids as a function of temperature
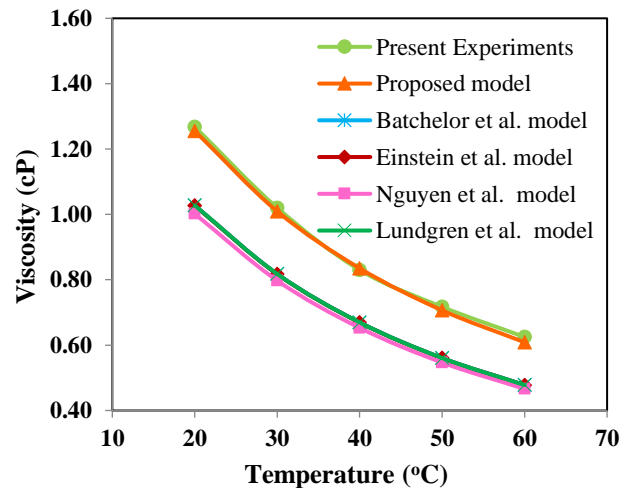
Fig 3.16 Comparison of proposed and existing correlations.

Comparisons were made between proposed correlation and various empirical relations available in the open literature and presented in Fig. 3.16. It can be observed from Fig. 3.16 that the proposed correlation has good agreement with the experimental results.

3.5.2 Thermal conductivity measurement

Thermal conductivity of all working fluids considered in the current work are measured using thermal conductivity analyzer (TPS 500S, Therm. Test Inc., Fredericton, Canada) as shown in Fig. 3.17 (a). The instrument is equipped with different types of sensors with software module interface to measure the thermal conductivity of different materials like bulk materials, powders, thin films, and wide range of liquids including nanofluids. The apparatus works based on transient plane source principle and follows ISO 22007-2.2 standards. In current work, 7552 Kapton sensor of 2 mm diameter is used to measure thermal conductivity of nanofluids at different particle concentrations. The equipment is supported with a thermostatic bath to facilitate to measure the thermal conductivity over a wide range of temperatures from -20 ºC to 200 ºC.

To measure the thermal conductivity of nanofluid Kapton sensor is immersed in the nanofluid filled attachment, so that both sides of sensor is having identical environment. The arrangement is kept ideal for 20 min to reach thermal equilibrium state and then thermal conductivity is measured from the software interface module. Each sample is tested three times under identical temperature conditions and averages of the readings are considered for the further analysis. The sensor-sample arrangement is as shown in Fig. 3.17 (b).

Fig. 3.17 (a) Thermal conductivity Analyzer   Fig. 3.17 (b) Conductivity measuring sensor

Thermal conductivity of CuO/water nanofluid at different particle concentrations is measured and compared the experimental outcomes with the analytical correlations available in the open literature as shown in Fig. 3.18. All correlations considered for the analysis are giving similar readings and overlapping each other. One can coherent from Fig. 3.18 that the established empirical relations are under predicting the thermal conductivity of a nanofluid and the degree of inaccuracies is increasing with the particle concentration. This is may be because of, in the empirical models may not considered the root causes for anomalous enhancement of thermal conductivity like Brownian motion, specific surface area, interfacial liquid layering, and surface chemistry, which will take part in the enhancement of thermal conductivity of a nanofluid. It can be observed from Fig. 3.18 that that thermal conductivity of nanofluid is progressively increasing with the particle concentration and it is amplifying at the higher concentrations. However, the deviation is less than 5 % compared to experimental data, therefore, no new correlation is developed for further analysis.

Experimentally measured thermal conductivity of different nanofluids at various concentrations is presented in Fig. 3.19. It is noticeable that the thermal conductivity of all nanofluids following the similar trend and are surpassing with the particle concentration As the particle concentration increases, the mean free path of the nanoparticles is decreased and leads to promote the lattice vibrations which is commonly known as percolation effect [176] that is may also one of the responsible root cause for the consequential enrichment of nanofluid thermal conductivity
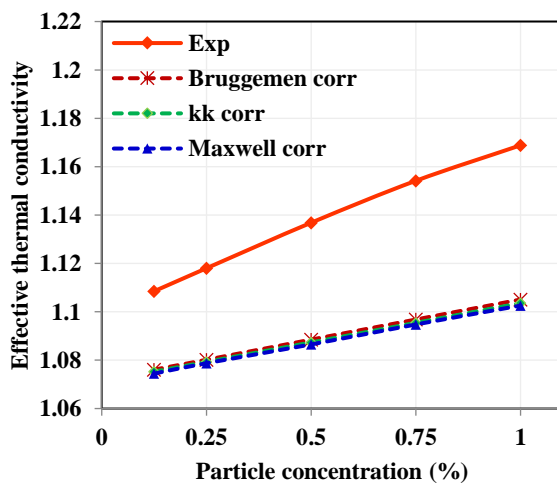
Fig. 3.18 Comparison of empirical and experimentally measured thermal conductivity of CuO/water nanofluid
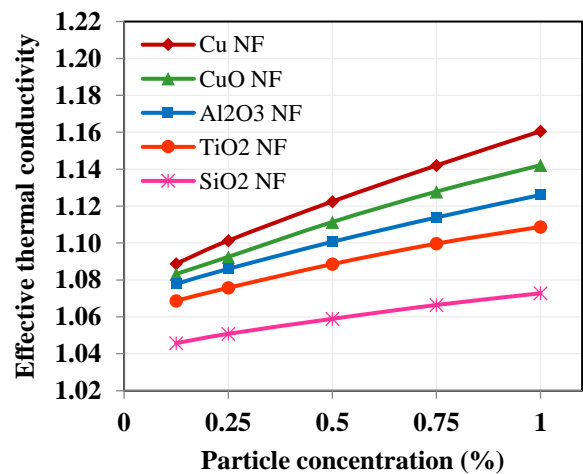
Fig. 3.19 Experimentally measured thermal conductivity of different nanofluids
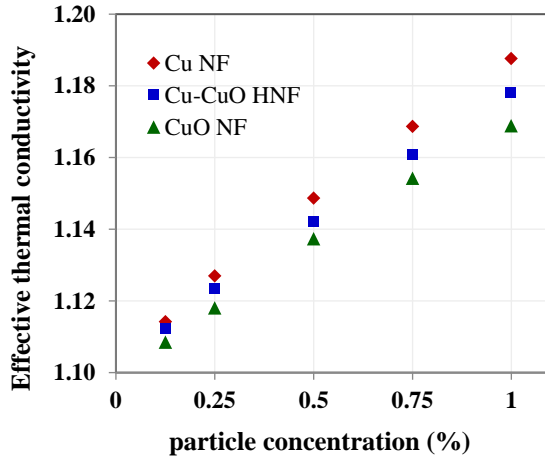
Fig. 3.20 Thermal conductivity of mono and hybrid nanofluids as a function of particle concentration
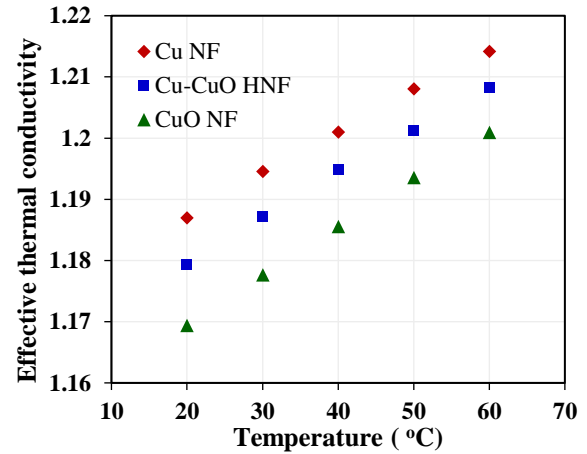
Fig. 3.21 Thermal conductivity of mono and hybrid nanofluids as a function of temperature

Thermal conductivity of mono-nanofluid and hybrid nanofluids as a function of particle concentration and temperature is experimentally measured and presented in Fig. 3.20 and Fig 3.21. It can be observed from Fig. 3.20 that the effective thermal conductivity of both mono and hybrid nanofluids enhances with the particle concentration and this enhancement is noticeably high at higher particle concentrations. The most prominent reasons for the marginal enhancement of thermal conductivity of a nanofluid is due to the Brownian motion of particles, larger specific surface area and formation of nanoclusters [173]. Similar mechanisms may also be ascribed for the enhancement of thermal conductivity of hybrid nanofluids as well. Precisely, when copper nanoparticles are hybridized with copper oxide nanoparticle thermal network is created at the interface of neibhouring particles as well as between particle and surrounded fluid layer is responsible for improved thermal conductivity of hybrid nanofluid [120]. Fig.3.22 describes the influence of nanofluid temperature on thermal conductivity. As the temperature of the nanofluid increase, the effective thermal conductivity of nanofluid also increased due to enhanced Brownian motion.
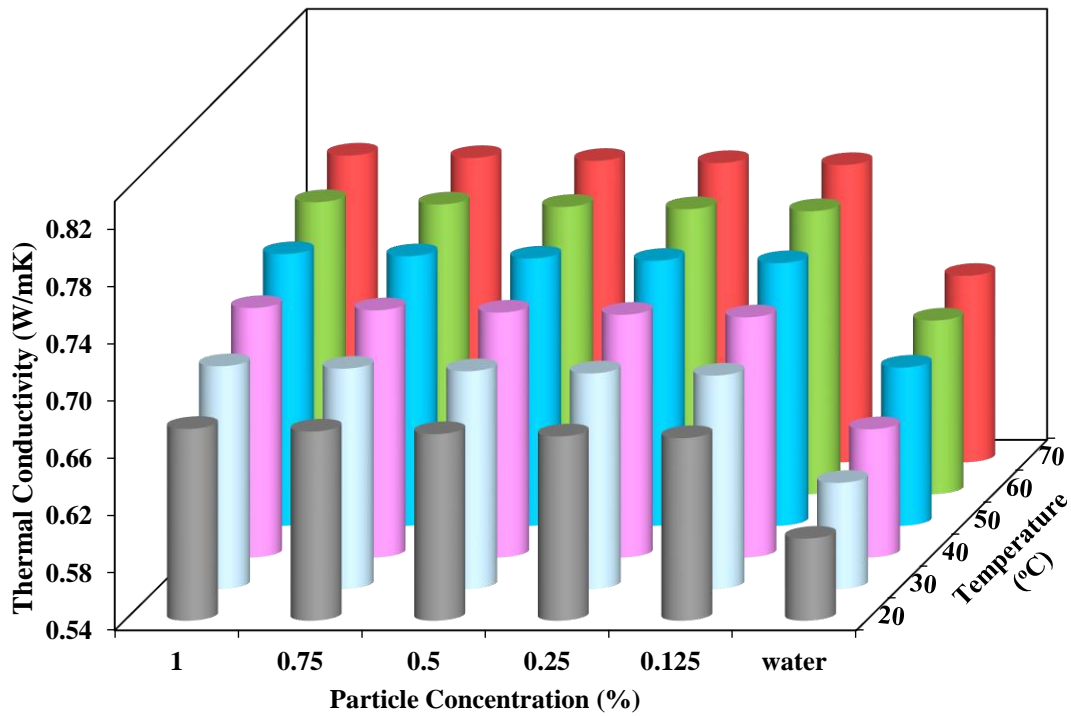
Fig. 3.22 Experimentally measured thermal conductivity of water and Cu/water nanofluid as a function of particle concentration and temperatures

Along with the particle concentration, effect of temperature on the enhancement of thermal conductivity of nanofluid is also studied and presented in Fig. 3.22. Together with particle concentration, temperature of nanofluid is also influences the thermal conductivity of nanofluid. This is because of, the inter particle cohesive forces and corresponding viscosity are diminished with the temperature raise which causes to ascend the Brownian motion. The increased random movement of nanoparticles promotes micro convection between nanoparticle and base fluid and leads to enhance the thermal conductivity of nanofluid. As elucidated in Fig. 3.22 thermal conductivity of Cu/water nanofluid is enhancing with particle concentration and temperature. The amelioration of thermal conductivity is depending on the properties of base fluid as well as nanoparticle material [177]. The thermal conductivity of Cu/water nanofluid is enhanced by 12.5 % at the particle concentration of 1.0 % and 20 $^{\circ}$C temperature and it is improved by 13.4 % for the same particle concentration at the temperature of 70°C.

3.6 Closure

This chapter discussed the selection of nanoparticle concentration for solar thermal collectors is explored in this chapter.

This chapter also scrutinizes the estimation of various thermophysical properties of mono and hybrid nanofluids from the correlations available in open literature. It also compares the experimentally measured properties with the empirical correlations. A considerable deviation is observed between the measured results and the empirical solutions. Therefore, a new correlation is developed to estimate the viscosity of nanofluids. Reasons to establish the new correlation is endorsed in this chapter.

Chapter - 4

Performance Evaluation of Forced Circulation Solar Thermal Collectors

4.1   Introduction

Thermodynamic analysis of any thermal system is a systematic study to know its thermal behaviour. It is inevitable to conduct the analysis by considering both first law and second law of thermodynamics to precisely study the energy distribution and thermal losses from a system. However, energy analysis alone cannot predict the functionality of the system. The energy analysis represents the amount of input energy converted into output in useful form but it cannot identify the ways of energy loss from the system. Therefore, second law analysis is required to know the transformation of energy in both available and unavailable forms. The second law describes the loss of energy to the environment from various parts of solar collector in terms of destroyed energy.

In solar thermal collector, the solar radiation incident on absorber surface is converted to heat energy and this heat energy is transferred to the working fluid flowing inside the riser tubes. The first law of thermodynamics reveals that only a portion of incident radiation is converted into useful form and remaining is lost to the environment in form of thermal losses. However, second law measures the degree of irreversibilities in terms of destroyed energy. The irreversibilities of the collector lead to rise the entropy generation. Entropy is nothing but the unrecoverable form of loss from a solar collector. Therefore, by controlling the degree of

irreversibilities from the solar collector one can minimise the entropy generation so that, the energy utilization can be maximised.

In the current research, thermodynamic analysis is carried out on SFPC operated on both forced circulation (active collectors) and natural circulation (passive collectors) modes and also on different absorption configurations like direct absorption and indirect absorption configurations. Analytical and experimental investigations are carried out on all four modes and comparative studies are reported. Figure 4.1 elucidates the solar collectors considered for the analysis within the scope of current research.
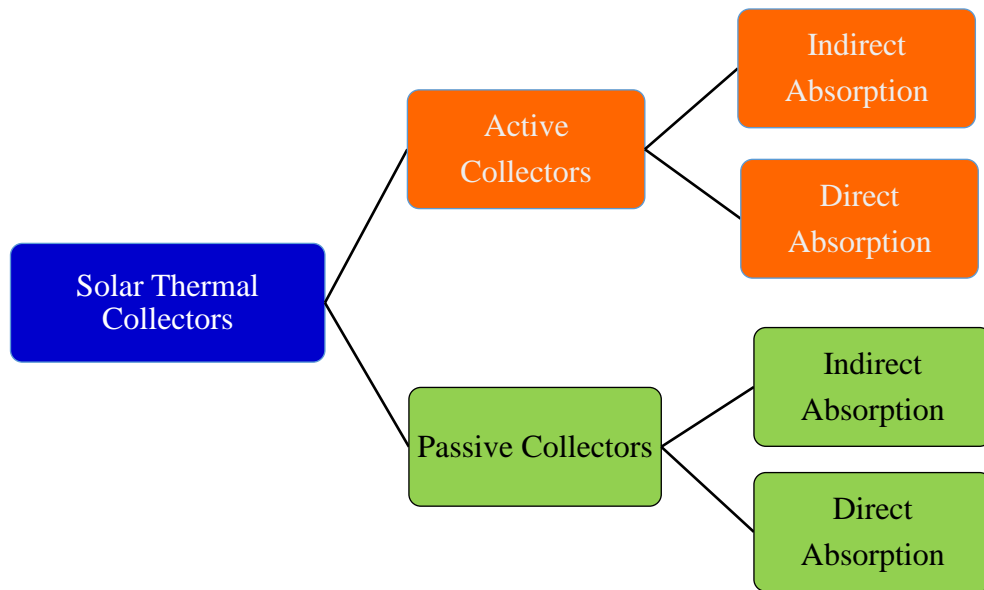
Fig. 4.1 Solar flat plate collectors analysed in current research

4.2 Forced Circulation In-Direct Absorption Solar Flat Plate Collector (FCIDASFPC)

Indirect absorption solar collector is the most common type of collector conventionally used for low temperature applications like water heating and space heating. Even though the solar collectors exist from dates back still it is suffering from lower thermal efficiency. Though, considerable research is carried out from the last six and half decades on the design changes of SFPC, the basic structure is still unaltered. SFPC is a most promising device with its simple construction and low maintenance. SFPC is a distinctive kind of heat exchanger that utilizes both beam and diffuse radiations at different wavelengths. Absence of tracking mechanism and larger collecting area make the SFPCs' desirable. However, SFPC's are suffering from lower thermal efficiency due to more convective and radiative losses because of its larger surface area

and lower convective heat transfer coefficients between absorber plate and working fluid [37]. The SFPC considered for the analysis in the current section is described in Fig. 4.2. Schematic view of indirect absorption solar collector is as shown in Fig. 4.3. A typical SFPC consists of glass cover, absorber plate, riser tubes, header pipes, and insulation. Glass cover will allow the maximum possible incident solar radiation on the absorber plate and create greenhouse effect to the incoming solar radiation. Absorber plate is made with copper and coated with low emissive surface coatings to absorb more incident solar radiation and this absorbed energy is transferred to the working fluid. The absorber plate is ultrasonically welded on top of the riser tubes. Bottom and edges of the collector are well insulated to minimize the convective and radiative heat losses to surroundings.
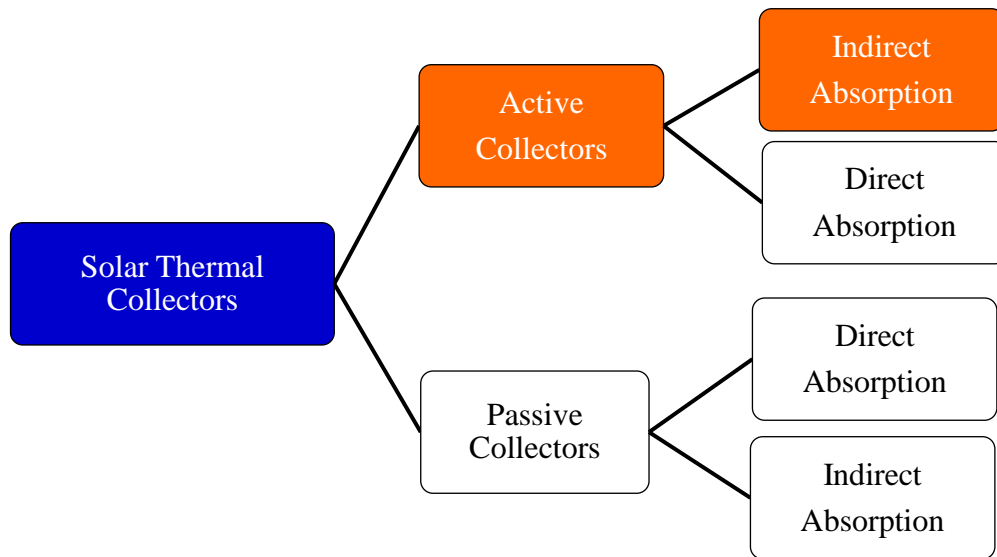
Fig. 4.2 Solar flat plate collector operating in indirect absorption configuration and active (Forced Circulation) mode

For SFPC, the intercepting area and radiation absorbing area are one and same. Thus, the amount of energy absorbed is linearly proportional to surface area of collector. However, the high surface area of SFPC causes for more heat losses that leads to reduce its thermal efficiency. The surface are of collector cannot be reduced therefore, the current study is concentrating on the enhancement of thermophysical properties of working fluid. The geometrical specifications, operating conditions, and environmental parameters for the current analysis are presented in table 4.1.
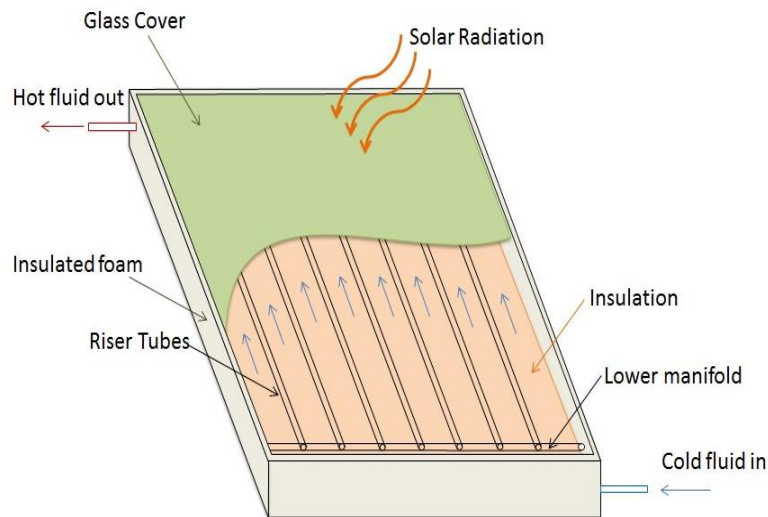
Fig. 4.3 Schematic view of indirect absorption solar flat plate collector

Table: 4.1 Specifications and environmental parameters of FCIDASFPC

Collector parameters	
Overall dimensions of collector	$550 \times 450 \text{mm}^2$
Glazing cover	Glass: Low iron toughened glass
	Number of Glass covers, N_g: Single
	Thickness: 3 mm
	Transmissivity, τ_g: 92 % of solar radiation
	Emissivity, ε_g: 88% of solar radiation
Absorber	Material: Copper
	Surface area: 0.211 m^2 coated with
	Selective black surface coating
	Absorptivity, α_p: 96% of solar radiation
	Emissivity, ε_p : 12% of solar radiation
Tubes	Material: Copper
	Number of tubes, n : 07
	External diameter, D_o: 10.1 mm
	Internal diameter, D_i: 9.5 mm
Insulation	Material: Rockwool
	Insulation density : 48 gm/m^3
	Base insulation thickness, t_b: 50 mm

	Edge insulation thickness, t_e: 25 mm
	Thermal conductivity, k_i: 0.04 W/mK
	Water
	Cu/Water nanofluid
	CuO/Water nanofluid
Working fluids	AL_2O_3/water nanofluid
	TiO_2/water nanofluid
	SiO_2/water nanofluid
	Cu-CuO/water hybrid nanofluid
Wind velocity, v_w	2 m/s
Collector tilt angle, β	18.59° latitude of NIT Warangal
Fluid inlet temperature, T_i	300 K
Apparent sun temperature T_{sun}	4350 K
Absorber plate thickness, t_p	0.12 mm
Transmittance-Absorptance product (ατ)	0.84
Tube pitch, W	45 mm

4.2.1 Thermodynamic analysis of FCIDASFPC

Thermodynamic analysis is carried out by amalgamating the energy and exergy analysis, which gave the impeccable perception on SFPC performance. In energy analysis, a comprehensive procedure is presented to estimate the useful heat gain by the working fluid and SFPC efficiency. Exergy analysis is provided in the subsequent section which describes the procedure to estimate the rate exergy destroyed and entropy generation. To establish the mathematical modeling for this thermal analysis, the following general assumptions are made:

a. The flow is turbulent, fully developed and uniform in all risers.
b. Intensity of incident solar radiation is uniform.

4.2.1.1 Energy Analysis

From the total solar radiation incident on SFPC, a fraction of radiation is transferred to the working fluid as useful heat gain, and remaining is lost to ambient in terms of radiation and

convection losses through different parts of the collector. The incidental solar radiation falling on SFPC is given by:

$$Q_i = I_t A_c \tag{4.1}$$

The incoming solar radiation is attenuated in the collector due to change of refractive index and wavelengths at collector cover. In the collector, a partial amount of radiation is absorbed by the glazing material, a fraction of radiation is reflected back to the environment and the remaining is transmitted to the absorber plate through the air gap. Therefore, the incident radiation reaching the absorber plate is given by:

$$Q_i = I_t (\tau\alpha) A_c \tag{4.2}$$

At the absorber plate, a portion of the received radiation is transmitted to the working fluid and converted it into useful heat gain. From the fundamentals of thermodynamics, the rate of useful heat gain by the working fluid is:

$$Q_u = \dot{m} C_p \left(T_{f,0ut} - T_{f,in} \right) \tag{4.3}$$

Eq 4.3 is not considering the effects of influencing parameters such as heat loss coefficient and optical efficiency of the glass cover. However, the amount of heat loss from the SFPC depends upon the overall heat loss coefficient of SFPC and absorber plate temperature. The net heat loss from the collector is:

$$Q_{loss} = U_l A_c \left(T_p - T_a \right) \tag{4.4}$$

Therefore, useful heat gain is the net effect of total incidental radiation on SFPC and heat loss from it [33]. So, the heat gain by the working fluid is given by:

$$Q_u = A_c \left[I_t (\tau\alpha) - U_l (T_p - T_a) \right] \tag{4.5}$$

$$Q_u = A_c F_R \left[I_t (\tau\alpha) - U_l (T_{f,in} - T_a) \right] \tag{4.6}$$

where F_R is the heat removal factor and it can be calculated by:

$$F_R = \left[\frac{\dot{m} C_p}{A_c U_l} \right] \left\{ 1 - exp \left(\frac{-A_c U_l F'}{\dot{m} C_p} \right) \right\} \tag{4.7}$$

In the above equation, F' is the collector efficiency factor, which depends on the convective heat transfer coefficient of the working fluid and fin efficiency of the absorber plate [178]. Collector efficiency factor F' is calculated by:

$$F' = \frac{1}{\left\{[WU_l/(\pi Dh_f)] + \left(\frac{1}{C_b}\right) + [W/(D+(W-D))F]\right\}}$$ (4.8)

Fin efficiency, 'F' can be calculated by:

$$F = \frac{tanh(m(W-D)/2)}{[m(W-D)/2]}$$ (4.9)

where, $m = \sqrt{U_l/(k_p t_p)}$

The overall heat loss coefficient is the sum of heat losses from top, edges and bottom of the collector [178].

The overall heat loss coefficient, $U_l = U_t + U_e + U_b$

Top heat loss coefficient, U_t is calculated by

$$U_t = \frac{1}{\frac{N_g}{\frac{C}{T_p}\left[\frac{T_p-T_a}{N_g+\tau}\right]^{0.33}} + \frac{1}{h_w}} + \frac{\sigma(T_p^2-T_a^2)(T_p+T_a)}{\frac{1}{\varepsilon_p+0.05N_g(1-\varepsilon_p)} + \frac{2N_g+\tau-1}{\varepsilon_g} - N_g}$$ (4.10)

where,

$$C = 520(1 - 0.000051\beta^2)$$ (4.10a)

$$\tau = (1 - 0.04h_w + 0.0005h_w^2)(1 + 0.091N_g)$$ (4.10b)

$$h_w = 5.7 + 3.8v_w$$ (4.10c)

T_p is the absorber plate mean temperature, which is given by

$$T_p = T_{f,in} + \frac{Q_u/A_c}{F_R U_l}(1 - F_R)$$ (4.11)

The initial guess of plate temperature is corrected by iteration technique and the benchmark for break-off of the iterations is

$$\left|\frac{(T_p)_{guess} - (T_p)_{calculated}}{(T_p)_{calculated}}\right| \leq 10^{-5}$$ (4.12)

Heat loss coefficient from bottom (U_b) and edges (U_e) of the SFPC can be calculated by using the following equations:

$$U_b = \frac{1}{\frac{t_b}{k_b} + \frac{1}{h_{ba}}}$$ (4.13)

$$U_e = \frac{1}{\frac{t_e}{k_e} + \frac{1}{h_{ea}}}\frac{A_e}{A_c}$$ (4.14)

The convective heat transfer coefficient of the working fluid flowing in risers is given by:

$$h_f = \frac{Nu.k}{D_i} \tag{4.15}$$

For the particular hydraulic diameter, h_f depends on Nusselt number and thermal conductivity of working fluid.

Nusselt number of SFPC operated in forced circulation mode can be estimated using Gnielinski's correlation [179]:

$$Nu = \frac{(f/8)(Re-1000)Pr}{1+1.27(f/8)^{0.5}(Pr^{0.66}-1)} \tag{4.16}$$

The above correlation can applied for a broad range of Prandtl number and Reynolds numbers, i.e. $0.5 \leq Pr \leq 2000$ and $3000 \leq Re \leq 5X10^6$

where, f is the Darcy friction factor, and it can be estimated by using Eq (4.17)

$$f = (0.79\ln(Re) - 1.64)^{-2} \tag{4.17}$$

From the definitions, Reynolds and Prandtl numbers of working fluid can be calculated by:

$$Re = \frac{4\dot{m}_r}{\pi D_i \mu} \tag{4.18}$$

$$Pr = \frac{\mu C_p}{k} \tag{4.19}$$

where $\dot{m}_r$ is the mass flow rate in any one riser.

The instantaneous thermal efficiency of SFPC for the incident solar radiation is the ratio of useful heat gain by the working fluid to the total solar radiation incident on collector area.

$$\eta = \frac{A_c F_R[I_t(\tau\alpha) - U_l(T_i - T_a)]}{I_t A_c} = F_R(\tau\alpha) - [F_R U_l(T_i - T_a)/I_t] \tag{4.20}$$

In which, $F_R(\tau\alpha)$ is the energy absorbed parameter, the term $(T_i - T_a)/I_t$ is the heat loss parameter, and $F_R U_l$ is called removed energy parameter [110].

A pump is an essential component to maintain the constant flow across the collector in forced circulation mode. While, the working fluid is circulating in entire collector, certain amount of pressure drop is inevitable. The total pressure drop in SFPC is encompassed with major and minor losses. The major head losses are generated due to friction between the working fluid and adjacent contact surfaces of SFPC, while the minor losses are due to changes in geometry and added components to the collector. Both major and minor losses are responsible for the

total pressure drop in collector [180]. Therefore, the total head loss in SFPC can be estimated by Eq 4.21:

$$h_l = h_{l,major} + h_{l,minor} = \frac{8\dot{m}_r^2}{\rho^2 g \pi^2 D_i^4}\left[f\frac{L_r}{D_i} + \sum_{i=1}^n K_l\right] \tag{4.21}$$

With the assumption of sharp edge fastening between the headers and risers, loss coefficient, K_l is taken as 0.5 at the entrance, and 1 at the exit [180], L_r is the length of each riser.

The pressure drop in the flat plate collector can be calculated by:

$$\frac{p_1}{\rho g} + z_1 = \frac{p_2}{\rho g} + z_2 + h_l \tag{4.22}$$

When the inclination of SFPC is β, then the vertical distance between the headers are equivalent to $L_r \sin\beta$.

Therefore, the total pressure drop in SFPC is:

$$\Delta p = p_1 - p_2 = \rho g(L_r \sin\beta + h_l) \tag{4.23}$$

The pumping power required for running the collector by considering the total pressure drop due to circulation of working fluid can be calculated by:

$$P = \frac{\dot{m}}{\rho_{nf}} . \Delta p \tag{4.24}$$

4.2.1.2 Exergy Analysis

Exergy of a solar collector is a qualitative measure of maximum useful work that can be extracted from the collector from the available solar radiation. The exergy analysis gives the direction to reduce the exergy losses.

The total exergy available at the collector includes the rate of exergy incident on the collector by the solar radiation and exergy of the working fluid at the inlet of SFPC [181]. The rate of exergy incident on SFPC by solar radiation is given by :

$$\dot{Ex}_{in,sun} = I_t A_c \left(1 - \frac{T_a}{T_s}\right) \tag{4.25}$$

The rate of exergy at the inlet of working fluid is given by:

$$\dot{Ex}_{in,f} = \dot{m}C_p\left[(T_i - T_a) - T_a ln\left(\frac{T_i}{T_a}\right)\right] \tag{4.26}$$

The outlet exergy rate of working fluid is given by:

$$\dot{E}x_{out,f} = \dot{m}C_p\left[(T_o - T_a) - T_a ln\left(\frac{T_o}{T_a}\right)\right]$$ (4.27)

The quantitative difference between inlet and outlet exergy rates should represent the destroyed exergy rate and it is given by:

$$\sum \dot{E}x_{in} - \sum \dot{E}x_{out} = \sum \dot{E}x_{dest}$$ (4.28)

Certain amount of exergy is lost to the environment in terms of destroyed exergy, and the exergy is destroyed by many reasons in several forms. The rate of exergy destroyed due to heat transfer at the finite temperature difference is in following forms [181].

a. Rate of exergy destroyed due to the temperature difference between the absorber plate surface and the sun:

$$\dot{E}x_{dest1,\Delta T_s} = I_t A_c T_a(\tau\alpha)\left(\frac{1}{T_p} - \frac{1}{T_{sun}}\right)$$ (4.29)

b. Rate of exergy destroyed due to radiation losses from the collector surface to the absorber plate:

$$\dot{E}x_{dest,2} = I_t A_c[1 - (\tau\alpha)]\left(1 - \frac{T_a}{T_{sun}}\right)$$ (4.30)

c. Rate of exergy destroyed due to the temperature difference between the absorber plate surface and the working fluid:

$$\dot{E}x_{dest,3} = \dot{m}C_p T_a\left[ln\left(\frac{T_o}{T_i}\right) - \left(\frac{T_o - T_i}{T_p}\right)\right]$$ (4.31)

Exergy is destroyed due to fluid flow in risers in terms of pressure drop. It can be calculated by[182].

$$\dot{E}x_{dest,\Delta P} = \frac{\dot{m}\Delta P}{\rho}T_a ln\frac{(T_o/T_a)}{(T_o/T_i)}$$ (4.32)

Certain amount of exergy is lost to the atmosphere in terms of leakage, the rate of exergy leakage to the environment due to improper fastening of collector components and it can be calculated by [183]:

$$\dot{E}x_{leakage} = A_c U_l(T_p - T_a)\left(1 - \frac{T_a}{T_p}\right)$$ (4.33)

Exergy efficiency of SFPC is the ratio of useful exergy gain by the working fluid to the inlet radiation exergy. The useful exergy gain by the working fluid is given by:

$$\dot{E}x_{gain} = \dot{E}x_{out,f} - \dot{E}x_{in,f}$$ (4.34)

Exergy efficiency can be estimated by:

$$\eta_{Ex} = \frac{\dot{Ex}_{gain}}{\dot{Ex}_{sun}} = \frac{\dot{Ex}_{out,f} - \dot{Ex}_{in,f}}{I_t A_c \left(1 - \frac{T_a}{T_s}\right)} \qquad (4.35)$$

The destroyed exergy leads to generate the entropy and the amount of entropy generated in SFPC is calculated in terms of work lost. The work lost in SFPC is the aggregation of destroyed and leakage exergy rates. Therefore, the total entropy generated, $\dot{S}_{gen}$ (W/K) is given by [184]:

$$\dot{S}_{gen} = \frac{\dot{W}_{lost}}{T_a} = \frac{\dot{Ex}_{dest} + \dot{Ex}_{Leak}}{T_a} \qquad (4.36)$$

In the SFPC, entropy is generated by two effects [185]

i.   Entropy generated by the heat transfer due to temperature gradients:

$$\left(\dot{S}_{gen}\right)_H = \frac{\dot{Ex}_{dest,1} + \dot{Ex}_{dest,2} + \dot{Ex}_{dest,3} + \dot{Ex}_{leak}}{T_a} \qquad (4.37)$$

ii.Entropy generated by the pressure drop due to frictional losses:

$$\left(\dot{S}_{gen}\right)_F = \frac{\dot{Ex}_{dest\Delta P}}{T_a} \qquad (4.38)$$

Thus, the overall entropy generated in a SFPC can be calculated by:

$$\dot{S}_{gen} = \underbrace{\eta_o I_t A_c \left(\frac{1}{T_p} - \frac{1}{T_s}\right) + \dot{m} C_p \left(ln\left(\frac{T_o}{T_i}\right) - \frac{(T_o - T_i)}{T_p}\right) + A_c U_l \left(\frac{T_p}{T_a} - 1\right)\left(1 - \frac{T_a}{T_p}\right)}_{(\dot{s}_{gen})_H} + \underbrace{\frac{\dot{m}\Delta P}{\rho} \frac{ln\left(\frac{T_o}{T_a}\right)}{(T_o - T_i)}}_{(\dot{s}_{gen})_F}$$
$$(4.39)$$

The impact of entropy generation due to heat transfer in the total entropy generated is represented by Bejan number and the Bejan number of SFPC is given by:

$$Be = \frac{(\dot{s}_{gen})_H}{\dot{s}_{gen}} \qquad (4.40)$$

4.2.2   Results and discussion

Efficiency of collector at different particle concentrations is presented in Fig. 4.4. To examine the effect of particle concentration, collector efficiency is analytical estimated up to 1.25 % and it is observed that the enhancement of collector efficiency is insignificant. Therefore, the particle concentration is limited to 1 %. The collector efficiency of SFPC with different working fluids such as Cu/water, CuO/water, Al$_2$O$_3$/water, TiO$_2$/water, SiO$_2$/water are estimated using Eq 4.20. From the incident solar radiation, the working fluid which attains more useful heat gain and less heat losses exhibits higher collector efficiency. The nanofluids

having lower specific heat possess more useful heat gain and subsequently higher collector efficiency. Since, the Cu/water nanofluid having lower heat capacity than the other nanofluids it exhibits higher collector efficiency.
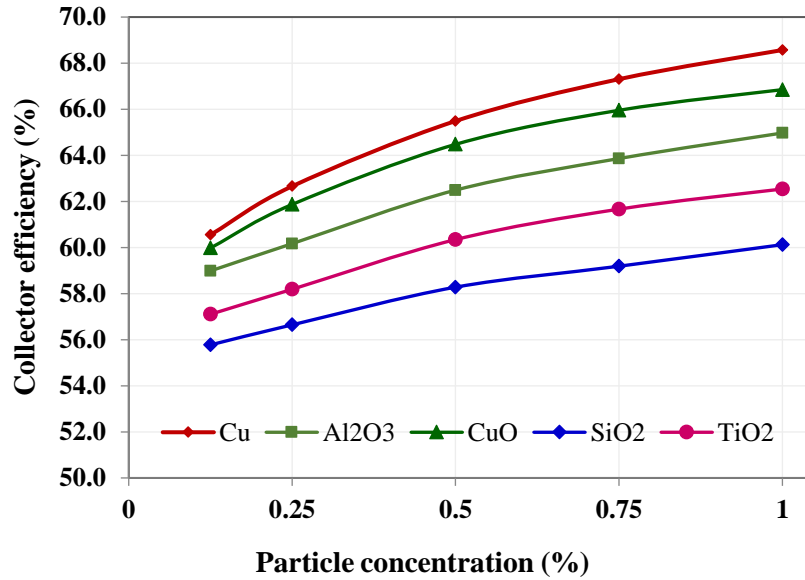
Fig. 4.4 Collector efficiency as a function of particle concentration

Though the addition of nanoparticles improve the energy efficiency of the SFPC, increasing pumping power to circulate the working fluid in collector is inevitable. Fig. 4.5 depicts the required pumping power as a function of particle concentration for different nanofluids.
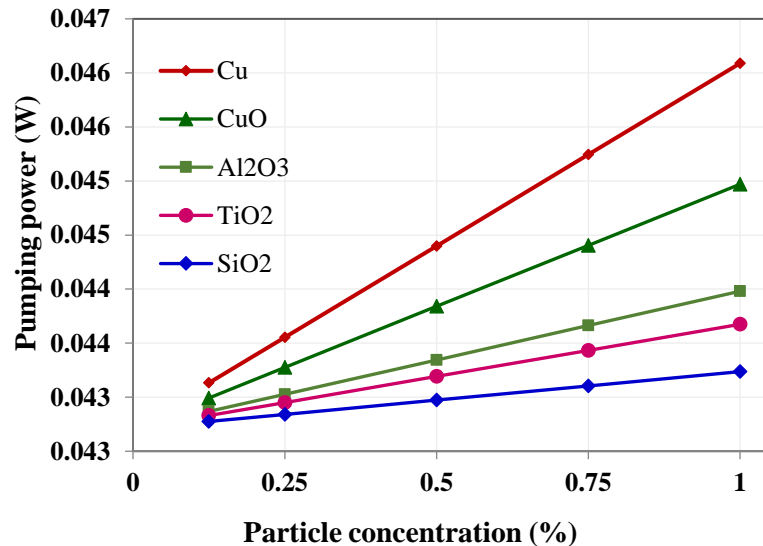
Fig. 4.5 Pumping power as a function of particle concentration

The pressure drop of all nanofluids is linearly increasing with increasing of particle concentration and the increasing trend is similar to all nanofluids. It is explicit from Eq (4.21)

and Eq (4.22) that both major and minor losses in SFPC are responsible for the pressure drop in collector. From Eq (4.21) it can be noted that the density of nanofluid is the other critical parameter that governs the pressure drop. For all the nanofluids, the density is proportionately increasing with the particle concentration and this increment is relatively more at higher concentrations. Therefore, at higher nanoparticle concentrations, density gradients and consequent frictional losses are gradually increasing. Pumping power of SFPC can estimate from Eq (4.24). Among all the nanofluids, since Cu/water nanofluid has higher density, it produces more pressure drop and consequently more pumping power is required than other nanofluids.

Exergy efficiency indicates the amount of exergy gain by the working fluid in a specified environment. The exergy efficiency of different nanofluids is estimated as a function of particle concentration and presented in Fig.4.6. The exergy efficiency of a SFPC can be estimated from Eq (4.35). It can be observed from Fig. 4.6 that, by increasing particle concentration, the useful exergy gain by the working fluid is also increasing and this increment is relatively more at higher particle concentration. For a specified geometry, at given ambient and inlet conditions, specific heat of the nanofluid has more impact on exergy gain. Since, specific heat of Cu/water nanofluid is 7.52 % less than water its exergy efficiency is enhanced by 18.07 % compared to water.
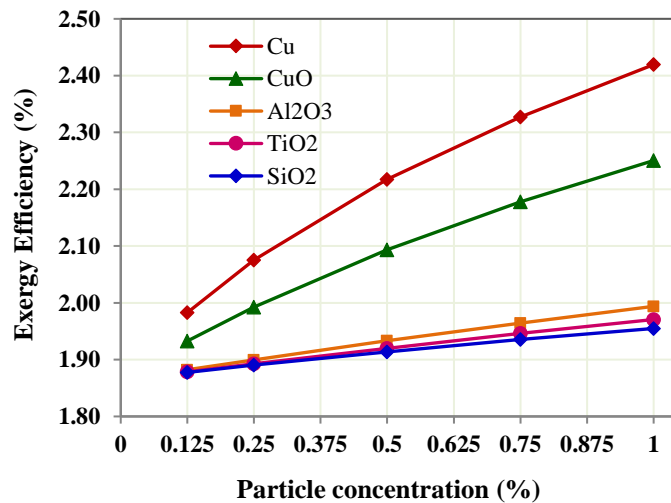
Fig.4.6 Exergy efficiency as a function of particle concentration

Total entropy generation is nothing but the sum of entropy generation due to heat transfer and entropy generation due to fluid flow. The total entropy generation by different working fluids as a function of particle concentration is presented in Fig. 4.7. By increasing the

73

nanoparticles concentration in base fluid, the entropy generation due to frictional resistance is increased. By increasing the particle concentration, the density gradients and subsequent frictional resistance increased and leads to increase the entropy generation due to fluid flow. However, the enhanced thermal transport properties of nanofluid leads to increase the convective heat transfer coefficients, which subsequently reduce the temperature gradients between the absorber plate and working fluid. Thereby, the convective and radiative losses from the hot absorber plate are minimised and improve the useful work potential in terms of exergy gain. Nevertheless, the increased entropy generation due to fluid flow is very much less and is dominated by the reduced entropy generation due to heat transfer rate. Therefore, the net entropy generation of a nanofluid is minimised.

It is noteworthy to understand that the Bejan number relates the various atmospheric and operating parameters that influences the entropy generation. Bejan number represents the impact of entropy generation due to heat transfer in the total entropy generated in a SFPC.
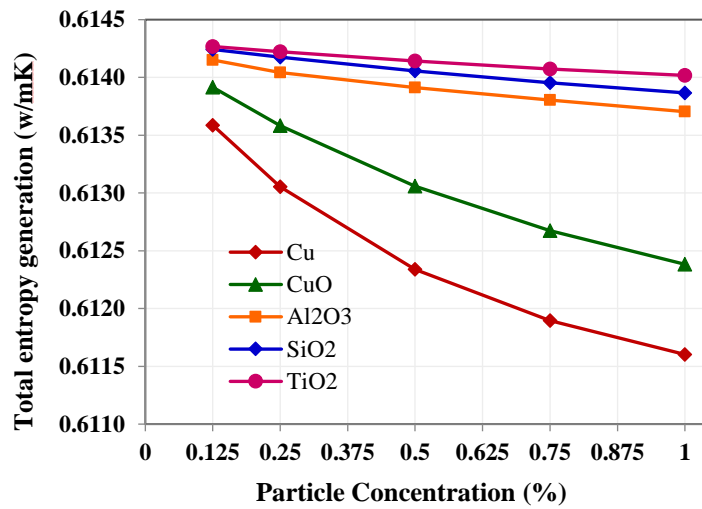
Fig. 4.7 Total entropy generation as a function of particle concentration
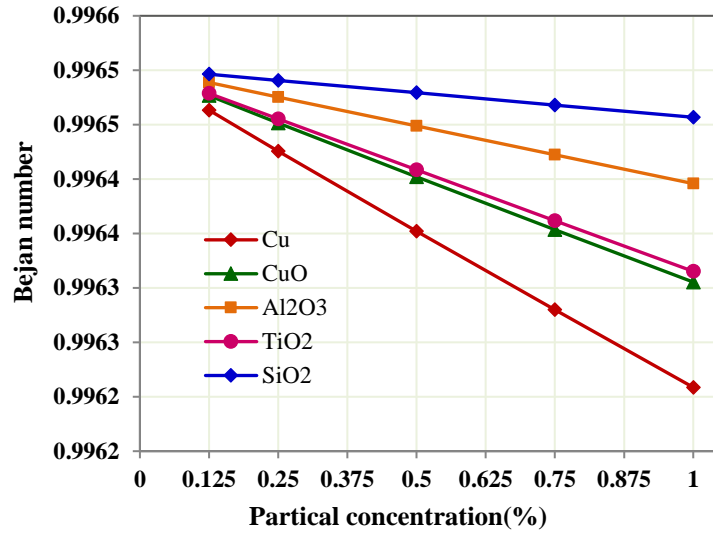
Fig. 4.8 Bejan number as a function of particle concentration

Fig. 4.8 shows the variation of Bejan number for different nanofluids as a function of particle concentration. In SFPC, entropy is generated due to heat transfer as well as fluid flow. It is clear from Eq (4.40) that the influence of entropy generation due to heat transfer is more on Bejan number. The nanofluid having lower entropy generation due to heat transfer will give lower Bejan number. Since, the Cu/water nanofluid exhibiting higher thermal transport properties, the Bejan number of Cu/water nanofluid is lower than other nanofluids and it is gradually reducing with particle concentration

4.2.3. Size reduction of SFPC with different working fluids

The enhanced thermal efficiency of SFPC using nanofluids as working fluid provides a platform to reduce the size of collector. For the equivalent thermal efficiency of SFPC with water as working fluid, the size of collector can be reduced in terms of collector area. Thermal efficiency of SFPC operated with any working fluid can be estimated by Eq (4.20). The possible reduction in area of the collector operating with different working fluids can be estimated by:

$$A_c = \frac{\dot{m}C_p(T_{f,out} - T_{f,in})}{I_t \eta} \tag{4.41}$$

The larger size of collectors not only increases the manufacturing cost but also increases the pressure drop across the collector. Along with the minimization of frictional resistance/pressure drop, the reduced size of the collector will also control the embodied energy associated with different materials used to fabricate the collector. The energy embodied in a material is nothing but the total energy associated with the material from the stage of extraction from ore to transforming the material into desired final goods [186]. By reducing the size of the collector,

corresponding embodied energy is minimized. The embodied energy of a typical SFPC materials is for glass 20.08 MJ/kg, copper 69.02 MJ/kg and rock wool 18.11 MJ/kg [187]. The embodied energy that can be saved by nanofluid based SFPC is presented in table 4.2.

Table 4.2 Total embodied energy associated with the SFPC operated with different working fluids, and the energy that can be saved with nanofluid based SFPC.

	Water	Al_2O_3/ water	Cu/ water	CuO/ water	SiO_2/ water	TiO_2/ water
Energy Embodied (MJ)	685.39	617.70	588.8522	599.5542	655.3883	627.3036
Energy that can be saved (MJ)		68.48	96.61	85.25	46.67	57.01

The enhanced thermophysical properties of nanofluid facilitate to scale down the surface area of SFPC without affecting the desired collector efficiency.

Fig. 4.9 Percentage of reduction in collector area with different nanofluids

The percentage of reduction in collector area with different nanofluids is exemplified in Fig. 4.9. From Eq (4.41) one can calculate the absorb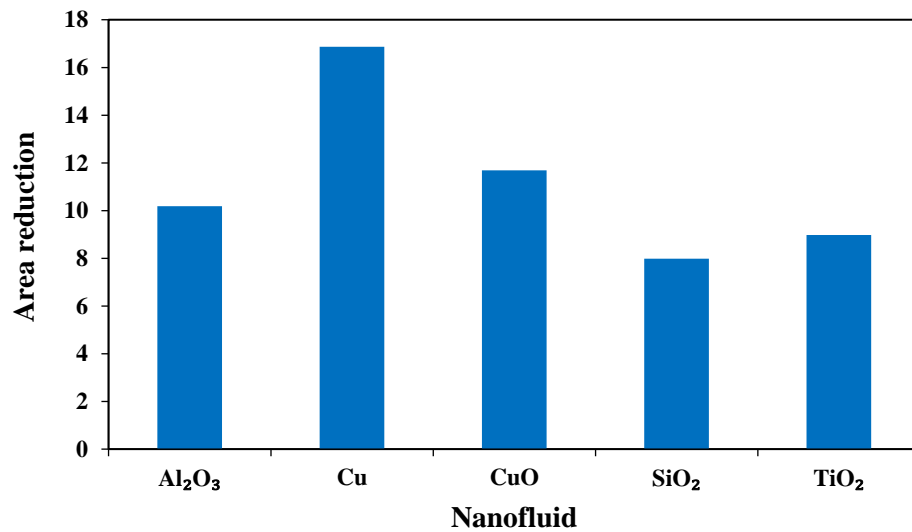er area of SFPC operated with nanofluids. From table 4.2, embodied energy that can be saved is also more for Cu/water nanofluid based SFPC followed by CuO/water nanofluid based SFPC.

4.2.4 Experimental studies on FCIDASFPC

Experiments are conducted on designed SFPC test rig in order to evaluate its performance. The schematic diagram of SFPC working under forced circulation that absorbs the incident radiation in indirect absorption mode is as shown in Fig. 4.10. The photographic view of FCIDSFPC test rig is presented in Fig. 4.11. The principle functionality of SFPC is, the absorber surface is heated up by the incident solar radiation falling on it and this absorbed heat is transferred to the working fluid. The working fluid is passing inside the riser tubes. The riser tubes are abided at the underneath of absorber plate. The optimum tilt angle of the collector is located at an angle approximately near to latitude of location. The variation of the collector's tilt angle is 5° to 10° for cooling applications, -10° to +10° for space heating and +5° is for water heating applications [188]. SFPC is oriented towards due south in northern hemispheric zone and vice versa for southern hemispheric zone locations to absorb more incident radiation [189]. Selection of appropriate materials for the various parts of collector is a critical stage, which affect the performance of collector. One has to choose the material such that it should have longer effective life despite of adverse effects from wide range of solar spectrum, environmental impacts, and corrosion and so on.

Glazing material: It should allow the maximum incident radiation falling on it and has to reduce the losses to environment to the extent possible. Low iron glass is the most common glazing material that transmits the maximum incident short wave radiation to the absorber plate and acts as opaque to long waves [190]. The transmittance of the glass is improved by optical polishing.

Absorber plate: The solar radiation reaches the absorber plate through the glazing material. The absorber plate should able to absorb the maximum possible radiation fall on it with minimum thermal losses to atmosphere and also it is thermally stable for a range of operating temperatures. The absorber plate is made with copper to absorb and transmit the maximum absorbed energy to the working fluid. The absorber plate is coated with Nichrom black selective coating as a thin layer to improve the absorptance of incident radiation and to lower the emissivity.

Risers: Risers are made with copper and welded at the underneath of the absorber plate. They should have good thermal bond with the absorber plate so as to reduce the conductive resistance and consequent thermal losses.

Insulation: The edges and bottom of the collector are well insulated with glass wool to minimize the heat loss to atmosphere.

The experiments are conducted with different working fluids such as water, Al_2O_3/water, Cu/water, CuO/water, TiO_2/water, and SiO_2/water nanofluids. All the experiments are conducted as per ASHRAE standards 93- 86 [190]. Based on independent scattering phenomenon the particle concentration in all nanofluids is restricted to 1.0 % only. The specifications of test rig used to conduct the experiments are presented in table 4.3.

Table 4.3 Specifications of FCIDASFPC experimental test rig

Collector over all dimensions		590X420X124 mm
Header	Copper	ϕ 25X450 mm
Riser	Copper	ϕ 10X500 mm
Absorber plate	Copper	0.15 mm
Absorber coating		Nichrome black coating
Glass	Toughened glass optically polished	3mm thickness
Insulation	Glass wool	75 mm thickness
Spacer	Wood	25 mm height
Frame	Wood	10 mm thick
Tank	Stainless steel tank	10 Litres capacity
Flow meter	Rotameter	0- 4 LPM
Thermocouples	K-Type	Ranging 0- 260 ºC
No of risers		7 No's
Pump		0.25 HP

Pilot experiments are conducted on SFPC in indirect absorption configuration operating in forced circulation mode with water and Cu/water, CuO/water, Al_2O_3/water, TiO_2 /water and SiO_2/water nanofluids. To examine and compare the instantaneous efficiency among different working fluids, maximum particle concentration of 1.0 % is considered for all nanofluids to avoid dependent scattering of nanoparticles. The instantaneous efficiency obtained by different working fluids is illustrated in Fig. 4.12 (a). Since all the nanofluids exhibiting higher efficiency at lower heat loss range, a closer view presented in Fig 4.12 (b). The instantaneous efficiency of SFPC with Cu/water, CuO/water, Al_2O_3/water, TiO_2 /water and SiO_2/water nanofluids is

16.86 %, 11.69 %, 10.18 %, 8.97 % and 7.98 % respectively compared to water. It is clear from the experimental results of SFPC operated with Cu/water exhibiting higher instantaneous efficiency than other nanofluids and it is followed by CuO/water nanofluid.
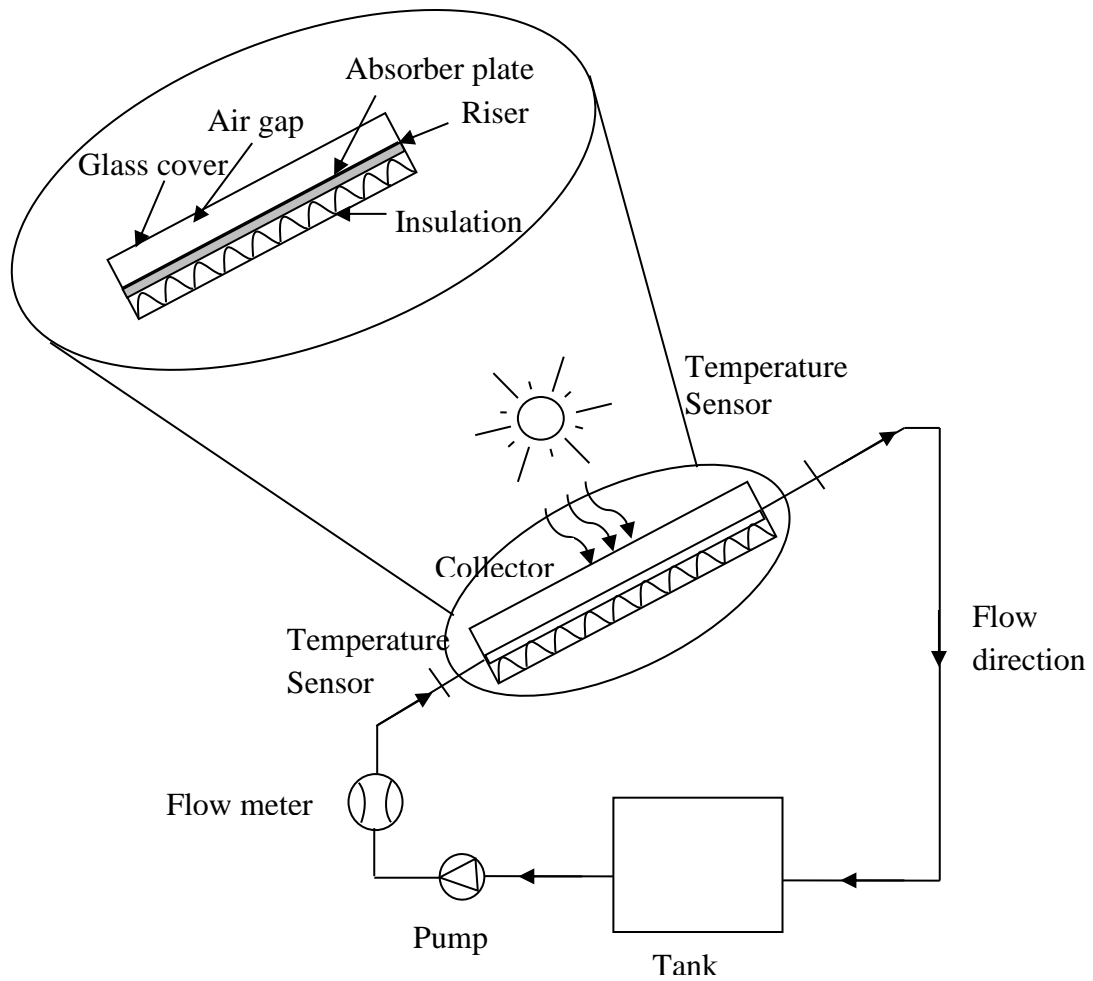
Fig. 4.10 Schematic diagram of FCIDASFPC

Fig. 4.11 Photographic view of FCIDASFPC with accessories.
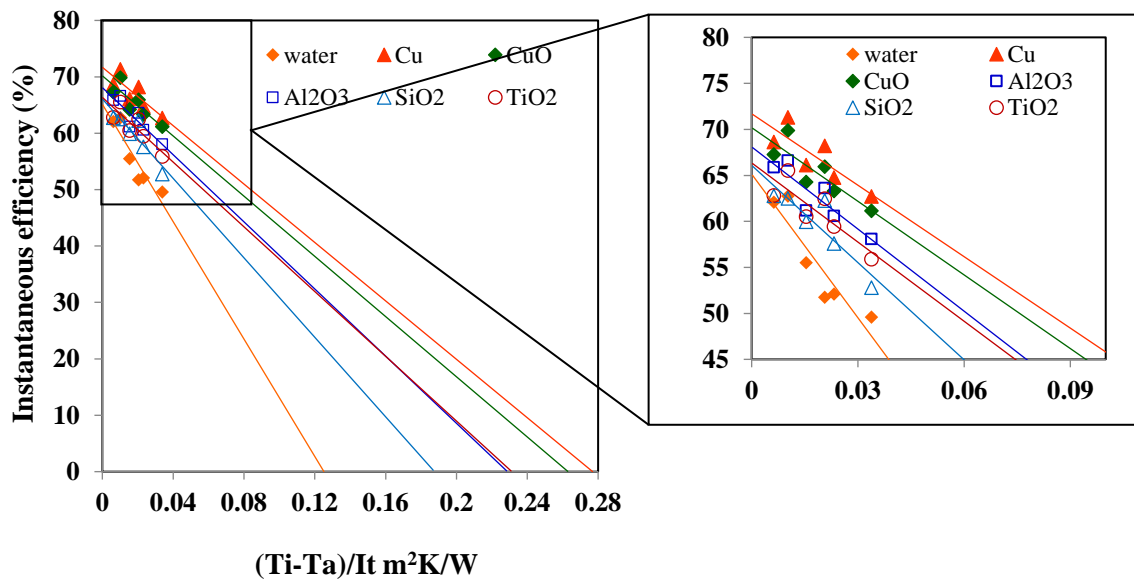
Fig 4.12 (a) Instantaneous efficiency of SFPC with different nanofluids

Fig 4.12 (b) Instantaneous efficiency at magnified view

4.2.5 Remarks from experimental, analytical, and size reduction analysis

Analytical, experimental and size reduction studies are conducted with different working fluids such as Cu/water, CuO/water, Al_2O_3/water, TiO_2/water, and SiO_2/water and water. It can be observed from the experimental, analytical, and size reduction evaluations that the collector

operated with Cu/water and CuO/water nanofluids exhibits higher thermal efficiency and lower collector area than all other working fluids.

Therefore, Cu/water and CuO/water nanofluids are considered for further analytical and experimental studies. Though, Cu/water nanofluid gives a higher thermal performance but it is highly reactive and it is economically not feasible. Therefore, by hybridising the Cu and CuO nanoparticles a new Cu-CuO hybrid nano composition is proposed. The thermophysical properties of hybrid nanofluids are discussed in earlier chapter in detail. The influence of amalgamated thermophysical properties due to synergistic effect on the performance of SFPC is discussed in foregoing sections.

The experimental studies are carried out on SFPC with indirect configuration operating on forced circulation mode operating with water, Cu-CuO/water hybrid nanofluid, mono nanofluids prepared by its individual constituents as working fluids. Initially experiments are conducted on SFPC to study the influence of particle concentration in mass flow rate on instantaneous efficiency. For this study, Cu/water nanofluid is considered as working fluid in SFPC.
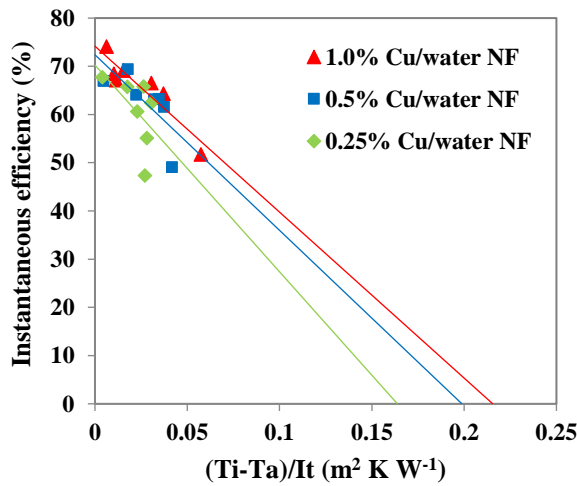
Fig. 4.13 Instantaneous efficiency of SFPC with Cu/water nanofluid as function of particle concentration
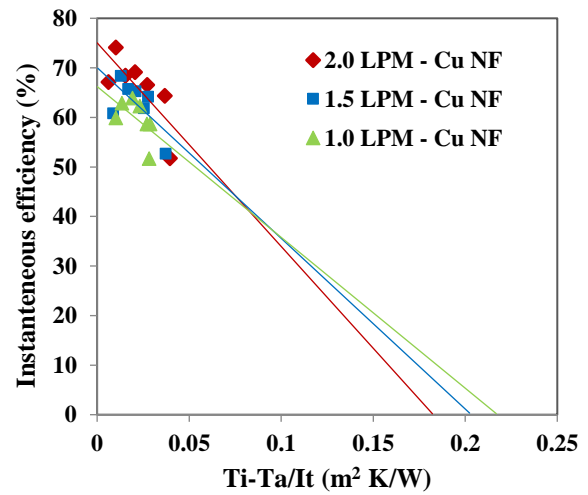
Fig. 4.14 Instantaneous efficiency of SFPC with Cu/water nanofluid as function of mass flow rate

It is clear from the experimental outcomes that, the instantaneous efficiency of SFPC is progressively increasing with the particle concentration and the maximum enhancement is noticed at 1.0 % particle concentration as shown in Fig 4.13. As mentioned in the chapter 3 the particle concentration is restricted to 1.0 % by considering independent scattering phenomenon. The instantaneous efficiency of SFPC is increasing with particle concentration due to the

enhanced thermal properties. The enhanced thermal transport properties of nanofluid with particle concentration promote the convective heat transfer coefficient, which in turn raise the heat removal factor and corresponding energy absorbed parameter of solar collector. In contrary, the heat loss parameter is also increasing with the particle concentration. Thus, further increment of particle concentration may lead to raise the heat losses from the collector that consequently lowers the instantaneous efficiency [191]. On the other hand, experiments are also conducted at different mass flow rates. Fig 4.14 elucidate that as the mass flow rate increases more amount of working fluid is in-contact with the collector tubes and hence the temperature gradients between the absorber plate and bulk fluid is reduced. The lower temperature gradient leads to reduce the heat loss parameter from the collector and improves the energy removal rate and corresponding instantaneous efficiency of collector.

It can be observed from the above experimental studies that, instantaneous efficiency of SFPC is higher particle concentration and mass flow rates. Therefore, all the foregoing experiments are carried out at 1.0 % particle concentration and 2.0 LPM mass flow rate. Fig. 4.15 interprets the instantaneous efficiency of SFPC with mono and hybrid nanofluids at 1.0 % particle concentration and 2 LPM flow rate. Amid all SFPC with Cu/water nanofluid exhibits the higher instantaneous efficiency that other working fluids due to more enhancements in thermal conductivity and consequent heat transfer coefficients. Increment in instantaneous efficiency of SFPC with CuO/water, Cu-CuO/water and Cu /water nanofluids is 9.81 %, 10.55 % and 16.86 % respectively compared to water.

The difference between analytical and experimental instantaneous efficiency under the similar operating conditions are illustrated in Fig. 4.16. It is noticed that the analytical approach is over estimating the collector efficiency by 4.42% to 11.39% than that of experimental approach. The considerable reasons for the marginal variation of instantaneous efficiency between analytical approach and experimental results are (i) in case of analytical approach the material properties and operating conditions are assumed to be ideal and constant but practically materials will not posses ideal characteristics (ii) solar radiation and ambient conditions are inconsistent in experimental studies. Error analysis is carried out to account the possible errors associated with the measuring devices while conducting the experiments. The errors associated with the experimental results are 2.97 % which is marginally lower than the enhanced instantaneous efficiency. Therefore, the enhanced instantaneous efficiency measured from the experimental results is true and reliable.
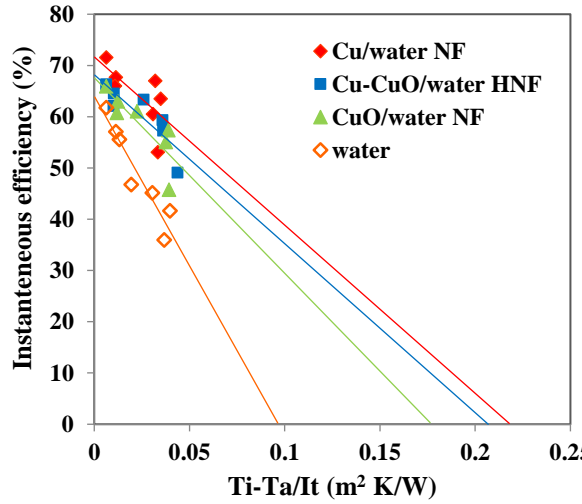
Fig. 4.15 Experimentally measured instantaneous efficiency of FCSFPC with water, mono and hybrid nanofluids
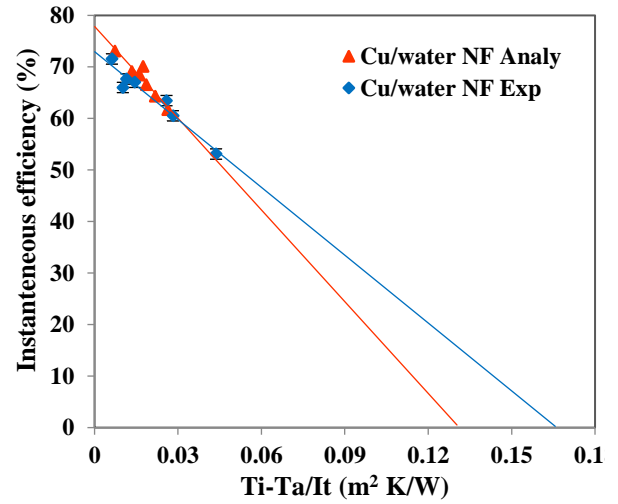
Fig. 4.16 Experimentally measured instantaneous efficiency of FCSFPC with water, mono and hybrid nanofluids

Instantaneous efficiency of indirect absorption SFPC operating in forced circulation mode is measured over a day, with different working fluids at different mass flows are presented in Fig. 4.17. The efficiency is estimated at NIT Warangal (79.53ºE and 17.98ºN) with latitude of location as tilt angle of collector and by keeping the collector orientation towards the due south.
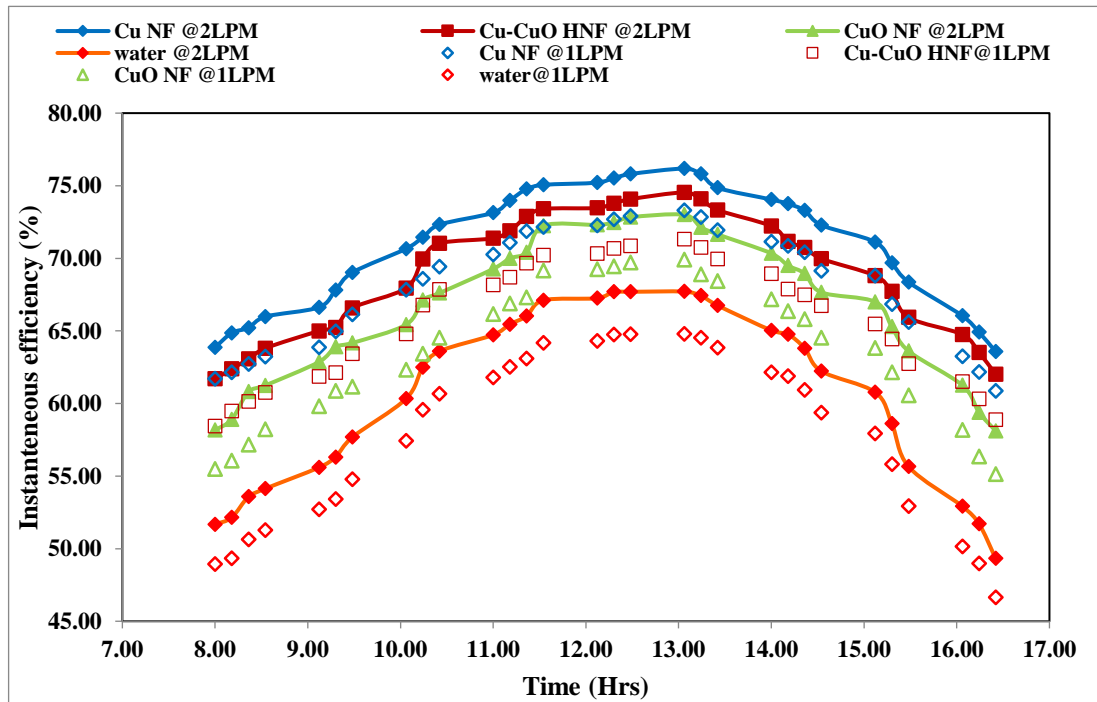
Fig. 4.17. Instantaneous efficiency of FCSFPC over a day operated with different working fluids at different mass flow rates

4.3 Forced Circulation Direct Absorption Solar Flat Plate Collector (FCDASFPC)

Another efficient configuration of solar collectors to convert the incident solar radiation into useful form of temperature rise of working fluid is direct absorption/volumetric collectors. In direct absorption collectors working fluid is flow between the absorber plate and glass cover. The upper side of collector is covered with the glass cover. The solar radiation incident on collector is passed through the glass cover and reaches the working fluid. The radiation transmitted through the glass cover is directly absorbed by the working fluid without any other thermal resistance like air gap, absorber plate, and risers. Bottom and sides of the collector is well insulated so as to make it adiabatic. In direct absorption configuration along with the thermophysical properties, optical properties of working fluid also play a key role on absorption of solar radiation incident on collector. By allowing the solar radiation directly on to the working fluid, thermal resistances associated with conduction and convection are marginally reduced and subsequently improves the collector efficiency. The type of collector used for the analysis is described in Fig. 4.18. The suspension of nanoparticles will significantly ameliorate the optical properties of nanofluid and causes for enhancing the radiation absorption capacity and consequent collector efficiency.
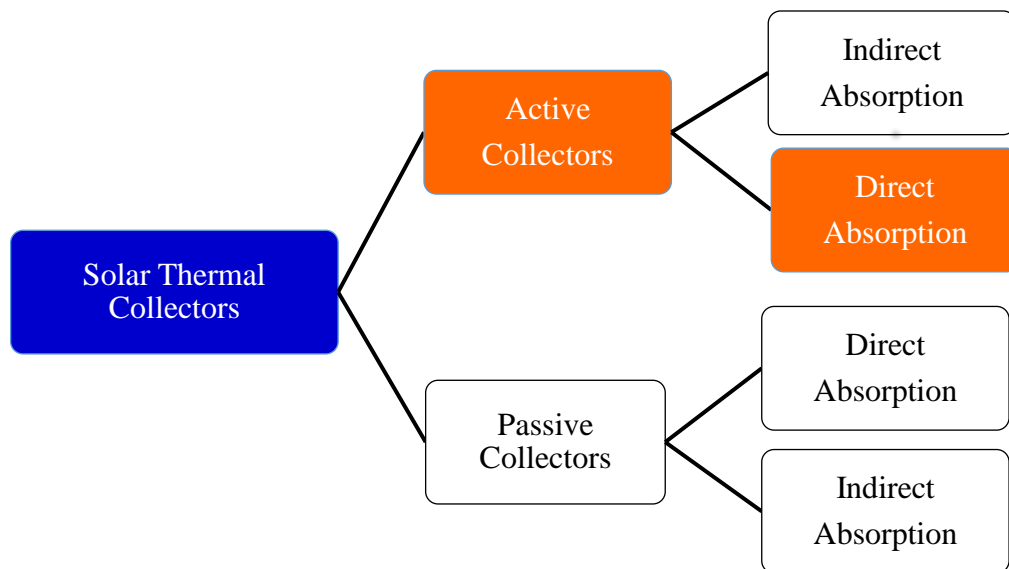
Fig. 4.18 Solar flat plate collectors operating in direct absorption configuration at active (Forced Circulation) mode

In direct absorption collector since the working fluid passes between the glass cover and absorber plate, some of the thermal resistances such as convective resistance between air and

absorber plate, conductive resistance between absorber and riser tubes and convective resistance between riser tubes are minimised. The reduced thermal resistance lead to improve the instantaneous efficiency of DASFPC. Specifications of collector and operating parameters of DASFPC are presented in table 4.4.

Table: 4.4 Specifications and operating parameters of DASFPC

Overall dimensions of collector	$550 \times 450 \text{mm}^2$
Glazing cover	Glass: Low iron toughened glass
	Number of Glass covers, N_g: Single
	Thickness: 3 mm
	Transmissivity, τ_g: 92 % of solar radiation
	Emissivity, ε_g: 88% of solar radiation
Absorber	Material: Copper
	Surface area: 0.211 m^2
Insulation	Material: Rockwool
	Insulation density : 48 gm/m^3
	Base insulation thickness, t_b: 50 mm
	Edge insulation thickness, t_e: 25 mm
	Thermal conductivity, k_i: 0.04 W/mK
Working fluid	Water
	Cu/Water nanofluid
	CuO/Water nanofluid
	Cu-CuO/water hybrid nanofluid
Wind velocity, v_w	2 m/s
Collector tilt angle, β	18.59^o latitude at NIT Warangal
Fluid inlet temperature, T_i	300 K
Apparent sun temperature T_{sun}	4350 K
Absorber plate thickness, t_p	0.12 mm
Transmittance-Absorptance product ($\alpha\tau$)	0.84

Fig. 4.19 Schematic view of direct absorption solar flat plate collector

4.3.1 Thermodynamic analysis of FCDASFPC

The energy conversion and energy transfer of a thermal system can be appropriately analyzed by conducting the thermodynamic analysis on it. In thermodynamic analysis first law quantifies the energy transfer and its influencing parameters, while second law is a qualitative measure of irreversibilities and associated entropy generations in solar collector.

4.3.1.1 Energy analysis on FCDASFPC

The net solar radiation incident on DASFPC is given by:

$$I_{b\lambda}(\lambda, T_{solar}) = \frac{2hC_0^2}{\lambda^5\left[exp\left(\frac{hC_0}{\lambda k_B T_{solar}}\right)-1\right]} \tag{4.41}$$

The intensity of incident solar radiation is assumed to vary in perpendicular direction to the fluid flow i.e. across the fluid film thickness only.

As the incident radiation passes through the working fluid its intensity is attenuated due to absorption and scattering phenomenon.

Absorption efficiency of nanoparticle can be estimated by:

$$Q_{a\lambda,np} = 4 \propto Im\left\{\frac{m^2-1}{m^2+2}\left[1+\frac{\propto^2}{15}\left(\frac{m^2-1}{m^2+2}\right)\right]\frac{m^4+27m^2+38}{2m^2+3}\right\} \tag{4.42}$$

and scattering efficiency of nanoparticle is:

$$Q_{s\lambda.np} = \frac{8}{3}\propto^4\left|\frac{m^2-1}{m^2+2}\right|^2 \tag{4.43}$$

where, size parameter, $\propto = \frac{\pi D}{\lambda}$

and complex refractory index, $m = \left(n_{np} + ik_{np}\right)/n_{bf}$

in which, 'n_{np}' is the real part of the refractive index that is responsible for the propagation of electromagnetic waves in the fluid medium while 'ik_{np}' is the imaginary part that is responsible

for the attenuation of incident radiation. The nanoparticles in the base fluid should be sufficiently dilute (maximum 1.0 % particle concentration) such that no interference of scattering occurs between the neighboring particles.

Sum of the absorption efficiency and scattering efficiency is commonly termed as extinction efficiency and it can be calculated by:

Extinction efficiency, $Q_{e\lambda} = Q_{a\lambda} + Q_{s\lambda}$ (4.44)

For pure liquids like water attenuation is caused by absorption only

Therefore, extinction coefficient of water, $K_{a\lambda} = \frac{4\pi k}{\lambda}$ (4.45)

where k is the absorption index.

In total radiation incident on fluid, maximum amount of radiation is absorbed by working fluid and very little amount is scattered due to the presence of nano sized solid particles in the fluid medium. However, the influence of scattering effect is negligible at the lower particle concentrations. Sum of the absorbed and scattered coefficients are termed as extinction coefficient.

The extinction coefficient of nanoparticle is given by: $K_{e\lambda} = \frac{3\phi_v Q_{e\lambda}}{D}$

where, $Q_{e\lambda}$ is the extinction efficiency, which is the sum of absorption and scattering efficiencies.

The extinction coefficient of nanofluid is the sum of extinction coefficients of base fluid and nanoparticle and it is estimated by:

$K_{e\lambda,nanofluid} = K_{e\lambda,water} + K_{e\lambda,nanoparticle}$ (4.46)

The radiative properties of the nanofluid are the sum of radiation properties of nanoparticle as well as the base fluid

The distribution of radiation intensity within the nanofluid is given by:

$\frac{\partial I_\lambda}{\partial y} = -K_{e\lambda,nanofluid} I_\lambda = -\left(K_{e\lambda,water} + K_{e\lambda,nanoparticle}\right) I_\lambda$ (4.47)

The energy balance equation of DASFPC accounts both thermophysical and radiative properties of working fluid and it is given by Eq 4.48:

$\rho C_p \frac{\partial T}{\partial t} = k \frac{\partial^2 T}{\partial y^2} + q(y)$ (4.48)

It is assumed that the heat would be lost to surrounds from the top surface of the receiver and it is depending on convective heat loss coefficient and thermal re-radiation of the fluid. Therefore, total heat loss from the collector is given by:

$$\frac{\partial T}{\partial t}_{y=0} = h(T_{top} - T_{amb}) + \varepsilon\sigma(T_{top}^4 - T_{amb}^4) \tag{4.49}$$

Bottom wall of the collector is assumed to be opaque and adiabatic, $\frac{\partial T}{\partial t}_{y=H} = 0$ (4.50)

The radiative transport equation in y-direction is given by:

$$q(y) - \frac{d}{dy}\int_0^\infty I(y)\,d\lambda \tag{4.51}$$

where, $I(y) = I_{b\lambda}(\lambda, T_{solar})\exp(-K_{e\lambda}y)$

The energy balance equation is solved by applying appropriate boundary conditions of Eq 4.49 and Eq 4.50 and estimated the outlet temperature of working fluid.

Therefore, the instantaneous efficiency of DASFPC, $\eta = \frac{\dot{m}C_p(T_{f,out}-T_{f,in})}{I_t A_c}$ (4.52)

4.3.1.2 Exergy analysis of FCDASFPC

With the assumption of no chemical reactions within the working fluid and by neglecting the kinetic energy variations of collector, the overall exergy balance of FCDASFPC is given by:

$$\sum\dot{Ex}_{in} - \sum\dot{Ex}_{out} = \sum\dot{Ex}_{dest} \tag{4.53}$$

which can be re-write as

$$\dot{Ex}_{heat} - \dot{Ex}_{work} + \dot{Ex}_{mass,in} - \dot{Ex}_{mass,out} = \dot{Ex}_{dest} \tag{4.54}$$

Exergy due to incident solar radiation, $\dot{Ex}_{heat,in} = \left(1 - \frac{T_{amb}}{T_{sol}}\right)\dot{Q}_{sol}$ (4.55)

where, $\dot{Q}_{sol} = I_t(\tau\alpha)A_c$

$$\dot{Ex}_{mass,in} = \dot{m}[(h_{in} - h_{amb}) - T_{amb}(S_{in} - S_{amb})] \text{ and} \tag{4.56}$$

$$\dot{Ex}_{mass,in} = \dot{m}[(h_{out} - h_{amb}) - T_{amb}(S_{out} - S_{amb})] \tag{4.57}$$

By making exergy balance

$$\left(1 - \frac{T_{amb}}{T_{sol}}\right)\dot{Q}_{sol} - \dot{m}C_p(T_{out} - T_{in}) + \dot{m}C_pT_{amb}ln\left(\frac{T_{out}}{T_{in}}\right) = \dot{Ex}_{dest} \tag{4.58}$$

and exergy efficiency, $\eta_{Ex} = 1 - \frac{\dot{Ex}_{dest}}{\left(1-\frac{T_{amb}}{T_{sol}}\right)\dot{Q}_{sol}}$ (4.59)

Total entropy generation in the collector, $\dot{S}_{gen} = \dot{m}C_pln\left(\frac{T_{out}}{T_{in}}\right) - \frac{\dot{Q}_{sol}}{T_{sol}} + \frac{\dot{Q}_{lost.amb}}{T_{amb}}$ (4.60)

4.3.2 Experimental investigations on FCDASFPC

Experimental investigations are carried out to study and compare the instantaneous efficiency of DASFPC operated with different working fluids. The influence of thermophysical and optical properties on collector efficiency is analyzed. Experiments are conducted on

designed test rig in direct absorption configuration operated in forced circulation mode. Cu/water, CuO/water, Cu-CuO/water nanofluids and water are considered as working fluids. The schematic diagram of DASFPC is as shown in Fig. 4.20 and the photographic view is presented in Fig. 4.21. The principle functionality of DASFPC is, the working fluid flow beneath the glass cover as a thin layer and it absorbers the incident radiation that passes through glass cover. In DASFPC, extinction coefficient of working fluid plays a crucial role to absorb the incident radiation. In total radiation incident on glass cover, most of the short wave radiation is penetrated through the cover and it is attenuated by absorption of working fluid. Extinction coefficient of working fluid is responsible for the penetration and absorption of incident radiation. Similar to the indirect absorption in the direct absorption configuration also the collector is oriented towards the due south with an optimum tilt angle of 18.59° E which is equivalent to the latitude of NIT Warangal.

Selection of appropriate materials for fabricating the test rig is a key stage and the details of material selection are discussed in the FCIDASFPC section. The geometrical and material specifications are presented in table 4.5.

Table 4.5 Specifications of FCDASFPC experimental test rig

Collector over all dimensions		590X420X124 mm
Header	Copper	ϕ 25X450 mm
Absorber plate	Copper	0.15 mm
Glass	Optically polished	3mm thickness
	Low iron toughened glass	
Insulation	Glass wool	75 mm thickness
Tank	Stainless steel tank	10 Litres capacity
Flow meter	Rotameter	0- 4 LPM
Thermocouples	K-Type	Ranging 0- 260 °C
Absorber coating		Nichrome black coating
Pump		0.25 HP
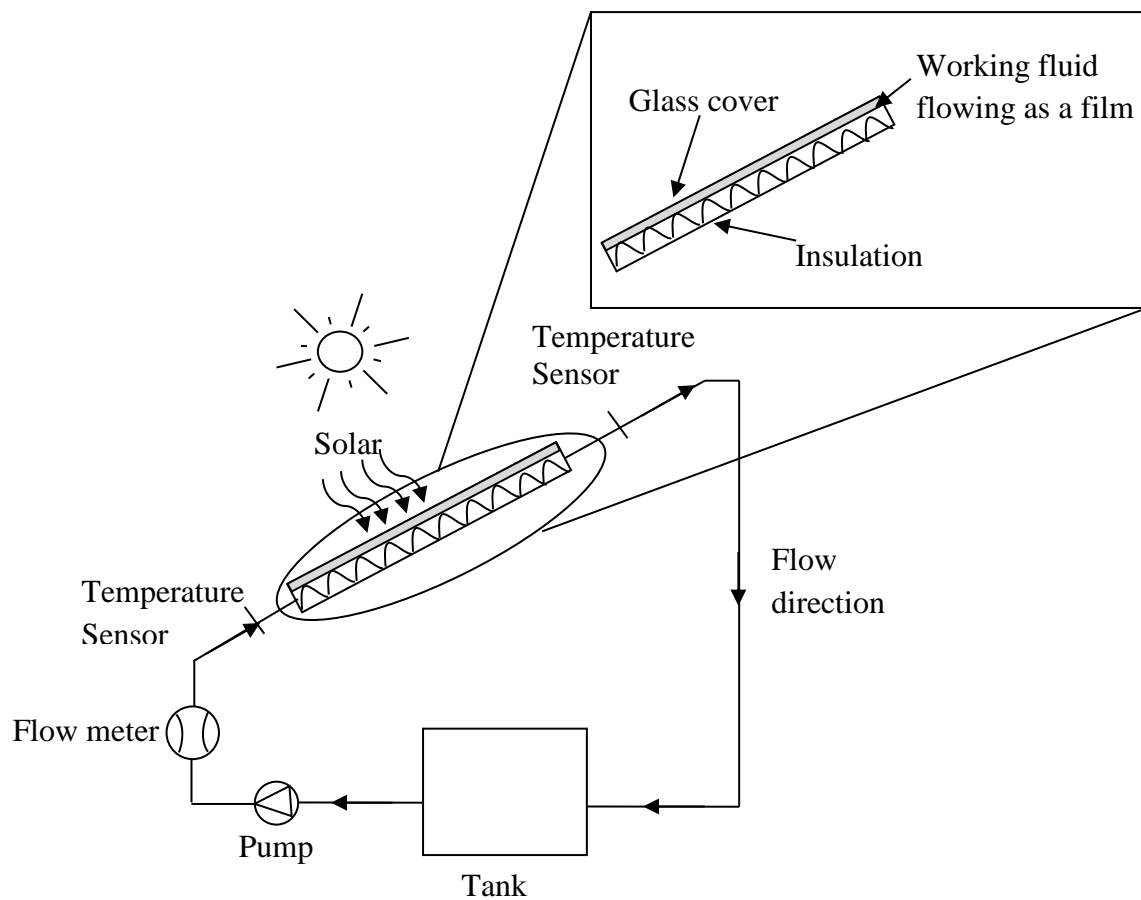
Fig. 4.20 Schematic diagram of forced circulation direct absorption solar flat plate collector

Major components

1.DASFPC

2.Temparature sensors

3.Tank

4. Connnecting pipes

5. Rotameter

Fig. 4.21 Photographic view of FCDASFPC experimental test rig with mass flow meter and temperature sensors

4.3.3 Results and discussion

In case of DASFPC, along with the thermophysical properties, contribution of optical properties is also pivotal. Most of the congenital energy in solar radiation is abide in the visible wavelength region but the conventional working fluid like water has poor absorption capability in this visible region [1]. The Fig 4.22 depicts the extinction coefficient of water as a function of wavelength. One can be observed from the graph that water has very low extinction coefficient for short wave radiation and it is relatively more for longer wavelengths. By suspending the nano sized solid particles in water, the resultant optical properties are intensified and absorb more incident radiation [108]. Fig. 4.22 describes the reinforcement of extinction coefficient by suspending copper nanoparticles in water at various particle concentrations. The homogenous suspension of copper nanoparticle should substantially increase the extinction coefficient of Cu/water nanofluid as shown in Fig. 4.22. It is clear from figure that the extinction coefficient of Cu/water nanofluid is substantially increasing with the particle concentration. It can be observed from Fig. 4.22 that Cu/water nanofluid exhibits higher extinction coefficients at ultraviolet and visible regions and it is relatively low in infrared region of solar spectrum. Since, the extinction coefficient of pure water as function of wavelength is presented in Fig. 4.22, scattering coefficient of Cu/water nanofluid is not delineated on it. However, the scattering coefficient is very less because of particle size is at nano scale and the particle concentration is within independent scattering region.
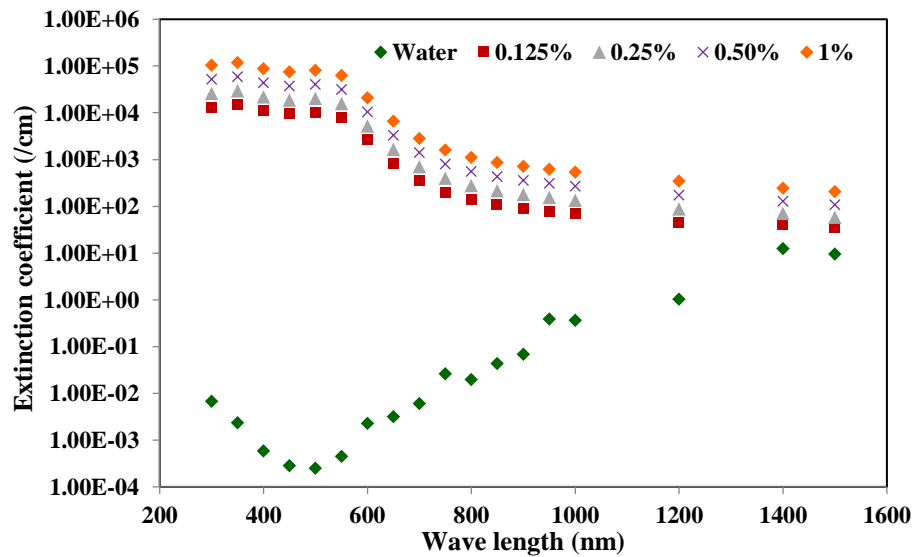
Fig.4.22 Extinction coefficient of Cu/water nanofluid at different concentrations as a function of wavelength

It can be observed from Fig 4.23 that, by suspending the CuO nanoparticle in water the extinction coefficient of CuO/water nanofluid is also enhancing compared to water and this enhancement is increasing with the particle concentration.

Fig. 4.23 Extinction and scattering coefficients of CuO/water nanofluid at different concentrations as a function of wavelength
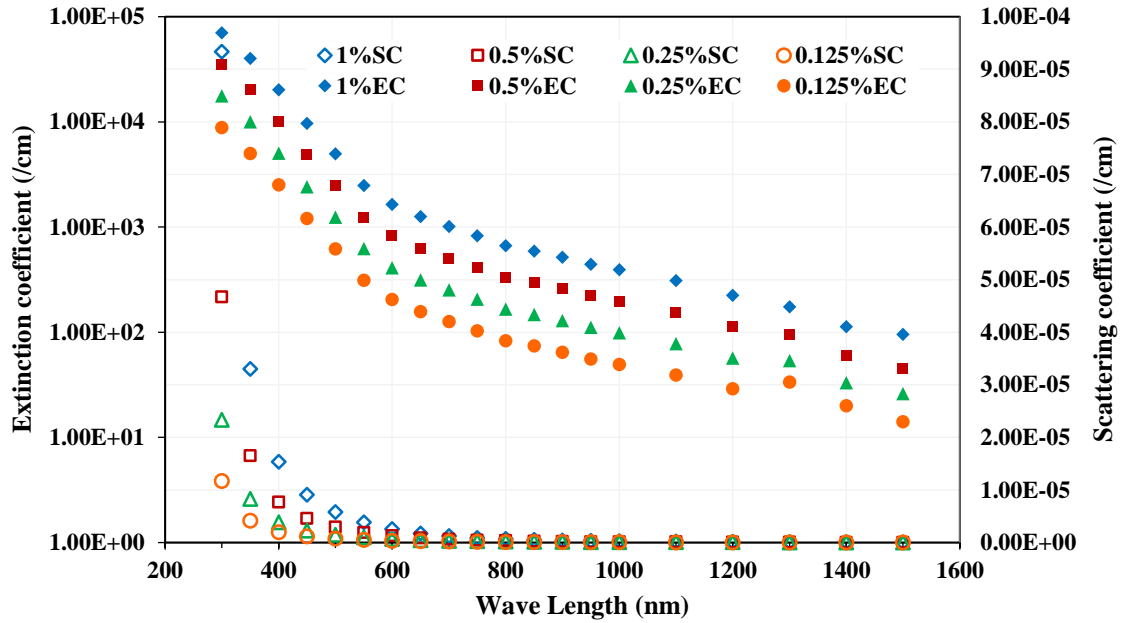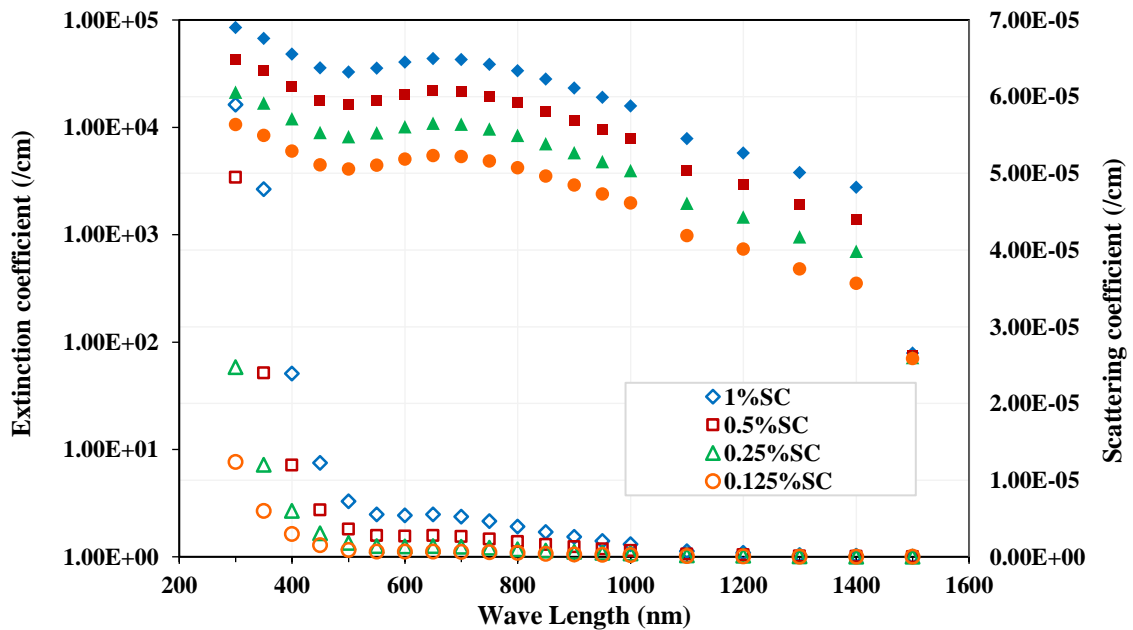

Fig.4.24 Extinction and scattering coefficients of Cu-CuO/water hybrid nanofluid at different concentrations as a function of wave length

It is clear from Fig. 4.23 that, CuO/water nanofluid exhibits higher extinction coefficient at ultraviolet region and it is exponentially decreasing from visible region to infrared region of

solar spectrum. Fig. 4.23 also depicts the scattering coefficient of CuO/water nanofluid at different particle concentrations and it can be estimated from Eq (4.43). One can be observed from the scattering efficiency equation that the scattering efficiency is varying with the fourth power of size parameter. Therefore, its influence is much less and negligible [191].

By hybridizing the Cu nanoparticles with CuO nanoparticles, the resultant extinction coefficient of Cu-CuO/water hybrid nanofluid is ameliorated. It can be observed from Fig. 4.24 that the extinction coefficient of Cu-CuO/water hybrid nanofluid is enhanced in ultraviolet and visible region and it is gradually decreasing in infrared. One can observe from Fig. 4.24 that the influence of scattering coefficient in radiation absorption is very less it can be neglected at low volume fractions.

The efficiency of FCDASFPC with mono and hybrid nanofluids is analytically estimated and presented in Fig. 4.25. Among all Cu-CuO/water hybrid nanofluid exhibits the higher collector efficiency than individual constituent mono nanofluids. In direct absorption configuration, the incident the incident radiation is directly absorbed by the working fluid rather than it passed through the series of thermal resistance such as air gap, absorber plate and riser tubes unlike indirect absorption configuration which improves the collector efficiency. In can be observed from Fig 4.24 that the extinction coefficient of hybrid nanofluid is more over a wide range of solar spectrum than mono nanofluids, it absorbs more incident radiation than its individual constituents. The enhanced photo-thermal properties of hybrid nanofluid and reduced thermal resistance lead to improve the collector efficiency as shown in Fig. 4.25. However, the improved photo-thermal properties of nanofluid not only increase the incident radiation absorption capabilities but also minimize the heat losses due to irreversibilities. Fig 4.26 shows the exergy efficiency of SFPC with mono and hybrid nanofluids as a function of particle concentration. It can be observed from Fig 4.26 that among all, SFPC with Cu-CuO/water hybrid nanofluid exhibits higher exergy efficiency because of its improved photo thermal properties and reduced heat losses. Amelioration of optical and thermophysical properties lead to improve the thermal efficiency of hybrid nanofluid by 13.13 % more than water while exergy efficiency is improved by 16.07 % compared to water.
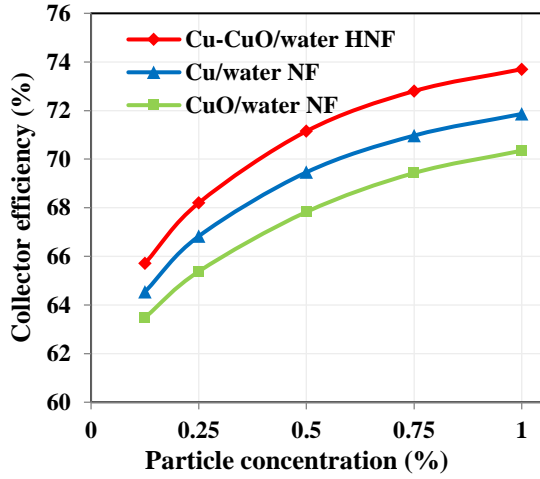
Fig. 4.25 Energy efficiency of SFPC with mono and hybrid nanofluids
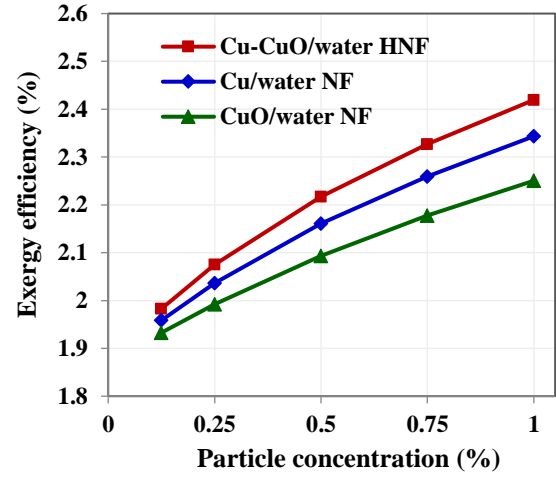
Fig. 4.26 Exergy efficiency of SFPC with mono and hybrid nanofluids

Experiments are conducted on direct absorption SFPC with water, mono nanofluid and hybrid nanofluid. It is clear from Fig. 4.27 that the instantaneous efficiency of Cu/water nanofluid is increasing with the particle concentration and higher instantaneous efficiency is noticed at 1.0 % nanoparticle concentration.
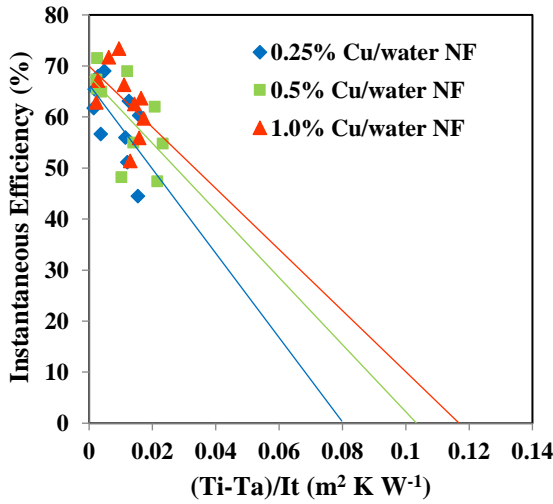
Fig. 4.27 Experimentally measured instantaneous efficiency of FCSFPC with Cu/water nanofluid
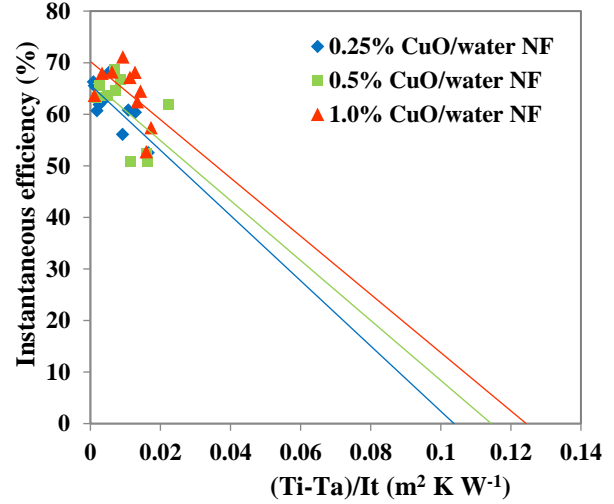
Fig. 4.28 Experimentally measured instantaneous efficiency of FCSFPC with CuO/water nanofluid

Similar kind of trend is observed for DASFPC with CuO/water and Cu-CuO/water nanofluids also as shown in Fig. 4.28 and Fig 4.29.

The instantaneous efficiency of DASFPC with both mono and hybrid nanofluids are presented in Fig. 4.30. It is observed that DASFPC with Cu-CuO/water hybrid nanofluid exhibits higher instantaneous efficiency than mono nanofluids. From Eq 4.51, the working fluid having higher extinction coefficient over a range of solar spectrum it absorbs more incident radiation and consequently instantaneous efficiency is improved.
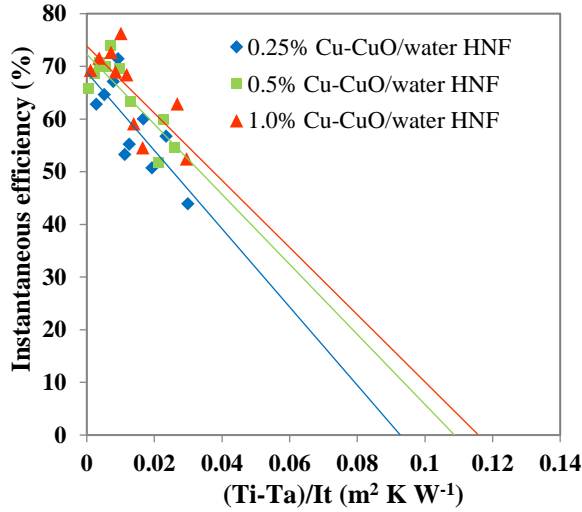
Fig. 4.29 Experimentally measured instantaneous efficiency of FCSFPC with Cu-CuO/water hybrid nanofluid
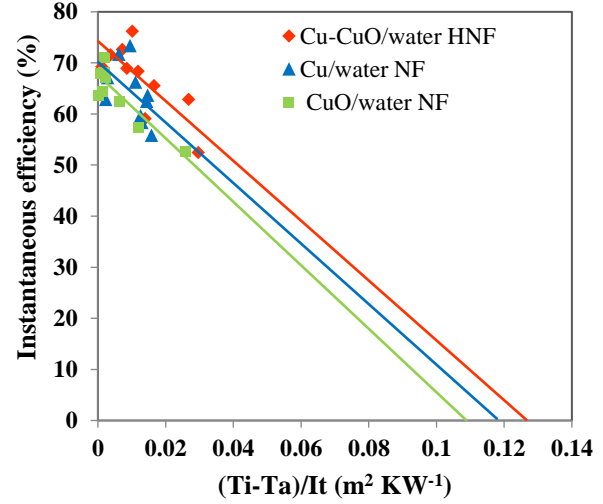
Fig. 4.30 Comparison of experimentally measured instantaneous efficiency of FCSFPC with mono and hybrid nanofluids

Though the thermophysical properties of Cu/water nanofluid are higher than that of hybrid nanofluid, the extinction coefficient of hybrid nanofluid plays a crucial role to improve the absorption capability of hybrid nanofluid. The instantaneous efficiency of DASFPC with Cu-CuO/water, Cu/water, CuO/water nanofluids are improved by 18.45 %, 13.64 %, and 11.34 % compared to water.

Comparatives studies are conducted between direct absorption and indirect absorption as illustrated in Fig. 4.31. Efficiency of both direct and indirect absorption collectors are compared by conducting the experiments at the same particle concentration of 1 % and at the mass flow rate of 2 LPM. Due to improved photo thermal properties and reduced thermal resistances direct absorption collector exhibits higher instantaneous efficiency than that of indirect absorption collectors. It is noticed that the direct absorption SFPC exhibits 7.9 % higher instantaneous efficiency compared to indirect absorption SFPC.
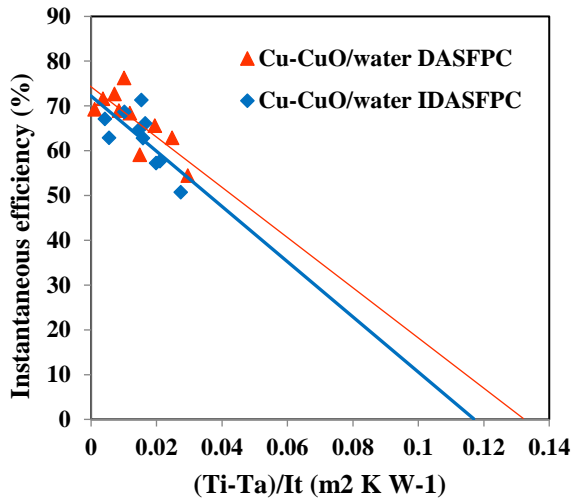
Fig. 4.31 Comparison of direct and indirect absorption configurations of FCSFPC with Cu-CuO/water hybrid nanofluid
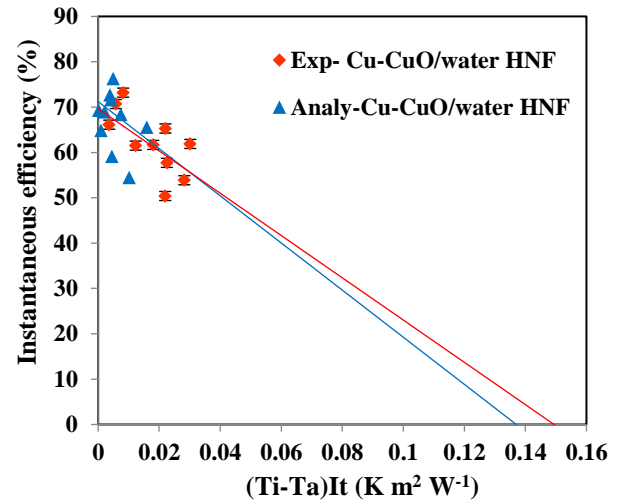
Fig. 4.32 Comparison of experimental and analytical instantaneous efficiency of FCSFPC with hybrid nanofluids

Comparative studies are also conducted between the analytical and experimental studies and presented in Fig. 4.32. It is noticed that analytical results are over estimating the collector efficiency by 3.18 % to 15.09 % than experimental results. The possible reasons are discussed in comparative studies in indirect absorption configuration. Error analysis is also conducted for the experimental studies by considering all possible errors of measuring devices and depicted in Fig. 4.32. It is estimated that the maximum possible errors during conducting the experiments are 3.76 %. The possible errors associated with the experimental studies are less than the improvement of instantaneous efficiency of the SFPC.

Instantaneous efficiency of direct absorption SFPC with different working fluids and mass flow rates operating in forced circulation configuration is estimated over a day is presented in Fig.4.33. It is noticed that among all working fluids, Cu-CuO/water hybrid nanofluid gives the higher instantaneous efficiency compared to water and other mono nanofluids. Maximum instantaneous efficiency is observed about 12.30 PM IST for all the nanofluids at both mass flow rates.
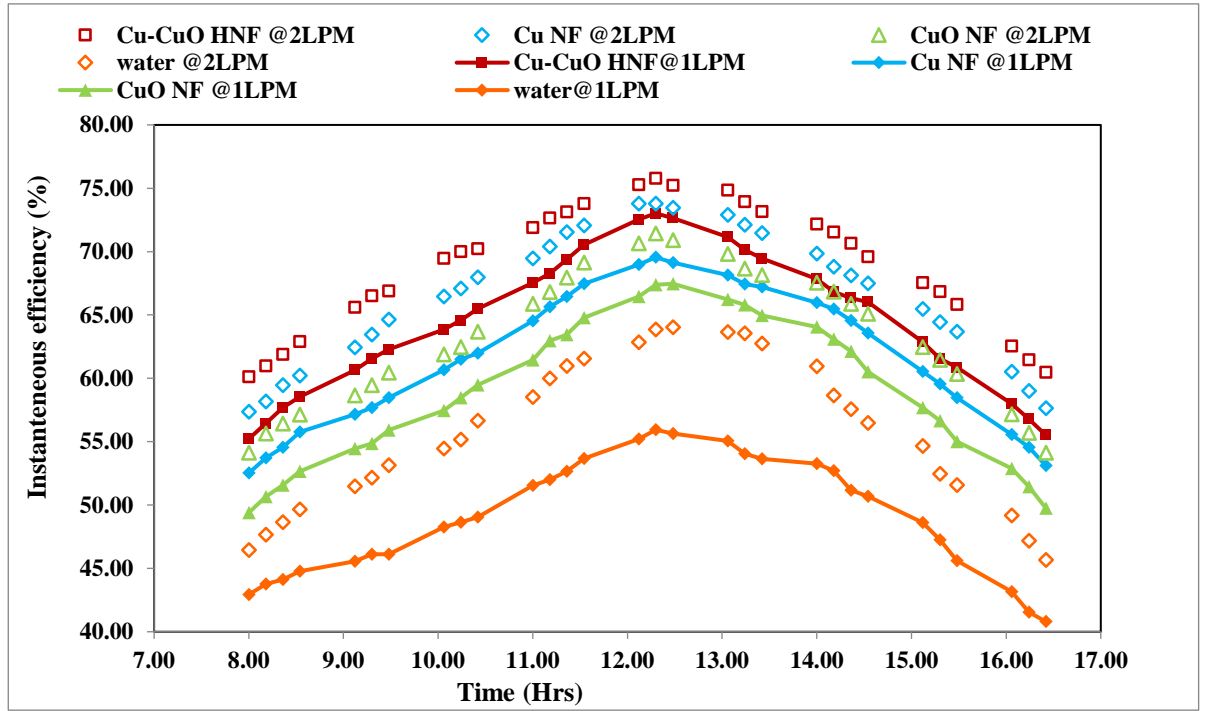
Fig. 4.33. Instantaneous efficiency of DASFPC over a day operated with different working fluids at different mass flow rates

4.4   Closure

This Chapter provides an elaborative discussion on thermodynamic analysis (energy and exergy) of SFPC which absorbs the incident radiation at both direct and indirect configurations and it is operated under forced circulation mode. Experimental studies are carried out with different working fluids such as Al_2O_3/water, Cu/water, CuO/water, TiO_2/water and SiO_2/water as working fluids and comparative studies are presented. It is noticed that, among all the nanofluids, Cu/water and CuO/water nanofluid exhibited higher thermal efficiency and lower entropy generation. However, Cu/water nanofluid is highly reactive and economically not feasible. Therefore, by combining the copper and copper oxide individual nanoparticles, a new hybrid nanofluid called Cu-CuO/water is proposed and studied in the current research. In further analysis, the instantaneous efficiency of nanofluid based SFPC is studied in different configurations such as direct and indirect absorption. This chapter explored the influence of thermophysical and optical properties on enhancement of instantaneous efficiency of solar collector operated in different configurations.

Chapter - 5

Performance Evaluation of Natural Circulation Solar Thermal Collectors

5.1   Natural Circulation Indirect Absorption Solar Flat Plate Collector (NCIDASFPC)

Most of the solar collectors used for the real time applications are operated on natural circulation mode (thermosyphon mode). In this mode, the solar radiation incident on collector will create temperature difference to the working fluid flowing inside the collector, which causes to induce density gradients in working fluid. The induced density gradients are responsible to develop the buoyancy and the fluid circulate in the collector due to this buoyancy [148]. Fig. 5.1 shows the configuration and mode of operation of SFPC for the current analysis. Low mass flow rate of the working fluid is the main drawback with the natural circulation collectors, which in turn causes for more heat losses and consequent lower thermal efficiency. However, the effective pressure difference created by the buoyancy is responsible to circulate the working fluid in NCIDASFPC. The working fluid circulated through the collector and tank by the buoyancy effect while, it descends to the inlet header by gravity [192]
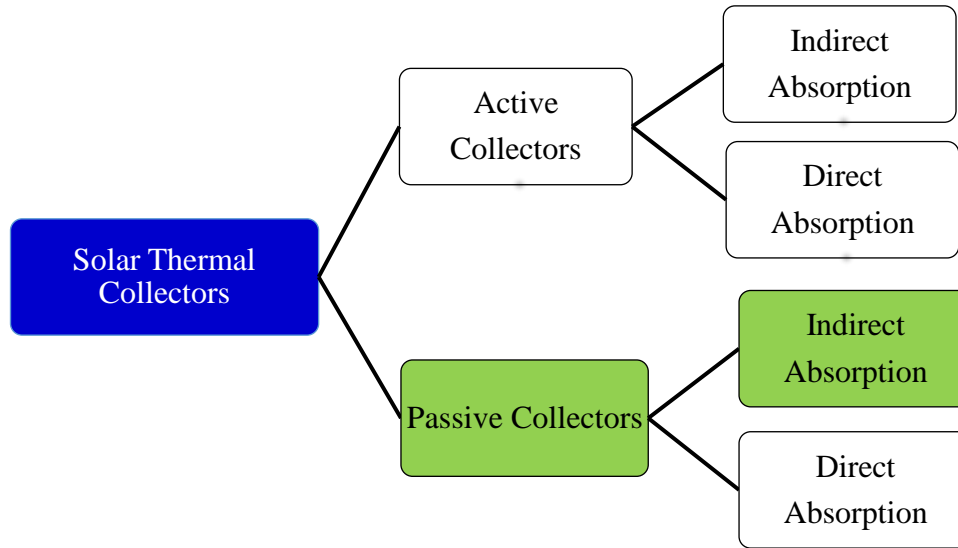
Fig. 5.1 Solar flat plate collectors operating in indirect absorption configuration and Passive (Natural Circulation) mode

The same old solar collector used in forced circulation mode is used natural circulation mode also to analyse the thermal performance and to conduct the experiments. However, in natural circulation mode the flow of the working fluid in collector is not relying on any external pumping agent. The geometrical specifications and operating conditions of the natural circulation collector is presented in table. 4.1.

5.1.1 Thermodynamic analysis of (NCIDASFPC)

In case of natural circulation mode, mass flow rate in the collector is a key parameter and it has to be estimated from the energy balance equation. By absorbing the incident radiation, the temperature of the working fluid flowing inside the riser tubes is getting heated. The hot working fluid enters into the tank. In tank temperature of the working fluid enters from collector is reduced and hence the density of the working fluid is increased. Then the low temperature working fluid from the tank is return back to the collector inlet and this phenomenon will continue till the density gradients are exists.

5.1.1.1 Energy Analysis of NCIDASFPC:

To circulate the working fluid in the collector, buoyancy created by the density gradients has to overcome the flow resistance due to friction

$$P_{bouyancy} = P_{friction} \tag{5.1}$$

Total buoyancy of the collector is nothing but the pressure difference created due to buoyancy in the collector as well as in connecting tubes and tank.

$$P_{bouyancy} = P_{collector} + P_{connecting\ tubes\ and\ tank} \tag{5.2}$$

$$= gsin\theta \int_0^{L_c}(\rho_{Ti} - \rho_{(x)})dx + (\rho_{Ti} - \rho_{To})gH \tag{5.3}$$

$$= \rho_o g\beta \left[sin\theta \int_0^{L_c}(T_x - T_{fi})dx + H(T_{fo} - T_{fi}) \right] \tag{5.4}$$

By assuming linear variation in temperature of the collector

$$\frac{(T_x - T_{fi})}{x} = \frac{(T_{fo} - T_{fi})}{L_c} \tag{5.5}$$

Hence, $\int_0^{L_c}(T_x - T_{fi})dx = (T_{fo} - T_{fi})L/2$ \tag{5.6}

By substituting temperature variation in net pressure balance equation

$$P_{Bouyancy} = \rho_o g\beta(T_{fo} - T_{fi})\left[\frac{Lsin\theta}{2} + H \right] \tag{5.7}$$

where β is the thermal expansion coefficient and it estimated by

$$\beta_{nf} = 7.56 \times 10^{-4} + 6.34 \times 10^{-7}T - 8.09 \times 10^{-4}(1 - \emptyset_{np}) \tag{5.8}$$

Total pressure loss in the system is the sum of pressure lost in collector and pressure loss in connecting tubes

$$P_t = P_c + P_{ct} \tag{5.9}$$

$$P_t = P_c\left[1 + \frac{P_{ct}}{P_c}\right] = P_c(1 + r_p) \tag{5.10}$$

where r_p is the pressure ratio of connecting tubes and collector

At steady state condition, buoyancy is balanced by frictional resistance

Therefore, $\rho_o g\beta(T_{fo} - T_{fi})\left[\frac{Lsin\theta}{2} + H \right] = P_c(1 + r_p)$ \tag{5.11}

Where $P_c = \frac{\rho f L_c v_c^2}{2d_c}$ in which $f = \frac{64\vartheta}{d_c v_c}$

Therefore, $P_c = 32\rho v_c L_c \frac{\vartheta}{d_c^2}$ \tag{5.12}

and $P_{ct} = 32\rho v_{ct} L_{ct} \frac{\vartheta}{d_{ct}^2}$ \tag{5.13}

From the continuity equation

$$\dot{m} = \rho A v_c = \rho A v_{ct} \tag{5.14}$$

and velocity of fluid, $v_c = \frac{4\dot{m}}{\rho \pi N d_c^2}$ \tag{5.15}

where N is the number of riser tubes.

Collector pressure can be estimated by substituting Eq 5.15 in Eq 5.12

Therefore, collector pressure, $P_c = 128\frac{\dot{m}L_c\vartheta}{\pi N d_c^{5.}}$ (5.16)

The pressure ratio r_p can be simplified by converting velocity ratio into diameters ratio

$\frac{v_{ct}}{v_c} = N\left(\frac{d_c}{d_{ct}}\right)^2$ (5.17)

Therefore, $r_p = N\frac{L_c}{L_{ct}}\left(\frac{d_c}{d_{ct}}\right)^4$ (5.18)

by substituting the pressure ratio in Eq (5.10)

$\rho_o g\beta(T_{fo} - T_{fi})\left[\frac{Lsin\theta}{2} + H\right] = 128\frac{\dot{m}L_c\vartheta}{\pi N d_c^4}\left(1 + N\frac{L_c}{L_{ct}}\left(\frac{d_c}{d_{ct}}\right)^4\right)$ (5.19)

From the fundamentals of thermodynamics heat gain the working fluid is given by:

$Q_u = \dot{m}C_p(T_{fo} - T_{fi})$ (5.20)

and useful heat gain by the working fluid in SFPC can be estimated by:

$Q_u = A_c F'\left[I_t(\tau\alpha) - U_l(T_{fm} - T_a)\right]$ (5.21)

By equating the useful heat gain equations, one can get the relation between temperature rise and mass flow rate

$\dot{m}C_p(T_{fo} - T_{fi}) = A_c F'\left[I_t(\tau\alpha) - U_l(T_{fm} - T_a)\right]$ (5.22)

$(T_{fo} - T_{fi}) = \frac{A_c F'}{\dot{m}C_p}\left[I_t(\tau\alpha) - U_l(T_{fm} - T_a)\right]$ (5.23)

By substituting the temperature gradient in Eq 5.19, one can get the mass flow rate in SFPC.

$\dot{m} = C^{1/2}\left(\frac{\rho_o\beta}{\vartheta C_p}F'\left[I_t(\tau\alpha) - U_l(T_{fm} - T_a)\right]^{1/2}\right)$ (5.24)

where, $C = \dfrac{g\pi N A_c d_c^4\left[\frac{Lsin\theta}{2} + H\right]}{128L_c\left(1 + N\frac{L_c}{L_{ct}}\left(\frac{d_c}{d_{ct}}\right)^4\right)}$

Therefore, efficiency of NCIDASFPC, $\eta = \dfrac{\dot{m}C_p(T_{fo} - T_{fi})}{I_t(\tau\alpha)A_c}$ (5.25)

Procedure to conduct the exergy analysis of NCIDASFPC is similar to that of FCIDASFPC. Therefore, no separate section is provided to the mathematical analysis on exergy. The pivotal parameter in the exergy analysis is the total entropy generation and it is discussed in the results and discussion section.

5.1.2   Experimental investigations on NCIDASFPC

Experimental studies are carried out on solar collector that absorbing the incident radiation in indirect configuration and operating in natural circulation mode. The schematic diagram of NCIDSFPC is as shown in Fig. 5.2. The fundamental energy transfer mechanism of converting the incident radiation into useful heat gain by the working fluid is one and similar to that of forced circulation mode.
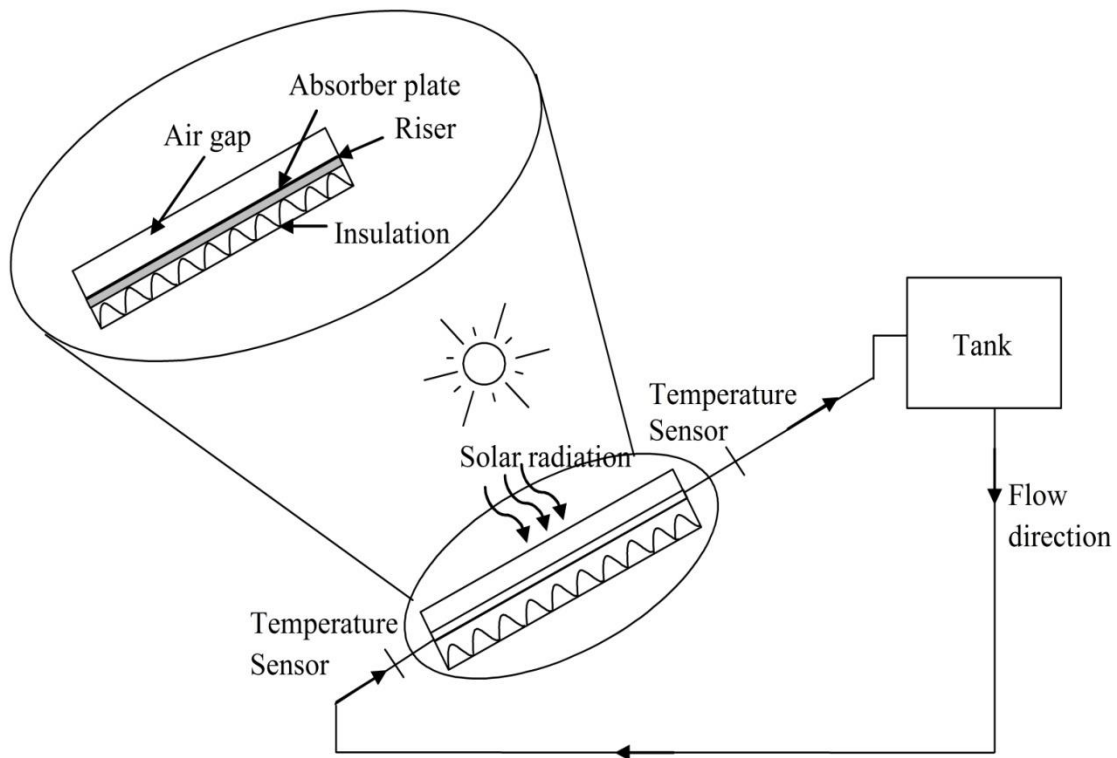
Fig. 5.2 Schematic diagram of NCIDASFC

Bottom and edges of the collector, all the connecting lines and tank are well insulated to prevent heat losses from various parts of collector. The collector connecting lines are kept sloped to prevent the formation of air pockets during circulation, which may prevent the circulation of working fluid. Construction details and material properties are already discussed in the FCIDASFPC section. Experiments are conducted with water, mono and hybrid nanofluids as working fluids. The photographic view of NCIDASFPC is shown in Fig 5.2. To study the effect of particle concentration, experiments are conducted at three different concentrations for all nanofluids.

Major components:

1. Tank
2. Collector
3. Connecting lines
4. Temperature
   indicator

Fig 5.3. Photographic view of NCIDASFPC

5.1.3   Results and discussion

In case of natural circulation along with the density and viscosity contribution of thermal expansion coefficient is also very critical. As elucidated in Fig. 5.4 thermal expansion coefficient of all the nanofluids is linearly increasing with the temperature. The enhanced thermal expansion coefficient leads to increase the mass flow rate in collector and consequently improves the collector efficiency.

Influence of particle concentration frictional pressure is illustrated in Fig. 5.5. The NCSFPC, frictional pressure of nanofluid is linearly increasing as a function of particle concentration. From Eq (5.1), buoyancy pressure of the collector is balanced by the frictional pressure hence the increasing frictional pressure represents the enhancement in buoyancy force and corresponding mass flow rate in the collector.
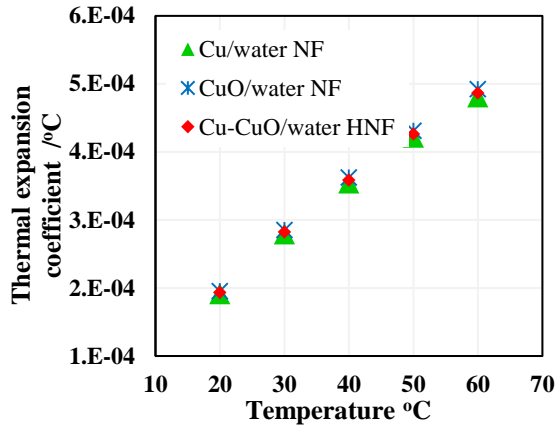
Fig. 5.4 Thermal expansion coefficient of mono and hybrid nanofluids
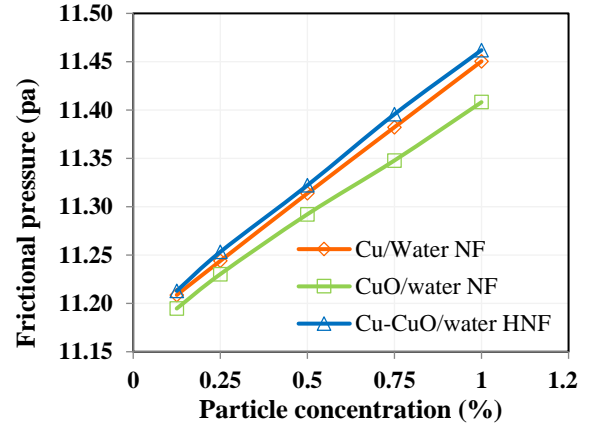
Fig. 5.5 Frictional pressure drops in the collector with mono and hybrid nanofluids

Thermal efficiency of the collector as function of particle concentration is presented in Fig. 5.6. The enhanced mass flow rate due to improved thermal expansion coefficient and friction pressure leads to improve the thermal efficiency of the collector. Since, the collector is operating in indirect absorption configuration, the contribution of thermophysical properties of working fluid have more influence than the optical properties. Increasing the particle concentration leads to increase the thermal conductivity and thermal expansion coefficient that causes to raise the buoyancy and subsequent collector efficiency. Since the Cu/water nanofluid possesses higher thermal properties than the other working fluids it exhibits the higher collector efficiency than other working fluids. Fig. 5.7 illustrates the total entropy generation by different working fluids as a function of particle concentration. In natural circulation operated collector, the effect of inconsistent solar radiation, ambient conditions are more on collector and leads to more entropy generation. Among the working fluids, Cu/water nanofluid posses lower entropy generation than other nanofluids and the possible reasons are discussed in the forced circulation mode.

Similar to indirect absorption forced circulation, natural circulation mode also instantaneous efficiency of SFPC is increasing the particle concentrations. The higher instantaneous efficiency is noticed at 1.0 % particle concentration as shown in Fig. 5.6, Fig. 5.7, Fig. 5.8 for Cu/water, CuO/water and Cu-CuO/water nanofluids respectively.
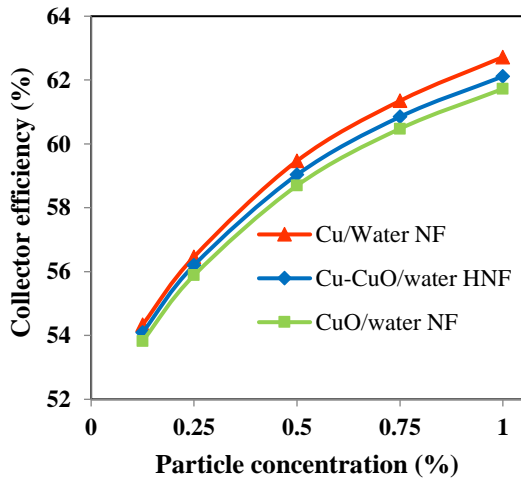
Fig.5.6. Collector efficiency as a function of particle concentration
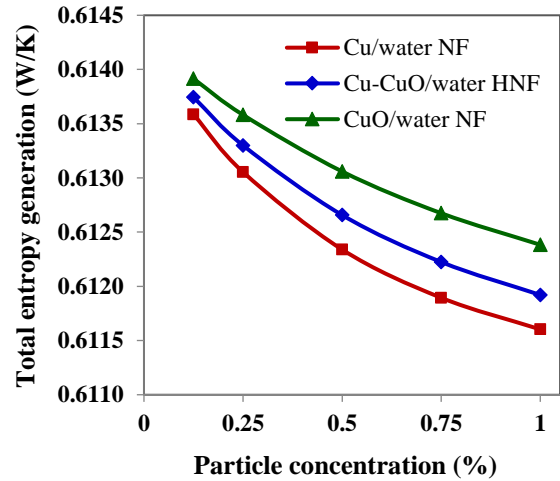
Fig.5.7. Total entropy generation as a function of particle concentration

Enhanced density and lower specific heat of the nanofluid cause to create more buoyancy to the nanofluids and it is increasing with the particle concentration. As the particle concentration increases the frictional pressure of working fluid is increasing and the total frictional pressure can be estimated from Eq 5.9. In natural circulation mode, this friction pressure is balanced by the buoyancy effect. Therefore, mass flow rate of the collector and corresponding instantaneous efficiency is improved.
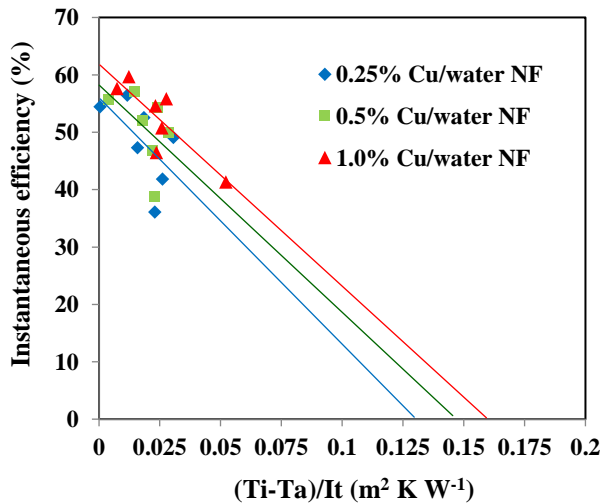
Fig. 5.8 Experimentally measured instantaneous efficiency of NCSFPC with Cu/water nanofluid
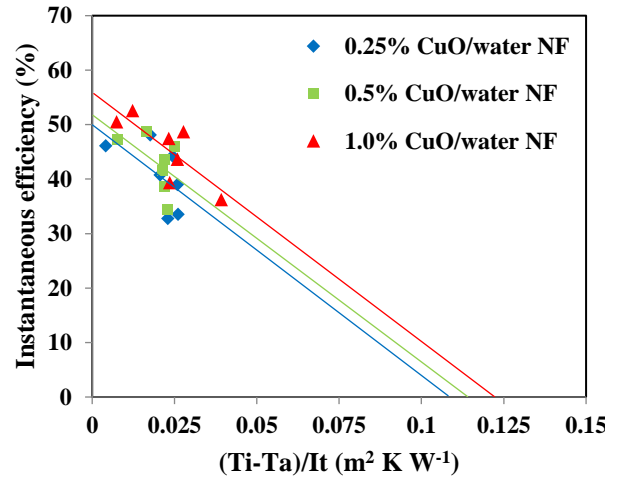
Fig. 5.9 Experimentally measured instantaneous efficiency of NCSFPC with CuO/water nanofluid

105

Another influencing parameter for the enhancement of instantaneous efficiency with the particle concentration in natural circulation mode is the thermal expansion coefficient. The increased thermal expansion coefficient causes for more mass flow rate and subsequently responsible for increased instantaneous efficiency.
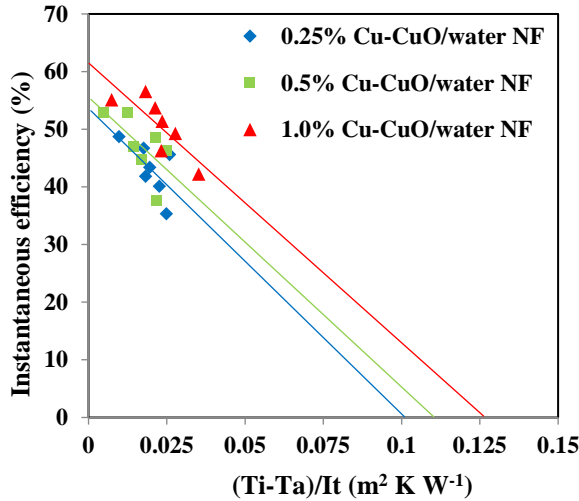
Fig.5.10 Experimentally measured instantaneous efficiency of NCSFPC with Cu-CuO/water hybrid nanofluid
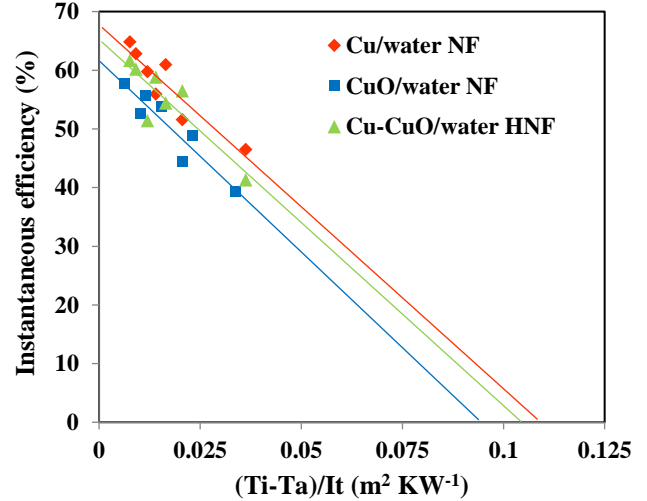
Fig. 5.11 Comparison of Instantaneous efficiency of NCSFPC with mono and hybrid nanofluids

It can be observed from Fig. 4.15 and Fig. 5.11 that the instantaneous efficiency of both natural circulation and forced circulation modes follow analogous trends. However, the instantaneous efficiencies of NCIDASFPC with Cu/water, Cu-CuO/water and CuO/water nanofluids are improved by 11.51%, 8.12%, and 6.84% respectively compared to water.
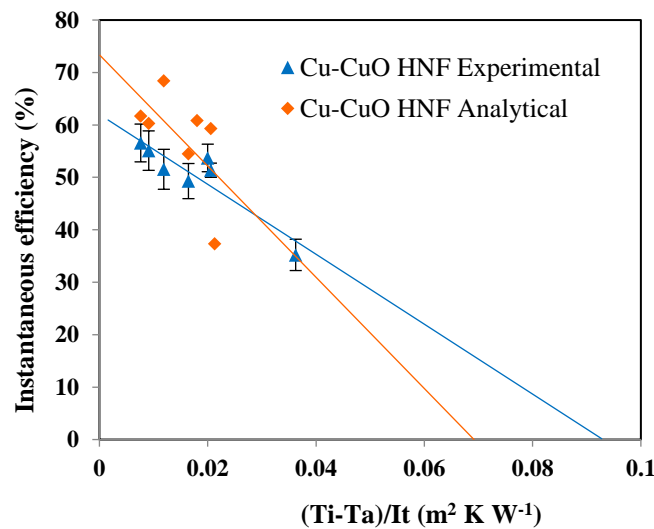
Fig. 5.12 Comparison of experimental and analytical results of NCIDASFPC

The instantaneous efficiency of NCIDASFPC is estimated both analytically and experimentally and presented in Fig. 5.12. It is noticed from the results that the deviation between experimental and analytical results are more in natural circulation mode compared to forced circulation. The possible reason could be in NC mode, the fluctuation of solar radiation and atmospheric conditions have more influence on the collector **efficiency**. Fig. 5.12 shows the comparison of analytical and experimental results. In order to consider the possible error occurred in the experimental work, error analysis is also carried out and the maximum possible error is 3.81 %.

5.2 Natural Circulation Direct Absorption Solar Flat Plate Collector (NCDASFPC)

The fundamental design and way of converting the incident radiation into useful heat gain is analogous for forced and natural circulation modes. In contrary, circulation of working fluid in natural circulation collector relies on buoyancy. However, the influence of optical properties is accountable in case of direct absorption collector unlike indirect absorption. In direct absorption, the incident radiation falling on glass cover is transmitted to the working fluid flowing underneath to it. The ameliorated photo-thermal properties of nanofluids causes to reduce the temperature gradients between the wall and bulk fluid and consequently improves the efficiency.
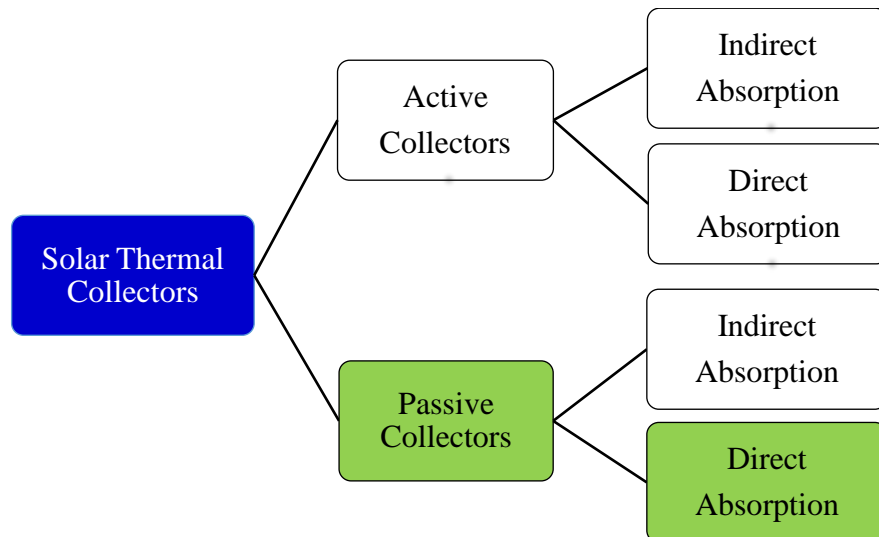
Fig. 5.13 Solar flat plate collectors operating in direct absorption configuration and passive (Natural Circulation) mode

In direct absorption configuration, the optical properties of working fluid have more influence on the absorption of incident solar radiation. In this configuration, the incident radiation is passed through the optically polished glass cover and reaches the working fluid. The incident radiation is attenuated in working fluid due to its photo-thermal properties. In direct absorption configuration, the reduced thermal resistance through the various parts of collector leads to increase the energy absorption capability of collector and subsequently improves the instantaneous efficiency. The specification of NCDASFPC test rig and operating parameters are as same as forced circulation mode and presented in table. 4.3. The schematic diagram of the NCDASFPC is as shown in Fig. 5.14. Experiments are conducted to study the influence of particle concentration and properties of the nanofluids and comparative studies are also conducted and presented. Investigations are also made to evaluate the variation of analytical and experimental studies. Test rig is designed and fabricated to carry out the experiments on direct absorption configuration under natural circulation mode.

5.2.1 Thermodynamic analysis of NCDASFPC

In case of direct absorption collector, the incident radiation passes through the glass cover would reach the working fluid without any intermittent thermal resistances.

The radiation incident on NCDASFPC, $I_{b\lambda}(\lambda, T_{solar}) = \dfrac{2hC_0^2}{\lambda^5\left[exp\left(\frac{hC_0}{\lambda k_B T_{solar}}\right)-1\right]}$ (5.26)

From the total incident radiation only a portion of radiation is transmitted to the working fluid. The amount of radiation absorbed and converted into useful heat gain is depends on the thermophysical and optical properties of the working fluid. The influence of photo-thermal properties of nanofluid on radiation absorption can be estimated by energy balance equation:

$$\rho C_p \frac{\partial T}{\partial t} = k \frac{\partial^2 T}{\partial y^2} + q(y) \quad\quad\quad (5.27)$$

The detailed procedure to estimate the outlet temperature of the working fluid is presented in the FCDASFPC.

Therefore, instantaneous efficiency of NCDASFPC is $\eta = \dfrac{\dot{m}C_p(T_{f,out}-T_{f,in})}{I_t A_c}$ (2.28)

The procedure used to carry out the exergy analysis of FCDASFPC is used to conduct exergy analysis on natural circulation mode also.

5.2.2 Experimental investigations on NCDASFPC

Experiments are conducted on SFPC configured for direct absorption of incident radiation and operated in natural circulation mode. The particle concentration is limited to 1.0 %

concentration as mentioned in forced circulation configuration. The schematic diagram of NCDASFPC is described in Fig. 5.14 and photographic view of the test rig is as shown in Fig. 5.15. Experiments are conducted with water, mono and hybrid nanofluids and results are presented in the foregoing section.
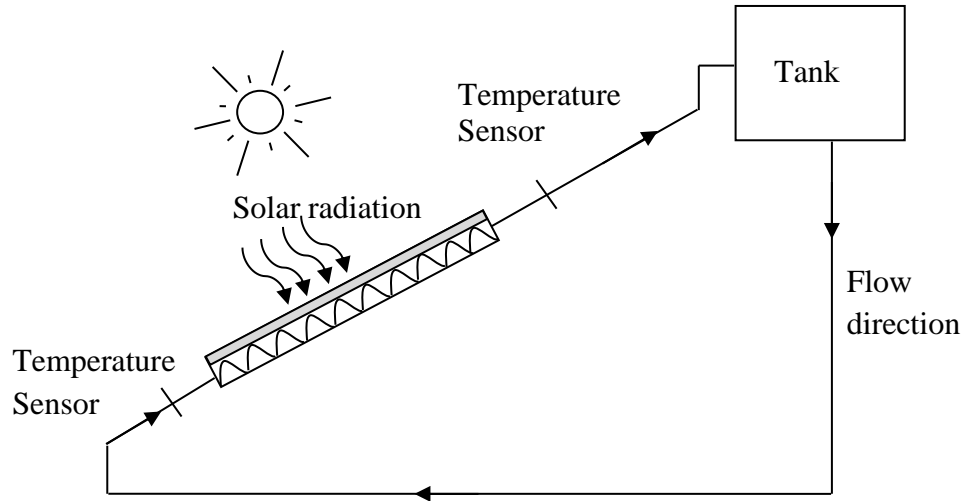
Fig. 5.14 Schematic diagram of natural circulation direct absorption solar flat plate collector

Major components

1. DASFPC
2. Tank
3. Connnecting pipes
4. Temperature analoger

Fig. 5.15 Photographic view of NCDASFPC experimental test rig with temperature sensors

5.2.3   Results and discussion

In case of natural circulation flows, the buoyancy is the dominance force to circulate the working fluid in entire system. Influence of particle concentration on collector efficiency is analytically estimated and presented in Fig. 5.16. It can be observed from Fig. 5.16 that the

collector gradually increasing with the particle concentration. Though the thermophysical properties of the Cu/water nanofluid is higher than other nanofluid, the ameliorated extinction coefficient of Cu-CuO/water hybrid nanofluid leads to exhibit higher collector efficiency than other nanofluids. The buoyancy is also increasing with the particle concentration that causes to increase the mass flow rate and consequently leads to improve the collector efficiency.
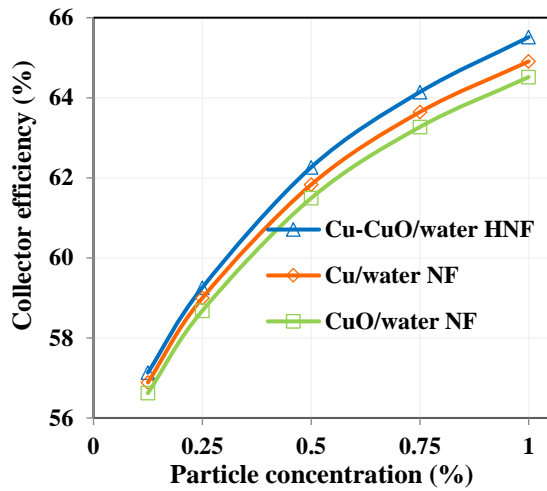
Fig. 5.16 Thermal efficiency of NCDASFPC as a function of particle concentration
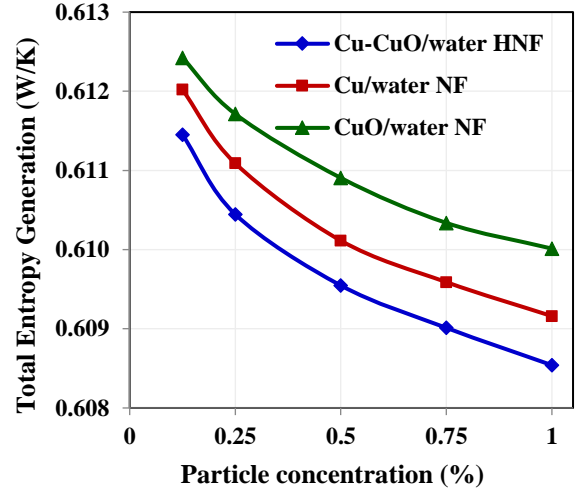
Fig. 5.17 Total entropy generation by NCDASFPC as a function of particle concentration

Fig. 5.17 shows the total entropy generated by different nanofluids as a function of particle concentration. The result shows that among the different nanofluids, Cu-CuO/water nanofluid exhibits the lower entropy generation as analogous to forced circulation mode.
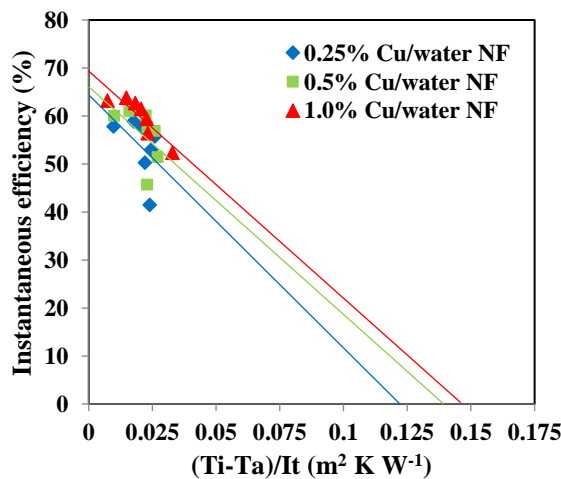
Fig. 5.18 Instantaneous efficiency of NADASFPC with Cu/water nanofluid
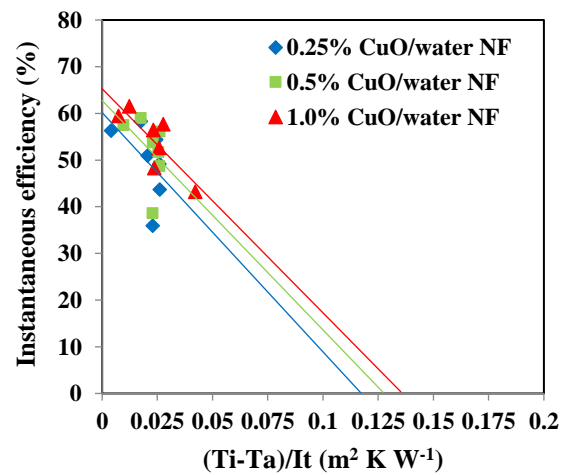
Fig. 5.19 Instantaneous efficiency of NADASFPC with CuO/water nanofluid

Experimental studies are carried out on NCDASFPC with Cu/water, CuO/water and Cu-CuO/water and water as working fluids. The instantaneous efficiency of NCDASFPC is increasing with the particle concentrations as shown in Fig. 5.18, Fig. 5.19 and Fig. 5.20 for Cu/water, CuO/water and Cu-CuO/water nanofluids respectively. It is clear from the all three graphs that higher instantaneous efficiency is noticed at 1.0 % particle concentration. Therefore, in further experimental part comparisons are made among all working fluids at 1.0 % particle concentration only. Fig. 5.21 shows the instantaneous efficiency of NCDASFPC with different working fluids. It can be observed from Fig. 5.21 that among all working fluids, Cu-CuO/hybrid nanofluid exhibits the higher instantaneous efficiency as similar to that of forced circulation. The probable reasons for higher instantaneous efficiency of hybrid nanofluid are analogous to that of forced circulation mode with direct absorption collector configuration.
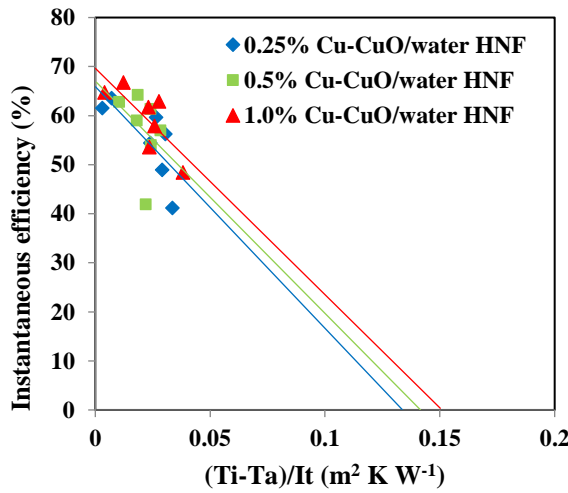
Fig. 5.20 Instantaneous efficiency of NADASFPC with Cu-CuO/water hybrid nanofluid
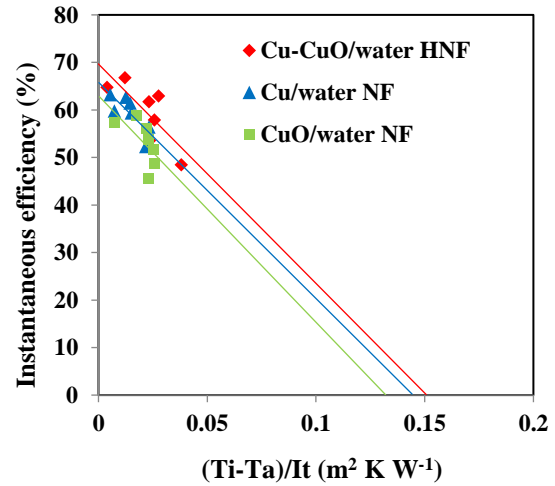
Fig. 5.21 Instantaneous efficiency of NADASFPC with mono and hybrid nanofluids

Comparison between analytical and experimental studies and presented in Fig. 5.22. It is noticed from the analytical studies that the analytical approach is over estimating the collector efficiency by 4 to 16.6 % than experimental results. Uncertainty analysis is conducted for the experimental test rig to account the inaccuracies of the measuring apparatus and noticed 3.76 % uncertainty is observed by considering all possible inaccuracies while conducting the experiments. The possible errors during the experimentation have less deviation than the enhanced instantaneous efficiency.
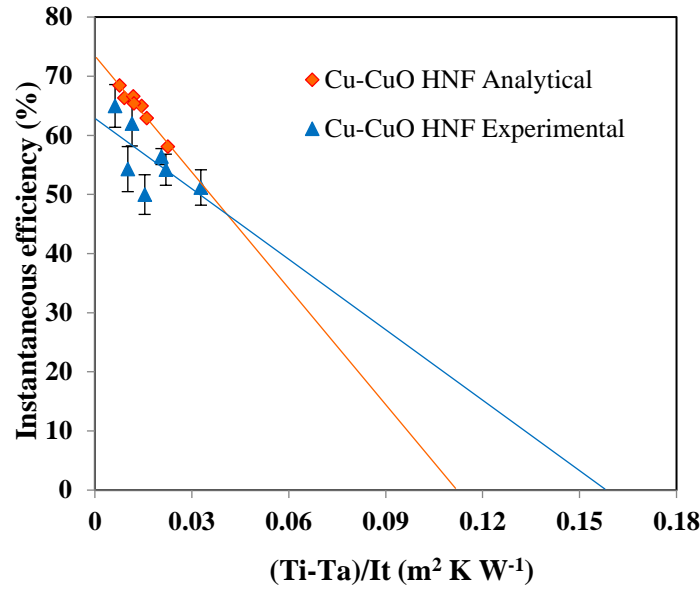
Fig. 5.22 Comparison of instantaneous efficiency of NADASFPC
with Cu-CuO/water hybrid nanofluid

5.3   Uncertainty analysis

This analysis is used to assess the uncertainty in a measurement.

Uncertainty of useful heat gain, $Q_u = \dot{m}C_p(T_{out} - T_{in})$ (5.29)

Uncertainty pertaining to rotameter, $\dot{m} = \pm 1.33$ %

Uncertainty pertaining to RTD at collector inlet, $T_i = \pm 0.2$ %

Uncertainty pertaining to RTD at collector outlet, $T_o = \pm 0.2$ %

Uncertainty pertaining to solar power meter, $I_t = \pm 2.67$ %

$$\frac{\partial Q_u}{Q_u} = \left[\left(\frac{\partial Q_u}{\partial \dot{m}}\omega_{\dot{m}}\right)^2 + \left(\frac{\partial Q_u}{\partial T_{out}}\omega_{T_{out}}\right)^2 + \left(\frac{\partial Q_u}{\partial T_{in}}\omega_{T_{in}}\right)^2\right]^{1/2}$$ (5.30)

$$= [(1.33)^2 + (0.2)^2 + (0.2)^2]^{1/2}$$

$$\frac{\partial Q_u}{Q_u} \leq 1.35\%.$$

Uncertainty of instantaneous efficiency of SFPC, $\eta_i = \frac{Q_u}{I_t A_c}$ (5.31)

$$\frac{\partial \eta_i}{\eta_i} = \left[\left(\frac{\partial \eta_i}{\partial \dot{m}}\omega_{\dot{m}}\right)^2 + \left(\frac{\partial \eta_i}{\partial T_{out}}\omega_{T_{out}}\right)^2 + \left(\frac{\partial \eta_i}{\partial T_{in}}\omega_{T_{in}}\right)^2 + \left(\frac{\partial \eta_i}{\partial I_t}\omega_{I_t}\right)^2\right]^{1/2}$$ (5.32)

$$= [(1.33)^2 + (0.2)^2 + (0.2)^2 + (2.67)^2]^{1/2}$$

$$\frac{\partial \eta_i}{\eta_i} \leq 2.99\%.$$

5.4   Closure

This Chapter provides a detailed discussion on thermodynamic analysis of SFPC that absorbs the incident solar radiation in both direct and indirect configurations operated under natural circulation mode. Both analytical and experimental studies are carried out using Cu/water, CuO/water and Cu-CuO/water nanofluids and comparative studies are presented. The current chapter explored the influence of thermophysical and optical properties on enhancement of instantaneous efficiency of solar collector operated under natural circulation mode in different configurations.

Chapter - 6

Salient Conclusions and scope of future work

6.1   General Conclusions

- Analytical and experimental studies are carried out on SFPC operating in different configurations and operating modes. Based on these studies the following conclusions are drawn

6.1.1   Thermophysical Properties

- Among several thermophysical properties of nanofluid density, specific heat, viscosity and thermal conductivity are the basic governing properties that influence the collector efficiency. However, along with these properties, thermal expansion coefficient also plays a vital role in thermosyphon mode operating collectors, whereas optical properties play a pivotal role in direct absorption collectors.

Analytical studies are carried out on solar collector, to study the influence of thermophysical and optical properties of working fluid on instantaneous efficiency experimental studies are also conducted to made comparative studies. A substantially variation in instantaneous efficiency of SFPC is noticed between analytical and experimental results. In order to identify the potential reason for this variation, thermal conductivity and viscosity of nanofluids are experimentally measured.

- Thermal conductivity of nanofluids is estimated from the existing empirical correlations and results are compared with the experimental results. It is found to be less than 5 % variation between the empirical and measured readings and hence any new correlation was developed.

- In case of viscosity, the results from the existing empirical correlations have a substantial deviation from experimental outcomes. For example, 18.58 % deviation is noticed at 1.0 % particle concentration of CuO/water nanofluid. Therefore, a new correlation is developed for precise calculation of viscosity of nanofluid and further analysis is carried out using the developed correlation.

6.1.2 Case 1 – Forced Circulation Indirect Absorption SFPC

- Thermodynamic analysis is carried out on the performance of the SFPC with different working fluids, and the analytical results are compared with the experimental outcomes.

- With basis of analytical results, pilot experiments are conducted with Cu, CuO, Al2O3, TiO2, and SiO2 nanoparticle suspensions in water to study the influence of nanoparticle type on the collector efficiency. Among all the nanofluids, Cu/water nanofluid based collector exhibits the highest thermal performance and it is followed by CuO/water nanofluid based collector.

- Though, Cu/water nanofluid based solar collector gives the higher thermal performance, the copper particles are highly reactive and chemically unstable. Therefore, CuO nanoparticles are hybridized with Cu nanoparticles, and a new hybrid nanofluid is proposed and studied in the current work. However, the hybridisation of Cu and CuO nanoparticle will significantly refine the optical properties.

- It is noticed from the experimental outcomes that, the instantaneous efficiency of SFPC increases with the particle concentration and mass flow rate. Among all working fluids, Cu/water nanofluid based solar collector giving higher instantaneous efficiency than other working fluids. The instantaneous efficiency of Cu/water, CuO/water and Cu-CuO/water nanofluids is 16.86 %, 10.55 %, and 9.81 % respectively.

6.1.3 Case 2 – Forced Circulation Direct Absorption SFPC

- In case of direct absorption configuration, along with the thermophysical properties, optical properties of the working fluid also play a key role in absorption of incident solar radiation.

- By hybridising Cu nanoparticles with CuO nanoparticles, absorption properties of hybrid nanofluid are substantially increased for a wide range of solar spectrum, when compared to water.

- In direct absorption SFPC, among all the working fluids Cu-CuO/water hybrid nanofluid exhibits higher instantaneous efficiency and it is 18.45 % more compared to water, that is 13.64 % and 11.34 % for Cu/water and CuO/water nanofluids.

- Comparative studies are conducted between indirect and direct absorption configurations under similar operating conditions. It is noticed that the direct absorption collector is giving 7.9 % higher instantaneous efficiency than indirect absorption.

6.1.4 Case 3 – Natural Circulation Indirect Absorption SFPC

- In natural circulation mode, thermal efficiency of the collector is relatively low due to more radiative and convective losses, however, the running cost of the collector is reduced due to the absence of pump.

- The trends and status of instantaneous efficiency of collector operated in natural circulation mode is like an analogous to forced circulation indirect absorption mode. Amid different working fluids, NCIDASFPC with Cu/water nanofluid exhibits the higher instantaneous efficiency of 11.51 %, it is 8.12 %, and 6.84 % respectively with Cu-CuO/water and CuO/water nanofluids compared to pure water.

6.1.5 Case 4 – Natural Circulation Direct Absorption SFPC

- Collector running in direct absorption configuration at natural circulation mode is found to be similar to that of forced circulation direct absorption collector.

- The experimental results resemble the forced mode collector among all working fluids Cu-CuO/water nanofluid give 13.25 % higher instantaneous efficiency than water and that is 9.53 % and 8.71 % for Cu/water and CuO/water nanofluids.

- From all the above experimental analysis, it can be noted that no single working fluid may be suitable for all absorption configurations and operating modes.

6.2 Scope of future work

- Researchers are already stepping towards the investigation of rheological and heat transfer behaviour of nanofluids. Further, investigations need to be carry out to address the root cause behind the peculiar changes in the hydrothermal and optical properties of mono and hybrid nanofluids.

- Another principal issue is, uneven augment in friction pressure drop characteristics, which is to be properly addressed to use them for solar thermal applications.

- In the current study, one combination of nanoparticles are considered to study the influence of amalgamated properties of hybrid nanofluid on the thermal performance of solar collectors, however, other combinations may also be suitable for the solar applications.

- Antifreezes like ethylene glycol also can be used as base fluid to prepare nanofluid

6.3 Closure

This chapter consolidates the important findings based on various cases studied in the thesis. The prominent conclusions and recommendations for future work are presented in this chapter.

Publications

International Journals

S.No.	Title of the paper	Name of the Journal and Publisher	Status
1	State of art review on hybrid nanofluids	*Renewable and sustainable energy reviews* (SCI) (IF: 8.05)	Published
2	Energy and exergy analysis of solar flat plate collector with hybrid nanofluid.	*World Journal of Engineering* **Emerald Publication (ESCI)**	Accepted
3	Numerical analysis and validation of heat transfer mechanism of solar flat plate collector	*Proceedia Engineering*, **Elsevier, (Scopus)**	Published
4	Miniaturization of nanofluid based solar flat plate collector: environmental and energy aspects	*Thermal Science,* **Vinca publication. (SCI)**	Communicated
5	Experimental studies on solar flat plate Collector with hybrid nanofluids	*Applied Thermal Engineering*, **Elsevier (SCI)**	Under Review
6	Comparison between different mode of operation of solar flat plate collectors with nanofluids	*Renewable Energy*, **Elsevier. (SCI)**	Under Review

International/ National Conferences

S.No.	Title of the paper	Name of the Conference	Status
1	An over view on preparation of and estimation of nanofluid properties	National Conference On Innovations in Engineering and Technology, NCIT-2013, GEC-Gudlavalleru, 27-28th December 2013. India	Presented
2	Nanofluids in Solar Flat Plate Collectors – A Review	NSMERS 2016, NIT Warangal 7th Oct, 2016. India	Presented
3	Numerical analysis of flat plate collectors thermal performance and validation of heat transfer mechanism	International Conference on frontiers in Chemical, energy and environment, INCEEE-2015, NIT Warangal, India	Presented
4	CFD Analysis of hybrid nanofluid based Solar Flat Plate Collector	International Conference on Recent Trends in Engineering, Science and Technology, 27-28th October 2016, Hyderabad, India	Presented.

References

[1]   Z. Abdin *et al.*, "Solar energy harvesting with the application of nanotechnology," *Renew. Sustain. Energy Rev.*, vol. 26, pp. 837–852, 2013.

[2]   Vaclav Smil, *E N E R G I E S*, First edit. London: The MIT Press, 1999.

[3]   O. Ibrahim, F. Fardoun, R. Younes, and H. Louahlia-Gualous, "Review of water-heating systems: General selection approach based on energy and environmental aspects," *Build. Environ.*, vol. 72, pp. 259–286, 2014.

[4]   C. U. Okujagu and S. K. Adjepong, "Performance of a simple flat plate solar collector at an equatorial location," *Sol. Wind Technol.*, vol. 6, no. 3, pp. 283–289, 1989.

[5]   K. P. Gertzos and Y. G. Caouris, "Optimal arrangement of structural and functional parts in a flat plate integrated collector storage solar water heater (ICSSWH)," *Exp. Therm. Fluid Sci.*, vol. 32, no. 5, pp. 1105–1117, 2008.

[6]   J. C. A. Maxwell, *Treatise on Electricity and Magnetism*, Second Edi. UK: Clarendon Press, Oxford, UK, 1881.

[7]   R. L. Hamilton and O. . Crosser, "Thermal Conductivity of Heterogeneous Two Component Systems," *Ind. Eng. Chem. Fundam.*, vol. 1, no. 3, pp. 187–191, 1962.

[8]   S. U. S. Choi, Z. G. Zhang, W. Yu, F. E. Lockwood, and E. A. Grulke, "Anomalous thermal conductivity enhancement in nanotube suspensions," *Appl. Phys. Lett.*, vol. 79, no. 14, pp. 2252–2254, 2001.

[9]   Z. Said, M. H. Sajid, R. Saidur, M. Kamalisarvestani, and N. A. Rahim, "Radiative properties of nanofluids," *Int. Commun. Heat Mass Transf.*, vol. 46, pp. 74–84, 2013.

[10]   R. Saidur, K. Y. Leong, and H. A. Mohammad, "A review on applications and challenges of nanofluids," *Renew. Sustain. Energy Rev.*, vol. 15, no. 3, pp. 1646–1668, 2011.

[11]   G. Huminic and A. Huminic, "Application of nanofluids in heat exchangers: A review," *Renew. Sustain. Energy Rev.*, vol. 16, no. 8, pp. 5625–5638, 2012.

[12]   K. H. Solangi *et al.*, "A comprehensive review of thermo-physical properties and convective heat transfer to nanofluids," *Energy*, vol. 89, pp. 1065–1086, 2015.

[13]   E. Sadeghinezhad *et al.*, "A comprehensive review on graphene nanofluids: Recent

research, development and applications," *Energy Convers. Manag.*, vol. 111, pp. 466–487, 2016.

[14] D. K. Devendiran and V. A. Amirtham, "A review on preparation, characterization, properties and applications of nanofluids," *Renew. Sustain. Energy Rev.*, vol. 60, pp. 21–40, 2016.

[15] K. Y. Leong, H. C. Ong, N. H. Amer, M. J. Norazrina, M. S. Risby, and K. Z. Ku Ahmad, "An overview on current application of nanofluids in solar thermal collector and its challenges," *Renew. Sustain. Energy Rev.*, vol. 53, pp. 1092–1105, 2016.

[16] K. V Sharma, L. Syam Sundar, and P. K. Sharma, "Estimation of heat transfer coefficient and friction factor in the transition flow with low volume concentration of Al2O3 nanofluid flowing in a circular tube and with twisted tape insert," *Int. Commun. Heat Mass Transf.*, vol. 36, pp. 503–507, 2009.

[17] A. R. Sajadi and M. H. Kazemi, "Investigation of turbulent convective heat transfer and pressure drop of TiO   2/water nanofluid in circular tube," *Int. Commun. Heat Mass Transf.*, vol. 38, no. 10, pp. 1474–1478, 2011.

[18] H. Zhu, C. Zhang, S. Liu, Y. Tang, and Y. Yin, "Effects of nanoparticle clustering and alignment on thermal conductivities of Fe3O4 aqueous nanofluids," *Appl. Phys. Lett.*, vol. 89, no. 2, 2006.

[19] S. W. Lee, S. D. Park, S. Kang, I. C. Bang, and J. H. Kim, "Investigation of viscosity and thermal conductivity of SiC nanofluids for heat transfer applications," *Int. J. Heat Mass Transf.*, vol. 54, no. 1–3, pp. 433–438, 2011.

[20] Y. Ding, H. Alias, D. Wen, and R. A. Williams, "Heat transfer of aqueous suspensions of carbon nanotubes (CNT nanofluids)," *Int. J. Heat Mass Transf.*, vol. 49, no. 1–2, pp. 240–250, 2006.

[21] W Duangthongsuk and S Wongwises, "Heat transfer enhancement and pressure drop characteristics of TiO2 –water nanofluid in a double-tube counter flow heat exchanger," *Int. J. Heat Mass Transf.*, vol. 52, no. 7, pp. 2059–2067, 2009.

[22] K. Y. Leong, R. Saidur, S. N. Kazi, and A. H. Mamun, "Performance investigation of an automotive car radiator operated with nanofluid-based coolants (nanofluid as a coolant in a radiator)," *Appl. Therm. Eng.*, vol. 30, no. 17–18, pp. 2685–2692, 2010.

[23] R. Nimmagadda and K. Venkatasubbaiah, "Conjugate heat transfer analysis of micro-channel using novel hybrid nanofluids (Al2O3 + Ag / Water)," *Eur. J. Mech. B/Fluids*, vol. 52, pp. 19–27, 2015.

[24] T. Yousefi, F. Veysi, E. Shojaeizadeh, and S. Zinadini, "An experimental investigation on the effect of Al   2O   3-H   2O nanofluid on the efficiency of flat-plate solar collectors," *Renew. Energy*, vol. 39, no. 1, pp. 293–298, 2012.

[25] I. Visa *et al.*, "Design and experimental optimisation of a novel flat plate solar thermal collector with trapezoidal shape for facades integration," *Appl. Therm. Eng.*, vol. 90, pp. 432–443, 2015.

[26] A. J. Moghadam, M. Farzane-Gord, M. Sajadi, and M. Hoseyn-Zadeh, "Effects of CuO/water nanofluid on the efficiency of a flat-plate solar collector," *Exp. Therm. Fluid Sci.*, vol. 58, pp. 9–14, 2014.

[27] J. Sarkar, P. Ghosh, and A. Adil, "A review on hybrid nanofluids: Recent research, development and applications," *Renew. Sustain. Energy Rev.*, vol. 43, pp. 164–177, 2015.

[28] M. Hemmat Esfe, S. Hadi Rostamian, and A. Alirezaie, "An applicable study on the thermal conductivity of SWCNT-MgO hybrid nanofluid and price-performance analysis for energy management," *Appl. Therm. Eng.*, vol. 111, p. , 2016.

[29] L.W. Florschuetz, "Extension of the Hottel–Whillier model to the analysis of com- bined photovoltaic/thermal flat plate collectors," *Sol. Energy*, vol. 22, no. 4, pp. 361–366, 1979.

[30] J. A. Ackermann, L. E. Ong, and S. C. Lau, "Conjugate heat transfer in solar collector panels with internal longitudinal corrugated fins-Part II: Local results," *Forsch. im Ingenieurwes. Eng. Res.*, vol. 61, no. 6, pp. 172–179, 1995.

[31] B. Hellstrom, M. Adsten, P. Nostell, B. Karlsson, and E. Wackelgard, "The impact of optical and thermal properties on the performance of flat plate solar collectors," *Renew. Energy*, vol. 28, no. 3, pp. 331–344, 2003.

[32] S. A. Kalogirou, "Flat-plate collector construction and system configuration to optimize the thermosiphonic effect," *Renew. Energy*, vol. 67, pp. 202–206, 2014.

[33] Z. Chen, M. Gu, and D. Peng, "Heat transfer performance analysis of a solar flat-plate collector with an integrated metal foam porous structure filled with paraffin," *Appl. Therm. Eng.*, vol. 30, no. 14–15, pp. 1967–1973, 2010.

[34] A. Hobbi and K. Siddiqui, "Optimal design of a forced circulation solar water heating system for a residential unit in cold climate using TRNSYS," *Sol. Energy*, vol. 83, no. 5, pp. 700–714, 2009.

[35] Y. Su, F. A. Kulacki, and J. H. Davidson, "Experimental and numerical investigations on a solar tracking concentrated photovoltaic-thermal system with a novel non-dimensional lattice Boltzmann method," *Sol. Energy*, vol. 107, pp. 145–158, 2014.

[36] M. Selmi, M. J. Al-Khawaja, and A. Marafia, "Validation of CFD simulation for flat plate solar energy collector," *Renew. Energy*, vol. 33, no. 3, pp. 383–387, 2008.

[37] Y. Tian and C. Y. Zhao, "A review of solar collectors and thermal energy storage in solar thermal applications," *Appl. Energy*, vol. 104, pp. 538–553, 2013.

[38] S. Saedodin, S. A. H. Zamzamian, M. E. Nimvari, S. Wongwises, and H. J. Jouybari, "Performance evaluation of a flat-plate solar collector filled with porous metal foam: Experimental and numerical analysis," *Energy Convers. Manag.*, vol. 153, no. September, pp. 278–287, 2017.

[39] M. A. Nima and A. M. Ali, "Effect of Metal Foam Insertion on Thermal Performance of Flat-Plate Water Solar Collector Under Iraqi Climate Conditions," *Arab. J. Sci. Eng.*, vol. 42, no. 11, pp. 4863–4884, 2017.

[40] R. Soloha, I. Pakere, and D. Blumberga, "Solar energy use in district heating systems. A case study in Latvia," *Energy*, vol. 137, pp. 586–594, 2017.

[41] S. K. Das, S. U. S. Choi, W. Yu, and T. Pradeep, *Nanofluids: Science and Technology*. 2007.

[42] S. Harikoshi and N. Serpone, *Microwaves in Nanoparticle Synthesis Fundamentals and Applications*, First edit. Tokyp: Willey, 2013.

[43] J. Vartiainen *et al.*, "Health and environmental safety aspects of friction grinding and spray drying of microfibrillated cellulose," *Cellulose*, vol. 18, no. 3, pp. 775–786, 2011.

[44] S. Sakthivel, V. V. Krishnan, and B. Pitchumani, "Influence of suspension stability on

wet grinding for production of mineral nanoparticles," *Particuology*, vol. 6, no. 2, pp. 120–124, 2008.

[45] S. Palaniandy, K. Azizi Mohd Azizli, H. Hussin, and S. Fuad Saiyid Hashim, "Mechanochemistry of silica on jet milling," *J. Mater. Process. Technol.*, vol. 205, no. 1–3, pp. 119–127, 2008.

[46] R. Rajkhowa, L. Wang, J. Kanwar, and X. Wang, "Fabrication of ultrafine powder from eri silk through attritor and jet milling," *Powder Technol.*, vol. 191, no. 1–2, pp. 155–163, 2009.

[47] M. J. Nine, B. Munkhbayar, M. S. Rahman, H. Chung, and H. Jeong, "Highly productive synthesis process of well dispersed Cu2O and Cu/Cu2O nanoparticles and its thermal characterization," *Mater. Chem. Phys.*, vol. 141, no. 2–3, pp. 636–642, 2013.

[48] R. Dvorský, A. Slíva, and Ň. Á. Č. Ek, "PREPARATION OF SILICON NANOPARTICLES BY MEANS OF DISINTEGRATION IN A CAVITATION WATER JET," 2010.

[49] C. J. Murphy *et al.*, "Anisotropic Metal Nanoparticles: Synthesis, Assembly, and Optical Applications," *J. Phys. Chem. B*, vol. 109, pp. 13857–13870, 2005.

[50] H. K. Chan and P. C. L. Kwok, "Production methods for nanodrug particles using the bottom-up approach," *Adv. Drug Deliv. Rev.*, vol. 63, no. 6, pp. 406–416, 2011.

[51] C. Keck, S. Kobierski, R. Mauludin, and R. H. Müller, "Second Generation of Drug Nanocrystals for Delivery of Poorly Soluble Drugs: Smartcrystals Technology," *Dosis*, vol. 24, no. 2, pp. 124–128, 2008.

[52] T. T. Baby and S. Ramaprabhu, "Experimental investigation of the thermal transport properties of a carbon nanohybrid dispersed nanofluid.," *Nanoscale*, vol. 3, no. 5, pp. 2208–14, 2011.

[53] R. Shende and R. Sundara, "Nitrogen doped hybrid carbon based composite dispersed nanofluids as working fluid for low-temperature direct absorption solar collectors," *Sol. Energy Mater. Sol. Cells*, vol. 140, pp. 9–16, 2015.

[54] S. C. Lyu, Y. Zhang, C. J. Lee, H. Ruh, and H. J. Lee, "Low-temperature growth of ZnO nanowire array by a simple physical vapor-deposition method," *Chem. Mater.*, vol. 15, no. 17, pp. 3294–3299, 2003.

[55]   R. B. Galindo *et al.*, "Synthesis of Copper Nanoparticles by Thermal Decomposition and Their Antimicrobial Properties," *J. Nanomater.*, vol. 2014, pp. 1–5, 2014.

[56]   J. P??rez-Juste, I. Pastoriza-Santos, L. M. Liz-Marz??n, and P. Mulvaney, "Gold nanorods: Synthesis, characterization and applications," *Coord. Chem. Rev.*, vol. 249, no. 17–18 SPEC. ISS., pp. 1870–1901, 2005.

[57]   M. B. Mohamed, Z. L. Wang, and M. a El-Sayed, "Temperature-Dependent Size-Controlled Nucleation and Growth of Gold Nanoclusters," *J. Phys. Chem. A*, vol. 103, no. 49, pp. 10255–10259, 1999.

[58]   * L. Rodríguez-Sánchez, M. C. Blanco, and and M. A. López-Quintela, "Electrochemical Synthesis of Silver Nanoparticles," *J. Phys. Chem. B*, vol. 104, no. 41, pp. 9683–9688, 2000.

[59]   S. M. Abbasi, A. Rashidi, A. Nemati, and K. Arzani, "The effect of functionalisation method on the stability and the thermal conductivity of nanofluid hybrids of carbon nanotubes/gamma alumina," *Ceram. Int.*, vol. 39, no. 4, pp. 3885–3891, 2013.

[60]   Y. J. Noh, S. I. Na, and S. S. Kim, "Inverted polymer solar cells including ZnO electron transport layer fabricated by facile spray pyrolysis," *Sol. Energy Mater. Sol. Cells*, vol. 117, pp. 139–144, 2013.

[61]   S. Suresh, K. P. Venkitaraj, P. Selvakumar, and M. Chandrasekar, "Synthesis of Al2O3-Cu/water hybrid nanofluids using two step method and its thermo physical properties," *Colloids Surfaces A Physicochem. Eng. Asp.*, vol. 388, no. 1–3, pp. 41–48, 2011.

[62]   L. S. Sundar, M. K. Singh, and A. C. M. Sousa, "Enhanced heat transfer and friction factor of MWCNT-Fe3O4/water hybrid nanofluids," *Int. Commun. Heat Mass Transf.*, vol. 52, pp. 73–83, 2014.

[63]   D. Madhesh, R. Parameshwaran, and S. Kalaiselvam, "Experimental investigation on convective heat transfer and rheological characteristics of Cu-TiO2 hybrid nanofluids," *Exp. Therm. Fluid Sci.*, vol. 52, pp. 104–115, 2014.

[64]   H. Yarmand *et al.*, "Graphene nanoplatelets-silver hybrid nanofluids for enhanced heat transfer," *Energy Convers. Manag.*, vol. 100, pp. 419–428, 2015.

[65]   L. Megatif, A. Ghozatloo, A. Arimi, and M. Shariati-Niasar, "Investigation of laminar convective heat transfer of a novel Tio2-carbon nanotube hybrid water-based nanofluid,"

Exp. Heat Transf., vol. 6152, no. November, pp. 1–15, 2015.

[66]   M. Batmunkh *et al.*, "Thermal conductivity of TiO2 nanoparticles based aqueous nanofluids with an addition of a modified silver particle," *Ind. Eng. Chem. Res.*, vol. 53, no. 20, pp. 8445–8451, 2014.

[67]   L. Chen, W. Yu, and H. Xie, "Enhanced thermal conductivity of nanofluids containing Ag/MWNT composites," *Powder Technol.*, vol. 231, pp. 18–20, 2012.

[68]   P. Selvakumar and S. Suresh, "Use of Al 2 O 3 – Cu / Water Hybrid Nanofluid in an Electronic Heat Sink," vol. 2, no. 10, pp. 1600–1607, 2012.

[69]   S. Suresh, K. P. P. Venkitaraj, P. Selvakumar, and M. Chandrasekar, "Effect of Al2O3– Cu/water hybrid nanofluid in heat transfer," *Exp. Therm. Fluid Sci.*, vol. 38, pp. 54–60, 2012.

[70]   H. Li, C.-S. Ha, and I. Kim, "Fabrication of Carbon Nanotube/SiO(2) and Carbon Nanotube/SiO(2)/Ag Nanoparticles Hybrids by Using Plasma Treatment.," *Nanoscale Res. Lett.*, vol. 4, no. 11, pp. 1384–1388, 2009.

[71]   L. F. Chen, M. Cheng, D. J. Yang, and L. Yang, "Enhanced Thermal Conductivity of Nanofluid by Synergistic Effect of Multi-Walled Carbon Nanotubes and Fe2O3 Nanoparticles," *Appl. Mech. Mater.*, vol. 548, pp. 118–123, 2014.

[72]   H. Chang, C. S. Jwo, P. S. Fan, and S. H. Pai, "Process optimization and material properties for nanofluid manufacturing," *Int. J. Adv. Manuf. Technol.*, vol. 34, no. 3–4, pp. 300–306, 2007.

[73]   M.-S. Liu, M. Ching-Cheng Lin, I.-T. Huang, and C.-C. Wang, "Enhancement of thermal conductivity with carbon nanotube for nanofluids," *Int. Commun. Heat Mass Transf.*, vol. 32, no. 9, pp. 1202–1210, 2005.

[74]   T. P. Teng, Y. H. Hung, T. C. Teng, H. E. Mo, and H. G. Hsu, "The effect of alumina/water nanofluid particle size on thermal conductivity," *Appl. Therm. Eng.*, vol. 30, no. 14–15, pp. 2213–2218, 2010.

[75]   B.-J. Huang *et al.*, "Maximum-power-point tracking control of solar heating system," *Sol. Energy*, vol. 86, no. 11, pp. 3278–3287, 2012.

[76]   Y. Hwang *et al.*, "Stability and thermal conductivity characteristics of nanofluids,"

Thermochim. Acta, vol. 455, no. 1–2, pp. 70–74, 2007.

[77] J. Huang, X. Wang, Q. Long, and L. Liming, "Influence of pH on the Stability Characteristics of Nanofluids," *Symp. Photonics Optoelectron.*, vol. 1, pp. 1–4, 2009.

[78] F. X. Li, D. S. Zhu, X. J. Wang, N. Wang, J. W. Gao, and H. Li, "Thermal conductivity enhancement dependent pH and chemical surfactant for Cu–H2O nanofluids," *Thermochim. Acta*, vol. 469, no. 1, pp. 98–103, 2008.

[79] D. Zhu, X. Li, N. Wang, X. J. Wang, J. W. Gao, and H. Li, "Dispersion behaviour and thermal conductivity characteristics of Al2O3–H2O nanofluids," *Curr. Appl. Phys.*, vol. 9, no. 1, pp. 131–139, 2009.

[80] J. L, G. L, and S. J, "Production of aqueous colloidal dispersions of carbon nanotubes," *J. Colloid Interface Sci.*, vol. 1, pp. 89–94, 2003.

[81] S. H. Kim, S. R. Choi, and D. Kim, "Thermal conductivity of metal-oxide nanofluids: particle size dependence and effect of laser irradiation," *J. Heat Transfer*, vol. 129, pp. 298–307, 2007.

[82] M. J. Assael, I. N. Metaxa, J. Arvanitidis, D. Christofilos, and C. Lioutas, "Thermal conductivity enhancement in aqueous suspensions of carbon multi-walled and double-walled nanotubes in the presence of two different dispersants," *Int. J. Thermophys.*, vol. 26, no. 3, pp. 647–664, 2005.

[83] I. Madni, C. Y. Hwang, S. D. Park, Y. H. Choa, and H. T. Kim, "Mixed surfactant system for stable suspension of multiwalled carbon nanotubes," *Colloids Surfaces A Physicochem. Eng. Asp.*, vol. 358, no. 1–3, pp. 101–107, 2010.

[84] Y. H. Wang, J. K. Lee, Y. M. Jeong, S. I. Cheong, Y. C. Ahn, and S. H. Kim, "Production and dispersion stability of nanoparticles in nanofluids," *Powder Technol.*, vol. 186, no. 2, pp. 145–153, 2008.

[85] C. Choi, H. S. Yoo, and J. M. Oh, "Preparation and heat transfer properties of nanoparticle-in-transformer oil dispersions as advanced energy-efficient coolants," *Curr. Appl. Phys.*, vol. 8, no. 6, pp. 710–712, 2008.

[86] M. Sato, Y. Abe, Y. Urita, R. D. Paola, A. Cecere, and R. Savino, "Thermal performance of self-rewetting fluid heat pipe containing dilute solutions of polymer capped silver nanoparticles synthesized by microwave-polyol process," *Proceeding ITP 2009*, 2009.

[87] C. Walleck, ", Development of Steady-State, Parallel-Plate Thermal Conductivity Apparatus for Poly-Nanofluids and Comparative Measurements with Transient HWTC Apparatus," Northern Illinois University United States, 2009.

[88] C. Cao, L. Zhang, X. X. Zhang, and F. P. Du, "Effect of gum arabic on the surface tension and surface dilational rheology of trisiloxane surfactant," *Food Hydrocoll.*, vol. 30, no. 1, pp. 456–462, 2013.

[89] A. T. Utomo, H. Poth, T. Philip, Robbins, and W. P. Pacek, "Experimental and theoretical studies of thermal conductivity, viscosity and heat transfer coefficient of titania and alumina nanofluids," *Int. J. Heat Mass Transf.*, vol. 55, pp. 7772–7781, 2012.

[90] P. C. Hiemenz and M. Decker, *Principles of colloid and surface chemistry*, Second Edi. New York: Dekker, 1986.

[91] P.C.Hiemenz and R. Rajagopalan, *Principles of colloids and surface chemistry*, 3rd Editio. Newyork: Madison Avenue, New york, 1997.

[92] S. U. S. Choi, "Thermal Conductivity of Fluids with Nanoparticles," *Dev. Appl. Non Newton. Flows*, vol. 231, no. 66, pp. 99–105, 1995.

[93] D. Wen and Y. Ding, "Experimental investigation into convective heat transfer of nanofluids at the entrance region under laminar flow conditions," *Int. J. Heat Mass Transf.*, vol. 47, no. 24, pp. 5181–5188, 2004.

[94] S. A. Angayarkanni and J. Philip, "Review on thermal properties of nanofluids: Recent developments," *Adv. Colloid Interface Sci.*, vol. 225, pp. 146–176, 2015.

[95] S. M. Fotukian and M. Nasr Esfahany, "Experimental investigation of turbulent convective heat transfer of dilute ??-Al2O3/water nanofluid inside a circular tube," *Int. J. Heat Fluid Flow*, vol. 31, no. 4, pp. 606–612, 2010.

[96] N. Ahammed, L. G. Asirvatham, and S. Wongwises, "Effect of volume concentration and temperature on viscosity and surface tension of graphene-water nanofluid for heat transfer applications," *J. Therm. Anal. Calorim.*, vol. 123, no. 2, pp. 1399–1409, 2016.

[97] R. Lenin and P. A. Joy, "Role of base fluid on the thermal conductivity of oleic acid coated magnetite nanofluids," *Colloids Surfaces A Physicochem. Eng. Asp.*, vol. 529, pp. 922–929, 2017.

[98] S. E. Ghasemi, A. A. Ranjbar, and M. J. Hosseini, "Experimental evaluation of cooling performance of circular heat sinks for heat dissipation from electronic chips using nanofluid," *Mech. Res. Commun.*, vol. 84, pp. 85–89, 2017.

[99] S. U. Ilyas, R. Pendyala, and M. Narahari, "Stability and thermal analysis of MWCNT-thermal oil-based nanofluids," *Colloids Surfaces A Physicochem. Eng. Asp.*, vol. 527, no. May, pp. 11–22, 2017.

[100] Y. Ueki, T. Aoki, K. Ueda, and M. Shibahara, "Thermophysical properties of carbon-based material nanofluid," *Int. J. Heat Mass Transf.*, vol. 113, pp. 1130–1134, 2017.

[101] T. T. Baby and S. Ramaprabhu, "Synthesis and nanofluid application of silver nanoparticles decorated graphene," *J. Mater. Chem.*, vol. 21, no. 26, p. 9702, 2011.

[102] B. Munkhbayar, M. R. Tanshen, J. Jeoun, H. Chung, and H. Jeong, "Surfactant-free dispersion of silver nanoparticles into MWCNT-aqueous nanofluids prepared by one-step technique and their thermal characteristics," *Ceram. Int.*, vol. 39, no. 6, pp. 6415–6425, 2013.

[103] X. Liu and Y. Chen, "Fluid flow and heat transfer in flat-plate oscillating heat pipe," *Energy Build.*, vol. 75, pp. 29–42, 2014.

[104] K. Motahari, M. Abdollahi Moghaddam, and M. Moradian, "Experimental investigation and development of new correlation for influences of temperature and concentration on dynamic viscosity of MWCNT-SiO2 (20-80)/20W50 hybrid nano-lubricant," *Chinese J. Chem. Eng.*, 2017.

[105] H. Li, L. Wang, Y. He, Y. Hu, J. Zhu, and B. Jiang, "Experimental investigation of thermal conductivity and viscosity of ethylene glycol based ZnO nanofluids," *Appl. Therm. Eng.*, vol. 88, pp. 363–368, 2014.

[106] O. Soltani and M. Akbari, "Effects of temperature and particles concentration on the dynamic viscosity of MgO-MWCNT/ethylene glycol hybrid nanofluid: Experimental study," *Phys. E Low-Dimensional Syst. Nanostructures*, vol. 84, pp. 564–570, 2016.

[107] S. Delfani, M. Karami, and M. A. Akhavan Bahabadi, "Experimental investigation on performance comparison of nanofluid-based direct absorption and flat plate solar collectors," *Int. J. Nano Dimens.*, vol. 7, no. 1, pp. 85–96, 2015.

[108] M. Karami, M. A. Akhavan-Behabadi, M. Raisee Dehkordi, and S. Delfani, "Thermo-

optical properties of copper oxide nanofluids for direct absorption of solar radiation," *Sol. Energy Mater. Sol. Cells*, vol. 144, pp. 136–142, 2016.

[109] A. Zamzamian, M. KeyanpourRad, M. KianiNeyestani, and M. T. Jamal-Abad, "An experimental study on the effect of Cu-synthesized/EG nanofluid on the efficiency of flat-plate solar collectors," *Renew. Energy*, vol. 71, pp. 658–664, 2014.

[110] S. Salavati, A. Kianifar, H. Niazmand, O. Mahian, and S. Wongwises, "Experimental investigation on the thermal efficiency and performance characteristics of a flat plate solar collector using SiO2/EG–water nanofluids," *Int. Commun. Heat Mass Transf.*, vol. c, pp. 71–75, 2015.

[111] M. Karami, M. A. Akhavan-Bahabadi, S. Delfani, and M. Raisee, "Experimental investigation of CuO nanofluid-based Direct Absorption Solar Collector for residential applications," *Renew. Sustain. Energy Rev.*, vol. 52, pp. 793–801, 2015.

[112] H. Kaya, K. Arslan, and N. Eltugral, "Experimental investigation of thermal performance of an evacuated U-Tube solar collector with ZnO/Etylene glycol-pure water nanofluids," *Renew. Energy*, vol. 122, pp. 329–338, 2018.

[113] T.Yousefi, E. Shojaeizadeh, F. Veysi, and S. Zinadini, "An experimental investigation on the effect of pH variation of MWCNT–H2O nanofluid on the efficiency of a flat plate solar collector," *Sol. Energy*, vol. 86, pp. 771–779, 2012.

[114] H. Chaji, Y. Ajabshirchi, E. Esmaeilzadeh, S. Z. Heris, M. Hedayatizadeh, and M. Kahani, "Experimental study on thermal efficiency of flat plate solar collector using tio2/water nanofluid," *Mod. Appl. Sci.*, vol. 7, no. 10, pp. 60–69, 2013.

[115] A. K. Tiwari, P. Ghosh, and J. Sarkar, "Solar Water Heating Using Nanofluids - a Comprehensive Overview and Environmental Impact Analysis," *Int. J. Emerg. Technol. Adv. Eng.*, vol. 3, no. 3, pp. 221–224, 2013.

[116] M. T. Jamal-abad, A. Zamzamian, E. Imani, and M. Mansouri, "Experimental Study of the Performance of a Flat-Plate Collector Using Cu–Water Nanofluid," *J. Thermophys. Heat Transf.*, no. August, pp. 1–5, 2013.

[117] A. E. Kabeel and E. M. S. El-Said, "Applicability of flashing desalination technique for small scale needs using a novel integrated system coupled with nanofluid-based solar collector," *Desalination*, vol. 333, no. 1, pp. 10–22, 2014.

[118] D. Anin Vincely and E. Natarajan, "Experimental investigation of the solar FPC performance using graphene oxide nanofluid under forced circulation," *Energy Convers. Manag.*, vol. 117, pp. 1–11, 2016.

[119] S S Meobodi, A. Kianifar, H. Niazmand, O. Mahian, and S. Wongwises, "Experimental investigation on the thermal efficiency and performance characteristics of a flat plate solar collector using SiO2/EG– water nanofluids," *Int. Commun. Heat Mass Transf.*, vol. 65, pp. 71–75, 2015.

[120] N. K. C. Sint, I. A. Choudhury, H. H. Masjuki, and H. Aoyama, "Theoretical analysis to determine the efficiency of a CuO-water nanofluid based-flat plate solar collector for domestic solar water heating system in Myanmar," *Sol. Energy*, vol. 155, pp. 608–619, 2017.

[121] M. Auffan, J. Rose, J. Y. Bottero, G. V. Lowry, J. P. Jolivet, and M. R. Wiesner, "Towards a definition of inorganic nanoparticles from an environmental, health and safety perspective," *Nat. Nanotechnol.*, vol. 4, no. 10, pp. 634–641, 2009.

[122] H. Tyagi, P. Phelan, and R. Prasher, "Predicted Efficiency of a Low-Temperature Nanofluid-Based Direct Absorption Solar Collector," *J. Sol. Energy Eng.*, vol. 131, no. 4, p. 41004, 2009.

[123] R. Saidur, T.C. Meng, Z. Said, M. Hasanuzzaman, and A Kamyar, "Evaluation of the effect of nanofluid-based absorbers on direct solar collector," *International J. heat mass Transf.*, vol. 55, pp. 5899–5907, 2012.

[124] L. Mercatelli *et al.*, "Absorption and scattering properties of carbon nanohorn-based nanofluids for direct sunlight absorbers," *Nanoscale Res. Lett.*, vol. 6, no. 1, p. 282, 2011.

[125] S. M. Ladjevardi, A. Asnaghi, P. S. Izadkhast, and A. H. Kashani, "Applicability of graphite nanofluids in direct solar energy absorption," *Sol. Energy*, vol. 94, pp. 327–334, 2013.

[126] Q. He, S. Wang, S. Zeng, and Z. Zheng, "Experimental investigation on photothermal properties of nanofluids for direct absorption solar thermal energy systems," *Energy Convers. Manag.*, vol. 73, pp. 150–157, 2013.

[127] T. B. Gorji, A. A. Ranjbar, and S. N. Mirzababaei, "Optical properties of carboxyl functionalized carbon nanotube aqueous nanofluids as direct solar thermal energy

absorbers," *Sol. Energy*, vol. 119, pp. 332–342, 2015.

[128] H. K. Gupta, G. Das Agrawal, and J. Mathur, "Investigations for effect of Al2O3–H2O nanofluid flow rate on the efficiency of direct absorption solar collector," *Case Stud. Therm. Eng.*, vol. 5, pp. 70–78, 2015.

[129] M. Vakili, S. M. Hosseinalipour, S. Delfani, and S. Khosrojerdi, "Photothermal properties of graphene nanoplatelets nanofluid for low-temperature direct absorption solar collectors," *Sol. Energy Mater. Sol. Cells*, vol. 152, pp. 187–191, 2016.

[130] R. Kaluri, S. Vijayaraghavan, and S. Ganapathisubbu, "Model Development and Performance Studies of a Concentrating Direct Absorption Solar Collector," *J. Sol. Energy Eng.*, vol. 137, no. 84, pp. 21005-1–12, 2015.

[131] W. Chen, C. Zou, and X. Li, "An investigation into the thermophysical and optical properties of SiC/ionic liquid nanofluid for direct absorption solar collector," *Sol. Energy Mater. Sol. Cells*, vol. 163, no. January, pp. 157–163, 2017.

[132] Y. Xuan, Q. Li, and H. Duan, "Enhancement of solar energy absorption using a plasmonic nanofluid based on Tio2/Ag composite nanoparticles," *RSC Adv.*, vol. 4, no. 31, pp. 16206–16213, 2014.

[133] A. Shitzer, D. Kalmanoviz, Y. Zvirin, and G. Grossman, "Experiments with a flat plate solar water heating system in thermosyphonic flow," *Sol. Energy*, vol. 22, no. 1, pp. 27–35, 1979.

[134] A. Zerrouki, A. Boumédien, and K. Bouhadef, "The natural circulation solar water heater model with linear temperature distribution," *Renew. Energy*, vol. 26, no. 4, pp. 549–559, 2002.

[135] K. Bouhadef, A. Zerrouki, and A. Boume, "The natural circulation solar water heater model with linear temperature distribution," vol. 26, pp. 549–559, 2002.

[136] P. Sae-Jung, T. Krittayanawach, P. Deedom, and B. Limmeechokchai, *An Experimental Study of Thermo-Syphon Solar Water Heater in Thailand*, vol. 79. Elsevier B.V., 2015.

[137] H. D. Koca, S. Doganay, and A. Turgut, "Thermal characteristics and performance of Ag-water nanofluid: Application to natural circulation loops," *Energy Convers. Manag.*, vol. 135, pp. 9–20, 2017.

[138] A. Saravanan, J. S. Senthilkumaar, and S. Jaisankar, "Performance assessment in V-trough solar water heater fitted with square and V-cut twisted tape inserts," *Appl. Therm. Eng.*, vol. 102, pp. 476–486, 2016.

[139] J. Ghaderian *et al.*, "Performance of copper oxide/distilled water nanofluid in evacuated tube solar collector (ETSC) water heater with internal coil under thermosyphon system circulations," *Appl. Therm. Eng.*, vol. 121, pp. 520–536, 2017.

[140] L. Sundar, M. Singh, V. Punnaiah, and A. Sousa, "Experimental investigation of Al2O3/water nanofluids on the effectiveness of solar flat-plate collectors with and without twisted tape inserts," *Renew. Energy*, 2017.

[141] O. Mahian, A. Kianifar, S. Zeinali Heris, and S. Wongwises, "First and second laws analysis of a minichannel-based solar collector using boehmite alumina nanofluids: Effects of nanoparticle shape and tube materials," *Int. J. Heat Mass Transf.*, vol. 78, pp. 1166–1176, 2014.

[142] S. Parvin, R. Nasrin, and M. A. Alim, "Heat transfer and entropy generation through nanofluid filled direct absorption solar collector," *Int. J. Heat Mass Transf.*, vol. 71, pp. 386–395, 2014.

[143] E. Shojaeizadeh, F. Veysi, and A. Kamandi, "Exergy efficiency investigation and optimization of an Al_2O_3-water nanofluid based Flat-plate solar collector," *Energy Build.*, vol. 101, pp. 12–23, 2015.

[144] Z. Said, R. Saidur, M. A. Sabiha, A. Hepbasli, and N. A. Rahim, "Energy and exergy efficiency of a flat plate solar collector using pH treated Al2O3 nanofluid," *J. Clean. Prod.*, vol. 112, pp. 3915–3926, 2016.

[145] Z. Said, R. Saidur, N. A. Rahim, and M. A. Alim, "Analyses of exergy efficiency and pumping power for a conventional flat plate solar collector using SWCNTs based nanofluid," *Energy Build.*, vol. 78, pp. 1–9, 2014.

[146] T. P. Otanicar, P. E. Phelan, R. S. Prasher, G. Rosengarten, and R. A. Taylor, "Nanofluid-based direct absorption solar collector," *J. Renew. Sustain. Energy*, vol. 2, no. 3, 2010.

[147] G. Sandhu, K. Siddiqui, and A. Garcia, "Experimental study on the combined effects of inclination angle and insert devices on the performance of a flat-plate solar collector," *Int. J. Heat Mass Transf.*, vol. 71, pp. 251–263, 2014.

[148] J. J. Michael and S. Iniyan, "Performance of copper oxide/water nanofluid in a flat plate solar water heater under natural and forced circulations," *Energy Convers. Manag.*, vol. 95, pp. 160–169, 2015.

[149] B. C. Pak and Y. I. Cho, "Hydrodynamic and Heat Transfer Study of Dispersed Fluids With Submicron Metallic Oxide Particles," *Exp. Heat Transf.*, vol. 11, no. 2, pp. 151–170, 1998.

[150] W. I. A. Aly, "Numerical study on turbulent heat transfer and pressure drop of nanofluid in coiled tube-in-tube heat exchangers," *Energy Convers. Manag.*, vol. 79, pp. 304–316, 2014.

[151] R. a Taylor, P. E. Phelan, T. P. Otanicar, R. Adrian, and R. Prasher, "Nanofluid optical property characterization: towards efficient direct absorption solar collectors.," *Nanoscale Res. Lett.*, vol. 6, no. 1, p. 225, 2011.

[152] C. L. Tien, "Thermal Radiation in Packed and Fluidized Beds," *J. Heat Transfer*, vol. 110, no. 4b, p. 1230, 1988.

[153] B. Takabi and H. Shokouhmand, "Effects of Al 2 O 3–Cu/water hybrid nanofluid on heat transfer and flow characteristics in turbulent regime," *Int. J. Mod. Phys.*, vol. 26, no. 4, pp. 1–25, 2015.

[154] L. S. Sundar, E. Venkata Ramana, M. P. F. Gra??a, M. K. Singh, and A. C. M. Sousa, "Nanodiamond-Fe3O4 nanofluids: Preparation and measurement of viscosity, electrical and thermal conductivities," *Int. Commun. Heat Mass Transf.*, vol. 73, pp. 62–74, 2016.

[155] C. J. Ho, J. B. Huang, P. S. Tsai, and Y. M. Yang, "Preparation and properties of hybrid water-based suspension of Al2O3 nanoparticles and MEPCM particles as functional forced convection fluid," *Int. Commun. Heat Mass Transf.*, vol. 37, no. 5, pp. 490–494, 2010.

[156] B. G. K. Batchelor, "The effect of Brownian motion on the bulk stress in a suspension of spherical particles," vol. 83, 1977.

[157] C. T. Nguyen *et al.*, "Temperature and particle-size dependent viscosity data for water-based nanofluids - Hysteresis phenomenon," *Int. J. Heat Fluid Flow*, vol. 28, no. 6, pp. 1492–1506, 2007.

[158] S. M. S. Murshed and P. Estellé, "A state of the art review on viscosity of nanofluids,"

Renew. Sustain. Energy Rev., vol. 76, no. April, pp. 1134–1152, 2017.

[159] D A G Bruggeman, "Calculation of Various Physics Constants in Heterogeneous Substances I Dielectricity Constants and Conductivity of Mixed Bodies from Isotropic Substances," *Ann. Phys.*, vol. 24, no. 7, pp. 636–664, 1935.

[160] J. Koo and C. Kleinstreuer, "A new thermal conductivity model for nanofluids," *J. Nanoparticle Res.*, vol. 6, no. 6, pp. 577–588, 2004.

[161] M. H, A. Ebata, K. Teramae, and N. Hishinuma, "Alteration of thermal conductivity and viscosity of liquid by dispersing ultra-fine particles (dispersion of γ-Al2O3, SiO2 and TiO2 ultra-fine particles)," *Netsu Bussei*, vol. 4, no. 4, pp. 227–233, 2010.

[162] J. Lee and I. Mudawar, "Assessment of the effectiveness of nanofluids for single-phase and two-phase heat transfer in micro-channels," *Int. J. Heat Mass Transf.*, vol. 50, no. 3, pp. 452–463, 2007.

[163] X. Wang, X. Xu, and S. U. S. Choi, "Thermal Conductivity of Nanoparticle - Fluid Mixture," *J. Thermophys. Heat Transf.*, vol. 13, no. 4, pp. 474–480, 1999.

[164] Y. Feng, B. Yu, P. Xu, and M. Zou, "The effective thermal conductivity of nanofluids based on the nanolayer and the aggregation of nanoparticles," *J. Appl. Phys.*, vol. 40, no. 10, pp. 3164–3171, 2007.

[165] S M S Murshed, K C Long, and C Yang, "Enhanced Thermal Conductivity of TiO2-Water Based Nanofluids," *Int. J. Therm. Sci.*, vol. 44, pp. 367–373, 2005.

[166] H. E. Patel, S. K. Das, and T. Sundararajan, "Thermal Conductivities of Naked and Monolayer Protected Metal Nanoparticle Based Nanofluids: Manifestation of Anomalous Enhancement and Chemical Effects," *Appl. Phys. Lett.*, vol. 83, no. 14, pp. 2931–2933, 2003.

[167] R. Prasher, I. Corporation, W. Chandler, and V. Boule, "Effect of Aggregation Kinetics on the Thermal Conductivity of Nanoscale Colloidal Solutions (Nanofluid)," pp. 8–12, 2006.

[168] X. ju Wang, D. sheng Zhu, and S. yang, "Investigation of pH and SDBS on enhancement of thermal conductivity in nanofluids," *Chem. Phys. Lett.*, vol. 470, no. 1–3, pp. 107–111, 2009.

[169] S. M. S. Murshed, C. A. N. De Castro, S. M. Sohel Murshed, and C. A. N. de Castro, "Contribution of Brownian Motion in Thermal Conductivity of Nanofluids," *Proc World Congr. Eng.*, vol. III, pp. 1905–1909, 2011.

[170] W. Evans, J. Fish, and P. Keblinski, "Role of Brownian motion hydrodynamics on nanofluid thermal conductivity," *Appl. Phys. Lett.*, vol. 88, no. 9, pp. 3–5, 2006.

[171] K. S. Suganthi, V. Leela Vinodhan, and K. S. Rajan, "Heat transfer performance and transport properties of ZnO-ethylene glycol and ZnO-ethylene glycol-water nanofluid coolants," *Appl. Energy*, vol. 135, pp. 548–559, 2014.

[172] NIST, "Standard Reference Database-REFPROP, Version 9.1." 2013.

[173] N. Putra, W. Roetzel, and S. K. Das, "Natural convection of nano-fluids," *Heat Mass Transf. und Stoffuebertragung*, vol. 39, no. 8–9, pp. 775–784, 2003.

[174] A. Einstein, "On the Motion of Small Particles Suspended in a Stationary Liquid, as Required by the Molecular Kinetic Theory of Heat," *Ann. Phys.*, vol. 322, pp. 549–560, 1905.

[175] M. T. Zafarani-Moattar and R. Majdan-Cegincara, "Effect of temperature on volumetric and transport properties of nanofluids containing ZnO nanoparticles poly(ethylene glycol) and water," *J. Chem. Thermodyn.*, vol. 54, pp. 55–67, 2012.

[176] P. M. Kumar, J. Kumar, R. Tamilarasan, S. Sendhilnathan, and S. Suresh, "Review on nanofluids theoretical thermal conductivity models," *Eng. J.*, vol. 19, no. 1, pp. 67–83, 2015.

[177] T. T. Baby and R. Sundara, "Synthesis and Transport Properties of Metal Oxide Decorated Graphene Dispersed Nanofluids," *J. Phys. Chem. C*, vol. 115, no. 17, pp. 8527–8533, 2011.

[178] J. Duffie and W. Beckman, *Solar Engineering of Thermal Processes, 3th ed.*, vol. 116. 2006.

[179] F P Incropara and D P De Witt, *Fundamentals of Heat and Mass Transfer*, 4th editio. New York: John Wiley and Sons, 1996.

[180] Y A Cengel and J M Cimbala, *Fluid Mechanics: Fundamentals and Applications*, @nd Editio. Mc. Graw-Hill Higher Education, 2009.

[181] H. Kargarsharifabad, M. Behshad Shafii, M. Taeibi Rahni, and M. Abbaspour, "Exergy Analysis of a Flat Plate Solar Collector in Combination with Heat Pipe," *Int. J. Environ. Res.*, vol. 8, no. 1, pp. 39–48, 2014.

[182] A. Suzuki, "General theory of exergy-balance analysis and application to solar collector," *Energy*, vol. 13, no. 2, pp. 153–160, 1988.

[183] Dutta Gupta kk and Saha SK, "Energy analysis of solar thermal collectors," *Renew. Energy Environ.*, vol. 5, pp. 283–287, 1990.

[184] O. Mahian, A. Kianifar, A. Z. Sahin, and S. Wongwises, "Entropy generation during Al2O3/water nanofluid flow in a solar collector: Effects of tube roughness, nanoparticle size, and different thermophysical models," *Int. J. Heat Mass Transf.*, vol. 78, pp. 64–75, 2014.

[185] A. Bejan, *Entropy Generation through Heat and Fluid Flow*, 1st editio. Newyork: Willey, 1982.

[186] S. Kalogirou, "Thermal performance, economic and environmental life cycle analysis of thermosiphon solar water heaters," *Sol. Energy*, vol. 83, no. 1, pp. 39–48, 2009.

[187] G. Hammond and C. Jones, "Inventory of Carbon and Energy," 2011.

[188] S. A. Kalogirou, *Solar thermal collectors and applications*, vol. 30, no. 3. 2004.

[189] Soteris Kalogirou, *Solar Energy Engineering Processes and systems*, 3 rd. California: Academic Press, 2009.

[190] American Society of Heating Refrigerating and Air-Conditioning Engineers, *2011 ASHRAE Handbook - HVAC Applications*. 2011.

[191] V. Khullar *et al.*, "Harvesting solar thermal energy through nanofluid-based volumetric absorption systems," *Int. J. Heat Mass Transf.*, vol. 77, pp. 377–384, 2014.

[192] D. A. G. Redpath, "Thermosyphon heat-pipe evacuated tube solar water heaters for northern maritime climates," *Sol. Energy*, vol. 86, no. 2, pp. 705–715, 2012.